

Copyright Warning & Restrictions

The copyright law of the United States (Title 17, United States Code) governs the making of photocopies or other reproductions of copyrighted material.

Under certain conditions specified in the law, libraries and archives are authorized to furnish a photocopy or other reproduction. One of these specified conditions is that the photocopy or reproduction is not to be “used for any purpose other than private study, scholarship, or research.” If a user makes a request for, or later uses, a photocopy or reproduction for purposes in excess of “fair use” that user may be liable for copyright infringement,

This institution reserves the right to refuse to accept a copying order if, in its judgment, fulfillment of the order would involve violation of copyright law.

Please Note: The author retains the copyright while the New Jersey Institute of Technology reserves the right to distribute this thesis or dissertation

Printing note: If you do not wish to print this page, then select “Pages from: first page # to: last page #” on the print dialog screen



The Van Houten library has removed some of the personal information and all signatures from the approval page and biographical sketches of theses and dissertations in order to protect the identity of NJIT graduates and faculty.

ABSTRACT

IONIC LIQUIDS AS ADDITIVES FOR BIODEGRADABLE POLYLACTIC ACID

by
Ku-II Park

In this study, two ionic liquids (IL) with different anions (decanoate, tetrafluoroborate) but with the same phosphonium based cation were evaluated as potential plasticizers and lubricants for polylactic acid (PLA) and also for their effects on its hydrolytic and thermal degradation. Both ILs at 5wt% were well dispersible and partly miscible with PLA as evidenced by scanning electron microscopy/energy dispersive x-ray scattering, SEM/EDX, and glass transition temperature, T_g , characterization, as well as from solubility parameters calculations.

The effects of the IL containing a decanoate anion were more pronounced on lubrication and degradation as evidenced by reduced melt viscosities and accelerated thermal/hydrolytic degradation; this IL could also be considered as a more effective plasticizer based on T_g suppression results although the degree of plasticization could also be affected by the observed excessive molecular weight, MW, degradation during melt processing. The IL containing the tetrafluoroborate anion increased the thermal stability of PLA as also confirmed from rate constants calculated from random chain scission statistics and activation energies from thermogravimetric analysis, and accelerated its hydrolytic degradation, but to a lesser extent than the decanoate based IL. The catalytic role of the decanoate anion in hydrolytic degradation was confirmed through experiments with a model compound.

Hydrolytic chain scission of ester bonds catalyzed by acid groups are the suggested mechanisms of hydrolytic degradation based on results of pH and acid number changes, although it appears that the presence of the phosphonium cation contributes also to accelerated degradation. Degradation results were confirmed by optical and SEM examination and experiments in “as received” and sterilized soil. The different surface characteristics of PLA/ILs were reflected in differences in coefficients of friction and contact angles. The tetrafluoroborate anion containing IL reduced the flexural modulus and strength of PLA, affecting much less its ductility than the decanoate anion containing IL.

IONIC LIQUIDS AS ADDITIVES FOR BIODEGRADABLE POLYLACTIC ACID

by

Ku-Il Park

**A Dissertation
Submitted to the Faculty of
New Jersey Institute of Technology
in Partial Fulfillment of the Requirements for the Degree of
Doctor of Philosophy in Materials Science and Engineering**

Materials Science and Engineering Program

August 2008

Copyright © 2008 by Ku-II Park

ALL RIGHTS RESERVED

APPROVAL PAGE

IONIC LIQUIDS AS ADDITIVES FOR BIODEGRADABLE POLYLACTIC ACID

Ku-II Park

Dr. Marino Xanthos, Dissertation Advisor Date
Professor, Otto H. York Department of Chemical, Biological and Pharmaceutical
Engineering, NJIT

Dr. Marios Avgousti, Committee Member Date
Research Associate, DuPont Engineering, Wilmington, DE

Dr. Reginald Farrow, Committee Member Date
Research Professor, Department of Physics, NJIT

Dr. Sergiu Gorun, Committee Member Date
Associate Professor, Department of Chemistry and Environmental Science, NJIT

Dr. Kun Sup Hyun, Committee Member Date
Research Professor, Otto H. York Department of Chemical, Biological and
Pharmaceutical Engineering, NJIT

Dr. Somenath Mitra, Committee Member Date
Professor, Department of Chemistry and Environmental Science, NJIT

Dr. Kwabena A. Narh, Committee Member Date
Professor, Department of Mechanical Engineering, NJIT

BIOGRAPHICAL SKETCH

Author: Ku-Il Park
Degree: Doctor of Philosophy
Date: August 2008

Undergraduate and Graduate Education:

- Doctor of Philosophy in Materials Science and Engineering, New Jersey Institute of Technology, Newark, NJ, 2008
- Master of Science in Materials Science and Engineering, New Jersey Institute of Technology, Newark, NJ, 2003
- Bachelor of Science in Textile Engineering, Kon-Kuk University, Seoul, Korea, 2000

Major: Materials Science and Engineering

Presentations and Publications:

Conference Proceedings

- K. Park, M. Xanthos, "Modification of Degradation and Processing Characteristics of Polylactic Acid with Ionic Liquids", *Proc. Polymer Processing Society PPS-24 Annual Meeting*, Paper S14-236, Salerno, Italy, June (2008).
- K. Park, M. Xanthos, "Ionic liquids as additives for polylactic acid", *Proc. 66th Annual Technical Conference Society of Plastics and Engineers, SPE*, 54, pp. 1687-1691, Milwaukee, WI, May (2008).
- K. Park, M. Xanthos, "Ionic liquids as additives for thermoplastics", *Proc. 65th Annual Technical Conference Society of Plastics and Engineers, SPE*, 53, pp. 2659-2662, Cincinnati, OH, May (2007).
- K. Park, M. Xanthos, "Preparation and Characterization of Polymeric Capsules Containing Functional Additives", *Proc. 64th Annual Technical Conference*

Society of Plastics and Engineers, SPE, 52, pp. 1515-1519, Charlotte, N.C, May (2006).

W. Feng, K. Park, Y. He, J. L. Zunino and M. Xanthos, “Environmentally Friendly Methods for Polymeric Paint Removal”, *Proc. Polymer Processing Society, PPS-21, N. American Meeting, Paper SL 14.1, Leipzig, Germany, June (2005).*

Posters

K. Park, M. Xanthos, “Modification of Polylactic acid with Ionic Liquids”, *NJIT Provost’s Student Research Day, April 2008*

K. Park, M. Xanthos, “Modification of Polylactic acid with Ionic Liquids”, *Green Polymer Symposium (ACS), Piscataway, NJ, November 2007.*

K. Park, M. Xanthos, “Preparation and application of microcapsules for depainting”, *NJIT Provost’s Student Research Day, April 2007.*

Dedicated to my mom, dad, wife, and BOSS (dog)

ACKNOWLEDGEMENTS

I would sincerely like to thank my advisors Dr. Marino Xanthos for his guidance and patience throughout this study. I could not have picked a better person to have worked in this area of study. After 4 years of spending time with him, he is more than an advisor to me. I also wish to thank Dr. Marios Avgousti, Dr. Reginald Farrow, Dr. Kun Sup Hyun, Dr. Somenath Mitra, Dr. Kwabena A. Narh, and Dr. Sergiu Gorun for their willingness to be on my committee.

Especially, Dr. Kun Sup Hyun who connected me with my advisor and provided constant support during my study through his knowledge and connections based on his work experiences during his whole life. I am indebted to my wife Soo Hyun, whose unconditional love, encouragement, and support during trying times I could not have done without. While the family pet cannot exactly provide anything resembling encouragement and support, he did provide plenty of unconditional love, and for that I wish to acknowledge the contributions of our dog, Boss.

I would like to thank my office mates Dr. Georgia Chouzouri, Mr. Jin Uk Ha, Ms. Kimberly Griswold and my friend Dr. Eun Kyu Lee for their help. I am very glad to have had the opportunity to work with each one of them, and I truly enjoyed their company in the office and school.

I would also like to acknowledge some of the people working at PPI whom helped with my experiments for this work. In no particular order, these are Dr. Victor Tan, Dr. Chen Wan, Dr. Byung Joon Jung, Dr. Kun Sup Hyun, Dr. David B. Todd, Mr. Dale Conti, and Mr. Michael Zawisa, who spent many hours of his own time helping me with

experiments.

I would like to acknowledge the assistance of Professor V. Flaris of CUNY with the contact angle measurements, also the assistance of Mr. Brian Gibson of Honeywell with the coefficient of friction measurement.

Financial support for this study was provided by the “Smart Coatings”, Active Coatings, and ACTOR research programs of Picatinny Arsenal at NJIT and also by the Materials Science and Engineering Program at NJIT.

TABLE OF CONTENTS

Chapter	Page
1 INTRODUCTION	1
1.1 Polylactic Acid (PLA)	1
1.1.1 General	1
1.1.2 Properties	3
1.2 Ionic Liquids (IL)	6
1.2.1 General	6
1.2.2 Characteristic Properties	7
2 BACKGROUND	10
2.1 Physical Chemistry of Ionic Liquids	10
2.1.1 Polarity of Ionic Liquids	10
2.1.2 Thermal Stability of Ionic Liquids in Polymer Systems	14
2.2 Ionic Liquids in Polymer Systems	19
2.2.1 Use of Ionic Liquids as Lubricants	19
2.2.2 Plasticization of Polymers with Ionic Liquids	22
2.2.3 Ionic Liquids and Nanoclays	25
2.3 Degradation Mechanisms of Polylactic Acid	27
2.3.1 Mechanisms of Thermal Degradation	27
2.3.2 Mechanisms of Hydrolytic Degradation	31
2.4 Objectives	37

TABLE OF CONTENTS
(Continued)

Chapter	Page
3 EXPERIMENTAL	38
3.1 Materials	38
3.1.1 Polylactic Acid	38
3.1.2 Ionic Liquids	38
3.1.3 Other Chemicals	39
3.1.4 Nanoclays	39
3.1.5 Degradation Media	41
3.2 Sample Preparation	41
3.2.1 Melt Compounding	41
3.2.2 Solvent Casting	42
3.2.3 Preparation of Ionic Liquid Modified Nanoclay	43
3.3 Testing and Characterization	43
3.3.1 Thermal Properties	43
3.3.2 Rheological Characterization	44
3.3.3 Isothermal Degradation	47
3.3.4 Hydrolytic Degradation	47
3.3.5 Soil Degradation Experiments	48
3.3.6 Gel Permeation Chromatography	48
3.3.7 pH and Acid Number	49

TABLE OF CONTENTS
(Continued)

Chapter	Page
3.3.8 Physical and Mechanical Properties.....	49
3.3.9 Surface Structure, Morphology and Crystallinity	52
4 RESULTS AND DISCUSSION	53
4.1 Miscibility of ILs and PLA	53
4.1.1 Predicted Miscibility of IL-4 and PLA	54
4.1.2 Predicted Miscibility of IL-5 and PLA	55
4.1.3 Visual Observation	56
4.1.4 SEM/EDX	56
4.1.5 Phase Separation of ILs in PLA	60
4.1.6 Glass Transition Temperature	62
4.2 Thermal Stability of ILs/PLA by TGA	65
4.2.1 Activation Energy by TGA	67
4.3 Flow Characteristics of ILs/PLA	68
4.3.1 Capillary Rheometer	68
4.3.2 Helical Barrel Rheometer	70
4.3.3 Torque Curves during Melt Mixing	71
4.4 Isothermal Thermal Degradation of PLA and PLA/ILs	72
4.4.1 Weight Changes as a Function of Time	72
4.4.2 Molecular Weight Changes as a Function of Time	74
4.4.3 Thermal Degradation and Modeling	75

TABLE OF CONTENTS
(Continued)

Chapter	Page
4.5 Hydrolytic Degradation of PLA and PLA/ILs	77
4.5.1 Visual Observation	77
4.5.2 Molecular Weight Changes as a Function of Time	79
4.5.3 Scanning Electron Microscopy	81
4.5.4 Acid Numbers and pH Changes as a Function of Time	83
4.6 Soil Degradation Characteristics of PLA and PLA/ILs	85
4.6.1 Visual Observation	85
4.6.2 Change of Crystallinity after Soil Degradation	87
4.7 Physical/Mechanical Properties	88
4.7.1 Coefficient of Friction of PLA and PLA/ILs	88
4.7.2 Contact Angle Measurements of PLA and PLA/ILs	90
4.7.3 Flexural Properties of PLA and PLA/ILs blends	90
5 CONCLUSIONS AND RECOMMENDATIONS	92
APPENDIX A CALCULATION OF SOLUBILITY PARAMETERS USING FEDORS METHOD	94
APPENDIX B SEM OF PLA AND PLA/ILS BLENDS AFTER HYDROLYTIC DEGRADATION	96
REFERENCES	104

LIST OF TABLES

Table		Page
1.1	Comparison of Mechanical Properties of PLA with Other Thermoplastics	4
2.1	Abbreviations and Chemical Names of Plasticizers and ILs	17
2.2	Tg Values and Dry Friction and Wear Coefficients for PS against AISI 52100 Steel as a Function of IL1 Content	20
2.3	Friction Coefficients for Several Frictional Pairs Lubricated with Various Lubricants	21
2.4	Long-term Thermal Stability of Bulk PMMA and Samples Plasticized with 1-butyl-3-methylimidazolium Hexafluorophosphate [bmim][PF ₆ ⁺] and Di(2-ethylhexyl) phthalate (DOP) at 170 °C for 21 Days	24
3.1	Technical Data of Cloisite [®] Na ⁺ (MMT-Na ⁺)	40
4.1	Group Contributions to <i>F</i>	54
4.2	EDX Elemental Analysis of PLA/ 5wt% IL-4 Surface	58
4.3	EDX Elemental Analysis of PLA/ 5 wt% IL-5 Surface	60
4.4	Tg Comparison of PLA vs. PLA Containing Different wt% of IL-4 and IL-5 .	63
4.5	MW Changes of Melt Processed PLA, PLA/5 wt% IL-4 and PLA/5 wt% L-5 Before and After Isothermal Heating at 160°C; M _p , M _n , and M _w are Peak MW, Number average MW, and Weight average MW Respectively	74
4.6	Peak MW, M _p , Changes of PLA, PLA/5 wt% IL-4 and PLA/5 wt% IL-5 before and after Hydrolytic Degradation (144 hrs)	79
4.7	Peak MW, M _p Changes of PLA, PLA/MMT-0, PLA/MMT-4, PLA/IL-4, and PLA/decanoic Acid Prepared by the Solvent Casting Method after 144 hrs Hydrolytic Degradation	80
4.8	Acid Numbers before and after Hydrolytic Degradation	85
4.9	Contact Angle and Coefficient of Friction Results	89

LIST OF FIGURES

Figures Page		
1.1	Polymerization routes to L- polylactic acid (PLLA)	2
1.2	Structures and melting points of lactide isomers	4
1.3	Structures of ionic liquids. X ⁻ represents any of a large number of anions, including nitrate [NO ₃], acetate [CH ₃ COO], trifluoroacetate [CF ₃ COO], tetrafluoroborate [BF ₄], triflate [CF ₃ SO ₃], hexafluorophosphate [PF ₆], and bis(trifluoromethylsulfonyl) imide [(CF ₃ SO ₂) ₂ N]	7
2.1	Structures of fluorescent probes and ionic liquids	11
2.2	Solute-solvent radial distribution functions showing hydrogen bonding between methanol (a) and water (b) and the charged regions of the ionic liquid	12
2.3	Solute-solvent radial distribution functions showing the position of the solutes relative to the different domains of the ionic liquid. The inserts indicate schematically the preference of each solute for the nonpolar (green) or charged (red) domains	12
2.4	Solubility of 1-octene in four different tri- <i>n</i> -alkylmethylammonium tosylate melts at 80° C	13
2.5	(a) Onset temperature for decomposition of different plasticizers when subjected to a temperature ramp of 10 °C/min, (b) percentage of weight remaining for different plasticizers when subjected to an isothermal condition at 200 °C for 30 min. Plasticizers, as denoted by different numbers, are as follows: 1. DEHP, 2. DIDP, 3. TOTM, 4. [tbPh ⁺][doss ⁻], 5. [hmim ⁺][doss ⁻], 6. [tbam ⁺][doss ⁻], 7. [thtdPh ⁺][deca ⁻], 8. [hmim ⁺][BF ₄ ⁻], 9. [thtdPh ⁺][Cl ⁻], 10. [bmim ⁺][PF ₆ ⁻], 11. [thtdPh ⁺][Tf ₂ N ⁻], 12. [hmim ⁺][PF ₆ ⁻], 13. [tbtdPh ⁺][mes ⁻], 14. [tbtdPh ⁺][dbs ⁻], 15. [thtdPh ⁺][mes ⁻], and 16. [thtdPh ⁺][dbs ⁻]	16
2.6	Structures of conventional plasticizers and selected ILs	18
2.7	Molecular structures of the ionic liquids L106 and L206 and traditional lubricants X-1P and PFPE	21

LIST OF FIGURES
(Continued)

Chapter	Page
2.8 Short-term thermal stability of bulk PMMA and samples containing 20 wt% 1-butyl-3-methylimidazolium hexafluorophosphate [bmim][PF ₆ ⁺], 20 wt% 1-hexyl-3-methylimidazolium hexafluorophosphate [hmim][PF ₆ ⁺], and 20 wt% di(2-ethylhexyl) phthalate (DOP) at 250 °C	23
2.9 Structure of 2:1 phyllosilicate clay	26
2.10 Mechanism of thermal degradation of PLLA	28
3.1 Structures of ILs: a) IL-4, b) IL-5	39
3.2 (a) Schematic of molecular structure of MMT-Na ⁺ , (b) Schematic side view of MMT-Na ⁺ between layers	40
3.3 Helical Barrel Rheometer	45
3.4 Configuration of friction tester	51
4.1 Photographs of PLA film samples containing 5 wt% of IL-4 and IL-5	56
4.2 SEM micrographs of cross-sections of (a) PLA, (b) PLA/ 5wt% IL-4, and (c) PLA/ 5wt% IL-5 produced by melt processing	57
4.3 (a) SEM micrograph of the surface of PLA/ 5 wt% IL-4 and (b) EDX elemental mapping of phosphorous	58
4.4 (a) SEM micrograph of the surface of PLA/ 5 wt% IL-5, (b) EDX elemental mapping of phosphorous, and (c) EDX elemental mapping of fluorine	59
4.5 SEM micrograph on fractured surface of PLA/ 5 wt% IL-4 one year after melt processing	61
4.6 SEM micrograph on fractured surface of PLA/ 5 wt% IL-5 one year after melt processing	61
4.7 DSC comparison of PLA vs. PLA containing different wt% of IL-4 and IL-5	63
4.8 TGA Comparison of IL-4, IL-5 and processed PLA	66

LIST OF FIGURES
(Continued)

Chapter	Page
4.9 TGA comparison of processed PLA with PLA containing 5wt% of IL-4 and IL-5	66
4.10 Friedman plots of $\ln(d\alpha/dt)$ or $\ln(1-\alpha)$ vs. $1/T$ for the direct calculation of E_a of thermal degradation at a heating rate of 20 °C /min under nitrogen	67
4.11 Apparent viscosity vs. apparent shear rate curves of PLA and PLA/IL-5 blends	69
4.12 Shear viscosity comparison of PLA, PLA/5 wt% IL-4 and PLA/5 wt% IL-5	70
4.13 Torque curves of PLA and PLA/IL blends during batch mixing	72
4.14 Weight loss of PLA, IL-4, IL-5, PLA/5wt% IL-4, and PLA/5 wt% IL-5 as a function of thermal degradation time at 160 °C in air	73
4.15 Thermal degradation data up to 19 hours for PLA, PLA/IL-4, and PLA/IL-5 based on $1/DP$ and Equation 4.8	77
4.16 (a) PLA, PLA/5 wt% IL-5 and PLA/5 wt% IL-4 before hydrolytic degradation (b) PLA, PLA/5 wt% IL-5 and PLA/5 wt% IL-4 after 144 hours of hydrolytic degradation	78
4.17 (a) SEM micrograph of PLA before immersion in PBS. (b) SEM micrograph of PLA after 144 hours of immersion in PBS. (c) SEM micrograph of PLA/IL-4 before immersion in PBS. (d) SEM micrograph of PLA/IL-4 after 144 hours of immersion in PBS. (e) SEM micrograph of PLA/IL-5 before immersion in PBS. (f) SEM micrograph of PLA/IL-5 after 144 hours of immersion in PBS	82
4.18 pH changes of PBS during hydrolytic degradation	84
4.19 Photographs of neat PLA and PLA/ILs blends before and after burial in soil/sterilized soil for 4 weeks. (a) PLA before burial, (b) PLA after burial in soil, (c) PLA after the burial in sterilized soil, (d) PLA/IL-4 before burial, (e) PLA/IL-4 after burial in soil, (f) PLA/IL-4 after burial in sterilized soil, (g) PLA/IL-5 before burial in soil, (h) PLA/IL-5 after burial in soil, (i) PLA/IL-5 after burial in sterilized soil	86

LIST OF FIGURES
(Continued)

Chapter	Page
4.20 XRD spectra of PLA before and after 4weeks of soil degradation	88
4.21 Flexural modulus and flexural strength of PLA, PLA/ 5 wt% IL-4, and PLA/ 5 wt% IL-5 by three point bending test. *Error bars indicate mean values \pm one standard deviation	91
B.1 SEM micrographs of after 144 hours of immersion in PBS	96
B.2 SEM micrograph of PLA/IL-4 after 144 hours of immersion in PBS.....	97
B.3 SEM micrograph of PLA/IL-5 after 144 hours of immersion in PBS.....	98

LIST OF SYMBOLS & ACRONYMS

a	Thickness of beam
C	Constant ($^{\circ}\text{K mol g}^{-1}$)
b	Width of beam
d	Depth of test beam
D	Diffusion coefficient
D_r	Rotor diameter (Helical Barrel Rheometer)
E	Flexural modulus
E_a	Activation energy
E_{coh}	Cohesive energy
E_h	Hydrogen bond energy
f	Load at a given point on the curve
F	Group molar attraction constant
H	Inside capillary tube diameter
h	Channel depth (Helical Barrel Rheometer)
k	Degradation rate constant
l	Span length between two support points
L	Capillary tube length
m	Initial slope of the load vs. deflection curve
M_n	Number average molecular weight
M_p	Peak molecular weight
M_w	Weight average molecular weight
n	Decomposition reaction order

N	Rotor speed (Helical Barrel Rheometer)
P	Pressure
Q	Volumetric flow rate
R	Gas constant
R_c	Inside capillary tube radius
S	Stress in the outer fibers at mid-span
t	Time
T, K	Absolute temperature
T_g	Glass transition temperature
v	Average fluid velocity
V	Molar volume
W_i	Weight of initial sample
W_t	Weight of sample at time t
w	Thickness
Z	Frequency factor
α	Weight loss of polymer, conversion
$\dot{\gamma}$	Shear rate
Δ	Difference or change
δ	Solubility parameter
δ_d	Solubility parameter of dispersion forces
δ_h	Solubility parameter of hydrogen bonding forces
δ_p	Solubility parameter of polar forces

η	Viscosity
λ	Wavelength
ρ	Density
τ	Shear stress
[bmim+][PF6-]	1-Butyl-3-methylimidazolium hexafluorophosphate
[hmim+][BF4-]	1-Hexyl-3-methylimidazolium tetrafluoroborate
[hmim+][doss-]	1-Hexyl-3-methylimidazolium dioctylsulfosuccinate
[hmim+][PF6-]	1-Hexyl-3-methylimidazolium hexafluorophosphate
[tbam+][doss-]	Tetrabutyl ammonium dioctylsulfosuccinate
[tbPh+][doss-]	Tetrabutyl phosphonium dioctylsulfosuccinate
[tbtdPh+][dbs-]	Tributyl (tetradecyl) phosphonium dodecylbenzenesulfonate
[tbtdPh+][mes-]	Tributyl (tetradecyl) phosphonium methanesulfonate
[THTDP][BF ₄] (IL-5)	Trihexyltetradecylphosphonium tetrafluoroborate
[THTDP][DE] (IL-4)	Trihexyltetradecylphosphonium decanoate
[thtdPh+][Cl-]	Trihexyl (tetradecyl) phosphonium chloride
[thtdPh+][dbs-]	Trihexyl (tetradecyl) phosphonium dodecylbenzenesulfonate
[thtdPh+][deca-]	Trihexyl (tetradecyl) phosphonium decanoate
[thtdPh+][mes-]	Trihexyl (tetradecyl) phosphonium methanesulfonate
[thtdPh+][Tf ₂ N-]	Trihexyl (tetradecyl) phosphonium bis(trifluoromethane) sulfonylimide

ASTM	American society for testing and materials
CEC	Cationic exchange capacity
COF	Coefficient of friction
DECA	Decanoic Acid
DEHP	Di(2-ethylhexyl) phthalate
DIDP	Diisodecyl phthalate
DP	Degree of polymerization
DSC	Differential scanning calorimetry
DTA-MMT	Dodecyltrimethyl ammonium bromide-montmorillonite
EDX	Energy dispersive x-ray analysis
GPC	Gel permeation chromatography
HBR	Helical barrel rheometer
HT	Hydrotalcite
IL	Ionic liquid
LLDPE	Linear Low Density Polyethylene
MMT	Montmorillonite
MMT-4	Montmorillonite modified with IL-4
MMT-Na ⁺	Sodium montmorillonite
MSDS	Materials safety data sheet
MW	Molecular weight
PA	Polyamide
PBMA	Poly n-butyl methacrylate

PBS	Phosphate buffer saline solution
PDLLA	Poly-DL-lactide
PEG	Poly(ethylene glycol)
PET	Polyethylene terephthalate
PFPE	Perfluoropolyether
PLA	Poly(lactic acid)
PLLA	Poly-L-lactide
PMMA	Polymethyl methacrylate
PP	Polypropylene
PS	Polystyrene
PVC	Polyvinylchloride
SEM	Scanning electron microscopy
TEM	Transmission electron microscopy
TGA	Thermogravimetric analysis
THF	Tetrahydrofuran
TOTM	Trioctyl trimellitate
UV	Ultra violet
XRD	X-ray diffraction

CHAPTER 1

INTRODUCTION

1.1 Polylactic Acid

1.1.1 General

Poly(lactic acid), PLA, is a rigid biodegradable linear aliphatic thermoplastic polyester, produced from renewable resources. PLA can be semicrystalline or totally amorphous, depending on the structure of the polymer backbone. L-lactic acid (2-hydroxy propionic acid) is the natural and most common form of the acid, but D-lactic acid can also be produced by racemization.

Due to its capability to be crystallized, impact modified, filled, copolymerized, and processed in most polymer processing equipment, it may become the polymer with the broadest range of applications [1]. PLA also has excellent organoleptic characteristics and is excellent for food packaging, biomedical and pharmaceutical controlled release applications.

PLA is not a new polymer introduced to the world. Carothers[2] investigated the production of PLA from the cyclic dimer (lactide) of lactic acid as early as 1932. Even before that time, low molecular weight dimers and oligomers were detected when water was removed from an aqueous solution of lactic acid as early as 1845 by Pelouze and later by Nef as described in ref. 1. The announcement of the formation of a new company, Cargill Dow LLC, in 1997 brought two large companies together to focus on the production and marketing of PLA with the intention of significantly reducing the cost of production and making PLA a large-volume plastic [1]. Concerning the green chemistry

and the environment, PLA has achieved spot lights in the marketplace. Lactic acid, the starting material for PLA, is made by a fermentation process using 100% annually renewable resources such as corn starch or sugar cane. PLA rapidly degrades in the environment and the by-products are of very low toxicity, eventually being converted to carbon dioxide and water which can be used for photosynthesis of natural resources.

PLA can be prepared by both direct condensation of lactic acid and by the ring-opening polymerization of the cyclic lactide dimer as shown in Figure 1.1. Most research work has been carried out on the ring-opening polymerization of lactide due to the difficulties of removing water in the late stages of polymerization of the lactic acid, which generally limit the ultimate molecular weight. In ring-opening polymerization, bacterial fermentation is used to produce lactic acid, which is oligomerized and then catalytically dimerized to make the monomer for the polymerization, which uses catalysts such as stannous octoate or stannous chloride.

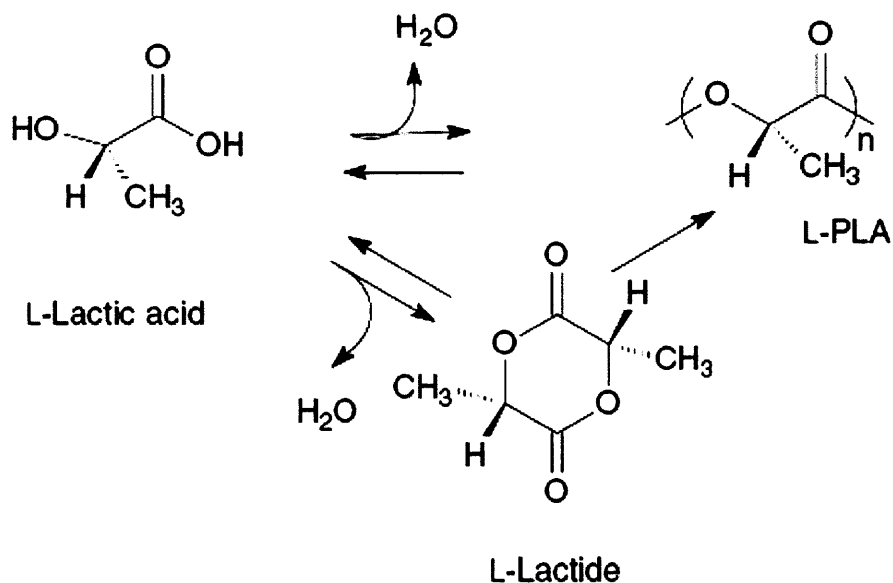


Figure 1.1 Polymerization routes to L- polylactic acid (PLLA) [1].

PLA can be processed like most thermoplastics into fibers, films or molded objects. PLA can also be employed in the preparation of bioplastics useful for producing loose-fill packaging, compost bags, food packaging as well as devices for a number of biomedical applications. Degradation times, which to a large extent involve hydrolytic degradation, vary depending on the medium and temperature. Biodegradation in soil for PLA takes typically longer (1 year) than other biodegradable polyesters such as poly(ϵ -caprolactone) and poly(butylene succinate) [3] whereas degradation in the human body may take as long as approximately 2 years [4].

1.1.2 Properties

PLA has a number of interesting properties including biodegradability and processability. Mechanical properties are satisfactory although, low elongation at break and high modulus have limited its applications in the packaging industry. Properties of PLA such as glass transition temperature (T_g) melting temperature (T_m), tensile strength and crystallinity are determined by the polymer architecture, (i.e. different proportions of L, D or meso-lactide shown in Figure 1.2) and molecular weight. The proportion of D and L lactides determines polymer morphology; PLA can be produced as totally amorphous or up to 40% crystalline. Due to the chiral nature of lactic acid several distinct forms of polylactide may exist. Poly-L-lactide (**PLLA**) is the product resulting from polymerization of lactic acid in the L form. PLLA has a crystallinity around 37%, a glass transition temperature between 50-80° C and a melting temperature between 173-178° C. The polymerization of a mixture of both L and D forms of lactic acid leads to the synthesis of poly-DL-lactide (**PDLLA**) which is amorphous (Figure 1.2).

The mechanical properties of PLA are compared to those of other plastics in Table 1.1 [5]. PLA shows similar mechanical properties to polystyrene (PS) and has higher yield strength than polyvinylchloride (PVC) and polypropylene (PP).

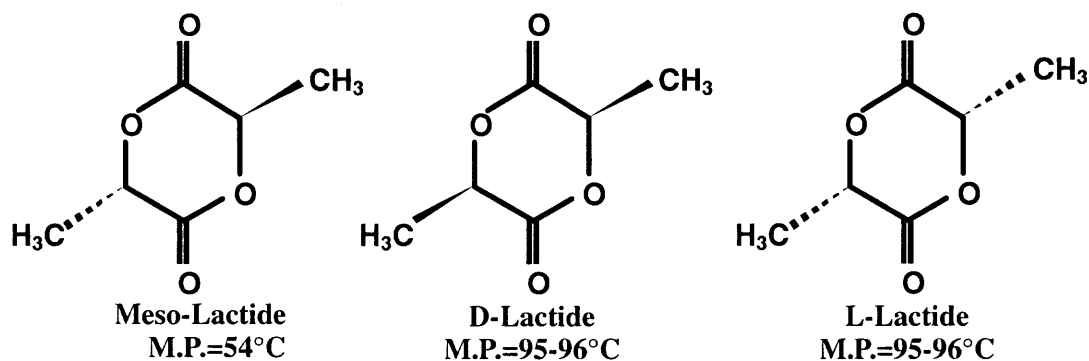


Figure 1.2 Structures and melting points of lactide isomers. [1]

Table 1.1 Comparison of Mechanical Properties of PLA with Other Thermoplastics [5]

Properties	PLA	PS	PVC	PP
Tensile Yield Strength, MPa	49	49	35	35
Elongation at break, %	2.5	2.5	3	10
Tensile Modulus, GPa	3.2	3.4	2.6	1.4
Flexural Strength, MPa	70	80	90	49

Bigg [6] reported on the effect of temperature on the degradation of PLA. PLA quickly loses its thermal stability when heated above its melting point. A significant level of molecular degradation occurred when PLA was held at 160 °C for a sustained period of time. Migliaresi et al. [7] have shown that thermal degradation was due to chain splitting and not hydrolysis. They observed molecular weight reductions as high as 50% and concluded that even larger molecular weight reduction was unavoidable.

The degradation process was complicated by more than just molecular weight reduction. Another process-limiting phenomenon associated with the upper limit of thermal processing was the development of color in the natural polymer when processed above 200 °C. When the residual monomer level of the polymer dropped during extrusion at 190 °C, color developed in the water white polymer [8].

1.2 Ionic Liquids

1.2.1 General

In general, Ionic Liquids (ILs) are liquid salts that consist of combinations of organic/organic or organic/inorganic cation/anions. While molten salts refer to high melting point, highly viscous substances, ILs are already liquid at low temperatures below 100 °C and have low viscosity. The salts that are liquid at room temperature are called room-temperature ILs. Component ions in ILs strongly interact with each other through coulombic forces, whereas normal liquids are bonded through Van der Waals forces and/or hydrogen bonding [9].

In addition to having a wide liquidus range, ionic liquids have the ability to dissolve both polar and non-polar compounds and, perhaps most importantly, they do not

evaporate due to their extremely low vapor pressure and, thus, cannot lead to fugitive emissions. The chemical and physical properties of ILs can, to some extent, be tailored by proper selection of the type of cation and anion that compose the IL, as well as any substituent groups [10].

Because of their insignificant vapor pressures, low melting points, good solvent characteristics for organic, inorganic and polymeric materials, adjustable polarity, selective catalytic effects, chemical and thermal stability, non-flammability and high ionic conductivity, ionic liquids have generated significant interest for a wide range of industrial applications [11]. Examples include organic synthesis where they are employed as green solvents replacing volatile organic compounds (VOC) or substituting for various organic solvents, catalysis, polymerization, bioprocessing operations, liquid-liquid extraction, gas separation, electrochemical processes, and heat transfer fluids. ILs have also the attractive benefit of easy recovery (recycling) since organic molecules can be easily separated by direct distillation without loss of the ionic liquids [12].

1.2.2 Characteristic Properties

The properties of ILs can be varied by the selection of proper cations and anions.

Examples of five different well-known types of organic cations which comprise typical ILs are shown in Figure 1.3. The cation substituent groups (the “R” groups) are typically alkyl chains but can contain any of a variety of other functional groups as well (e.g., fluoroalkyl, alkenyl, methoxy, etc.).

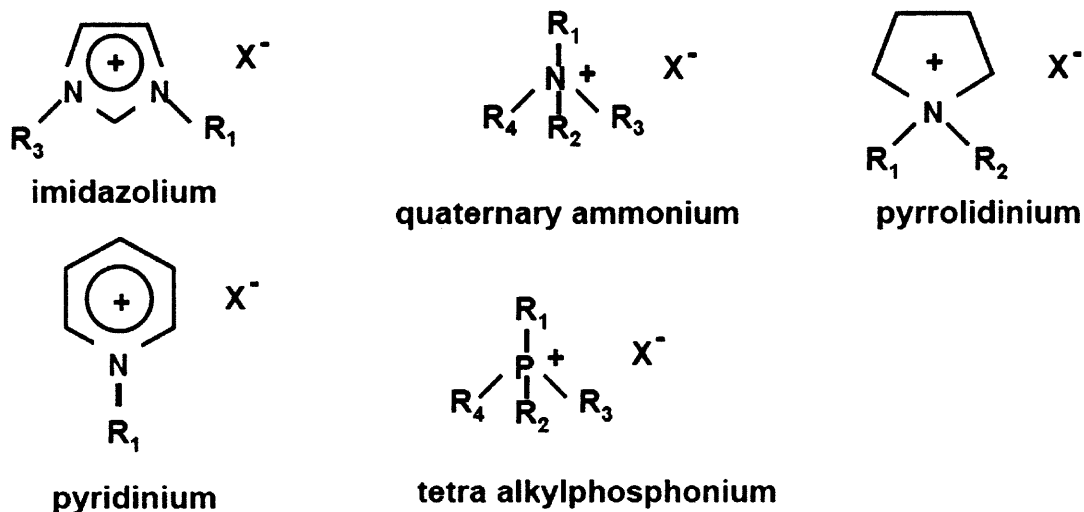


Figure 1.3 Structures of ionic liquids. X^- represents any of a large number of anions, including nitrate $[NO_3]$, acetate $[CH_3COO]$, trifluoroacetate $[CF_3COO]$, tetrafluoroborate $[BF_4]$, triflate $[CF_3SO_3]$, hexafluorophosphate $[PF_6]$, and bis(trifluoromethylsulfonyl) imide $[(CF_3SO_2)_2N]$.

As mentioned above, a key feature of ILs is that their physical properties can be tailored by proper selection of cation, anion and substituents. For example, the water solubility of an alkylimidazolium based IL can be controlled by the nature of the alkyl chain. Increasing the length of the alkyl chain tends to decrease water solubility by increasing the hydrophobicity of the cation. In addition, the water solubility of the IL can be changed dramatically by the choice of anion. At ambient conditions, water is completely miscible with 1-n-butyl-3-methylimidazolium [bmim] tetrafluoroborate $[BF_4]$, but is almost completely immiscible with [bmim] hexafluorophosphate $[PF_6]$. A solid understanding of how the molecular structure of an IL affects its thermophysical properties, transport properties, and phase equilibrium behavior is necessary to facilitate the design of ILs that can be used for a specific industrial task, will not pose a serious

health hazard if released in a chemical spill, and can be produced in large quantities at a low cost.

Melting points of ILs can be affected by either different cations or anions due to their symmetry [13], weak intermolecular interaction, good distribution charge in the cation [14] and size of anion.

Thermal stability is another significant advantage of ILs which allows their use in a wide temperature range. It is not unusual for organic salts to decompose upon heating but the ILs resist weight loss at higher temperatures [15]. Thermal stabilities of ILs depend on their structure, both cations and anions. The relative anion stabilities were observed as $\text{Tf}_2\text{N}^- > \text{PF}_6^- > \text{BF}_4^- > \text{Cl}^-$. Most ILs are liquids over a wide temperature range (-104 to 350 °C) and begin to decompose around 350 °C [13]. In the case of cations, for applications requiring temperatures in excess of 100 °C, phosphonium salts provide superior thermal stability over analogous ammonium salts [16].

The viscosity of ILs is determined by their tendency to form hydrogen bonding and by the strength of their Van der Waals interactions. It is shown that stronger hydrogen bonding and Van der Waals interactions result in a higher viscosity of the IL. Comparison of the viscosities of $[\text{BMIM}]^+\text{CF}_3\text{SO}_3^-$ with $[\text{BMIM}]^+(\text{CF}_3\text{SO}_2)_2\text{N}^-$ reveals a lower viscosity for $[\text{BMIM}]^+\text{CF}_3\text{SO}_3^-$ despite stronger Van der Waals interactions for ILs with the $(\text{CF}_3\text{SO}_2)_2\text{N}^-$ ion. In this case, the almost complete suppression of hydrogen bonding overcompensates for the expected increase in viscosity [18]. In some cases, the viscosity of IL can be lowered drastically by slightly increasing the temperature.

Besides lower vapor pressure, density is another characteristic that distinguishes ILs. Generally, the density of ILs decreases as the bulkiness of the organic cation

increases. Slight structural changes of the cation allow a fine adjustment of the density. Density measurements of ILs with triflate or trifluoroacetate ions confirmed the more general result that a certain density range is established by the choice of anion [18].

CHAPTER 2

BACKGROUND

2.1 Physical Chemistry of Ionic Liquids

2.1.1 Polarity of Ionic Liquids

In order to use ILs in polymer systems, there is a need to understand of how the structure of the IL affects its physical properties, solvent strength as well as its polarity. Since polarity and polarizability are the simplest indicators of solvent strength, organic solvents are frequently classified based on their ability to dissolve and stabilize dipolar or charged species. The following are some examples of recent studies.

According to Sudhir et al. [19], fluorescent probes that are commonly used to determine the solvent strength of organic solvents can also be used to determine the solvent strength of ILs]. For example, Bonhote et al. found that the solvent strength of 1-ethyl-3-methylimidazolium bis-(triflyl)amide, using pyrene and pyrenecarbaldehyde probes, was similar to ethanol and hexane respectively, depending on the choice of the fluorescent probe [18]. Figure 2.1 shows the structures of several ILs, (I to IV) and two fluorescent probes (V, VI) used to estimate their polarities.

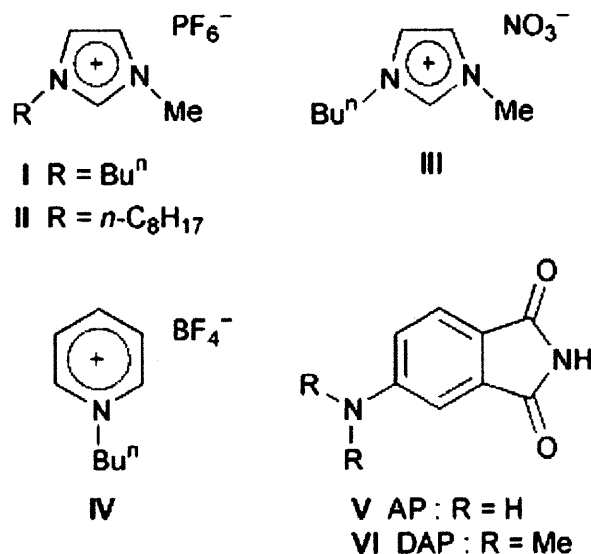


Figure 2.1 Structures of fluorescent probes and ionic liquids. [19]

The results show that both I and III ILs have more polar characteristic environments than II and IV ILs. By comparing IL- I with IL- II, the fact that IL- II has an octyl group which is non-polar (hydrophobic) leads to the conclusion that IL-I is more polar than IL-II which has a shorter butyl substituent. In the case of IL- III and IL- IV comparison, polarity difference maybe due to the presence of different cations (imidazolium vs pyridinium).

Canongia Lopes et al. [20] reported from their molecular simulation study that interaction of water with the PF₆ anions in 1-butyl-3-methylimidazolium hexafluorophosphate [C4mim][PF₆] are dominated by hydrogen bonding. The radial distribution functions between a given solute and IL are shown in Figure 2.2. The H-P bonding between IL and water was picked by the second H-P peak at 4.4 Å, a feature that is obviously absent in methanol. The major difference between water and methanol is the stronger interaction between the acidic hydrogen atom of the cation and the oxygen atom

of water, when compared to that of methanol as shown in Figure 2.3. Since water is smaller than methanol, its oxygen atom can interact more easily with the hydrogen atoms of the cation.

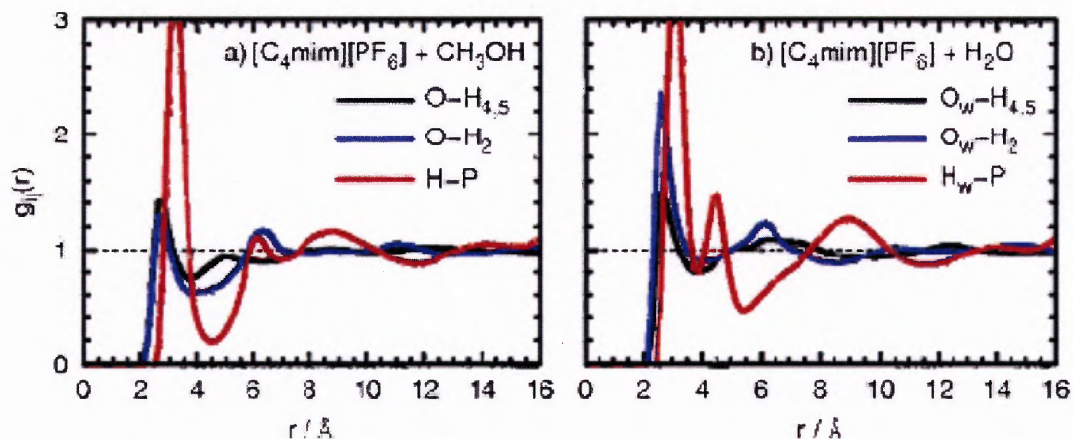


Figure 2.2 Solute-solvent radial distribution functions showing hydrogen bonding between methanol (a) and water (b) and the charged regions of the ionic liquid.

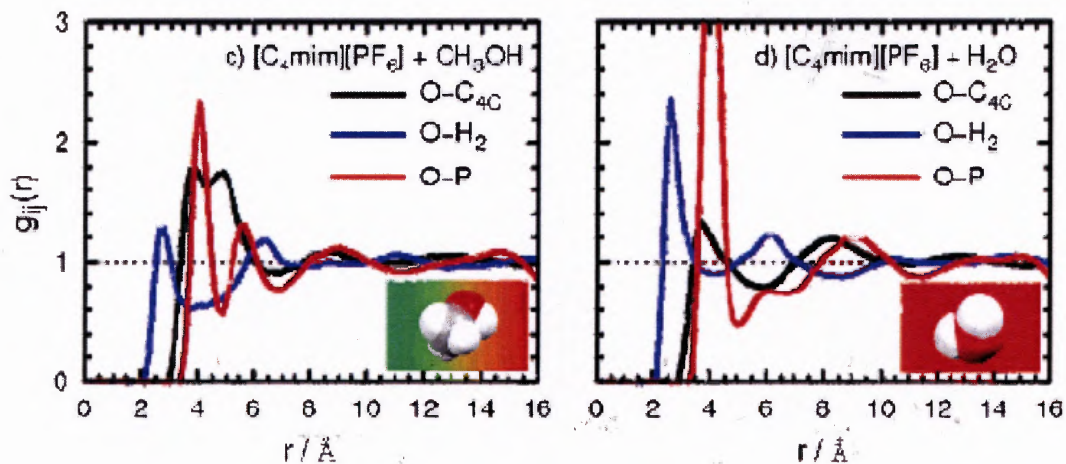


Figure 2.3 Solute-solvent radial distribution functions showing the position of the solutes relative to the different domains of the ionic liquid. The inserts indicate schematically the preference of each solute for the nonpolar (green) or charged (red) domains [20].

The complex microscopic structure of the ionic liquids can be demonstrated by the differences in relative position, orientation, and specific interactions between water or methanol and the different regions of the ionic liquid such as polar imidazolium ring, nonpolar aliphatic chain, and anions (PF_6).

Similar information based on the polarity of ILs, can be used to predict and explain interactions between the relatively polar PLA polymer and ILs in the molten or solid state or water and ILs during hydrolytic degradation.

Wasserscheid and Keim [21] described the tuning of the solubility properties of ionic liquids by the choice of cations and anions depending on their polarities. It is shown in Figure 2.4 that variation of the alkyl group length on the ammonium cation of four ILs having the same tosylate anion significantly affects the solubility of 1-octene. As expected, by increasing the nonpolar character of the cation, the solubility of 1-octene in the melt increases.

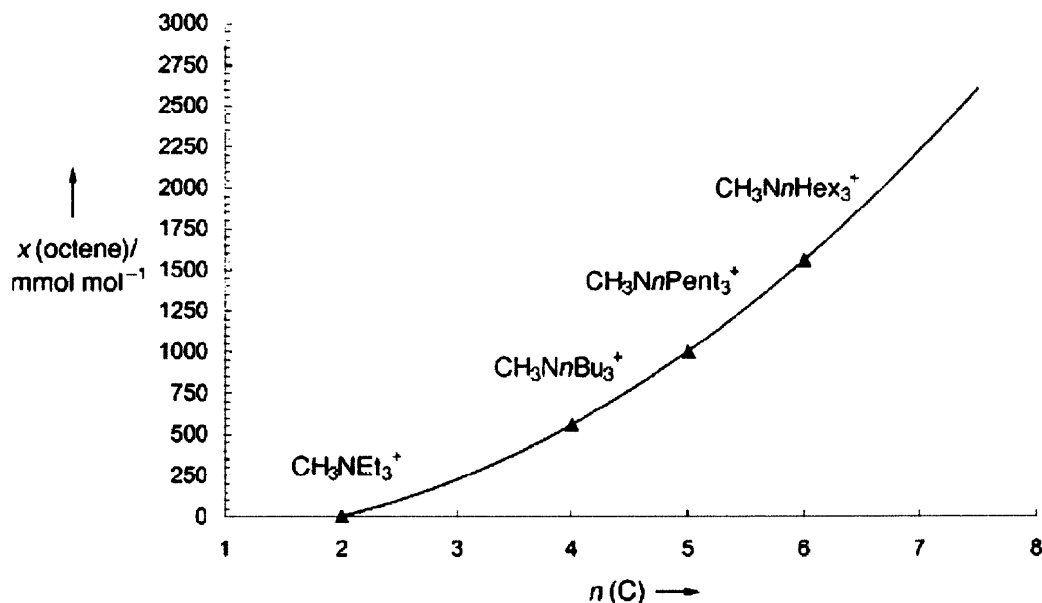


Figure 2.4 Solubility of 1-octene in four different tri-*n*-alkylmethylammonium tosylate melts at 80° C [21].

The influence of anions on the solubility characteristics of ILs was determined by the water solubility of ILs having the same cation but different anions. While $[\text{BMIM}]^+\text{Br}^-$, $[\text{BMIM}]^+\text{CF}_3\text{COO}^-$, and $[\text{BMIM}]^+\text{CF}_3\text{SO}_3^-$ are highly water soluble, ILs with the same cation but with a PF_6^- or $(\text{CF}_3\text{SO}_2)_2\text{N}^-$ anion formed biphasic mixtures with water.

2.1.2 Thermal Stability of Ionic Liquids

ILs are well known for their high thermal stability due to their negligible low vapor pressure. Great attention has been given to quaternary nitrogen based ILs (e.g., ammonium, imidazolium, pyridinium, etc) in recent years. Their thermal stability by TGA has been shown to largely depend on the anion type with BF_4^- providing higher decomposition temperatures. For example, the thermal stability of three pyridinium and imidazolium ILs was ranked as $[\text{Etpy}]^+ [\text{BF}_4]^- > [\text{EMIM}]^+ [\text{Br}]^- > [\text{HXMIM}]^+ 22^-$ [23, 24]. However, specific accounts of ILs containing quaternary phosphonium cations have been less common [25]. Phosphonium based ILs have been shown to have better overall properties than many nitrogen based ILs, especially thermal properties [26, 27]. Although the decomposition temperature of phosphonium ILs on heating varies, depending on the anion, a thermal stability of over 300°C has been observed for many species [28].

Brazel et al. [29] compared the thermal stabilities of various ILs with conventional polyvinylchloride (PVC) plasticizers. Figure 2.5a shows the decomposition temperature for various ILs and traditional plasticizers as observed during a TGA temperature ramp of $10^\circ\text{C}/\text{min}$. It is clear that all three traditional phthalate and mellitate

plasticizers (DEHP, DIDP, TOTM) have lower thermal stability compared to the ILs studied, which were found to be fairly stable up to and above 300 °C. Abbreviations of plasticizers and ILs used in Figure 2.5 are shown in Table 2.1. In an ideal plasticizer, the solvating groups are usually located internally rather than at the ends of the plasticizer molecule [30]. The compatibility is controlled by the solvating groups along with the significant influence of the non-polar groups creating a barrier between polymer chains. The phthalate and trimellitate plasticizers studied, as shown in Figure 2.6, clearly fall into this category as well as the ILs used in their study [29].

Significant differences were observed between the ILs and the conventional plasticizers when those were subjected to an isothermal condition heating at 200° C for 30 min. As shown in Figure 2.5b, all of the ILs displayed good stability, losing 5wt% or less of their initial weight, whereas DIDP and DEHP lost around 20% and 65% weight, respectively. This suggests that among ILs those having a good miscibility with the polymer have a strong potential to be used as a new generation plasticizers since they were shown to have better thermal stability than conventional plasticizers.

Conventional plasticizers of PLA such as tributyl citrate, polyethylene glycol, diethylene glycol successfully lowered the glass transition temperature of PLA. However, all of them decreased the thermal stability of the polymer.

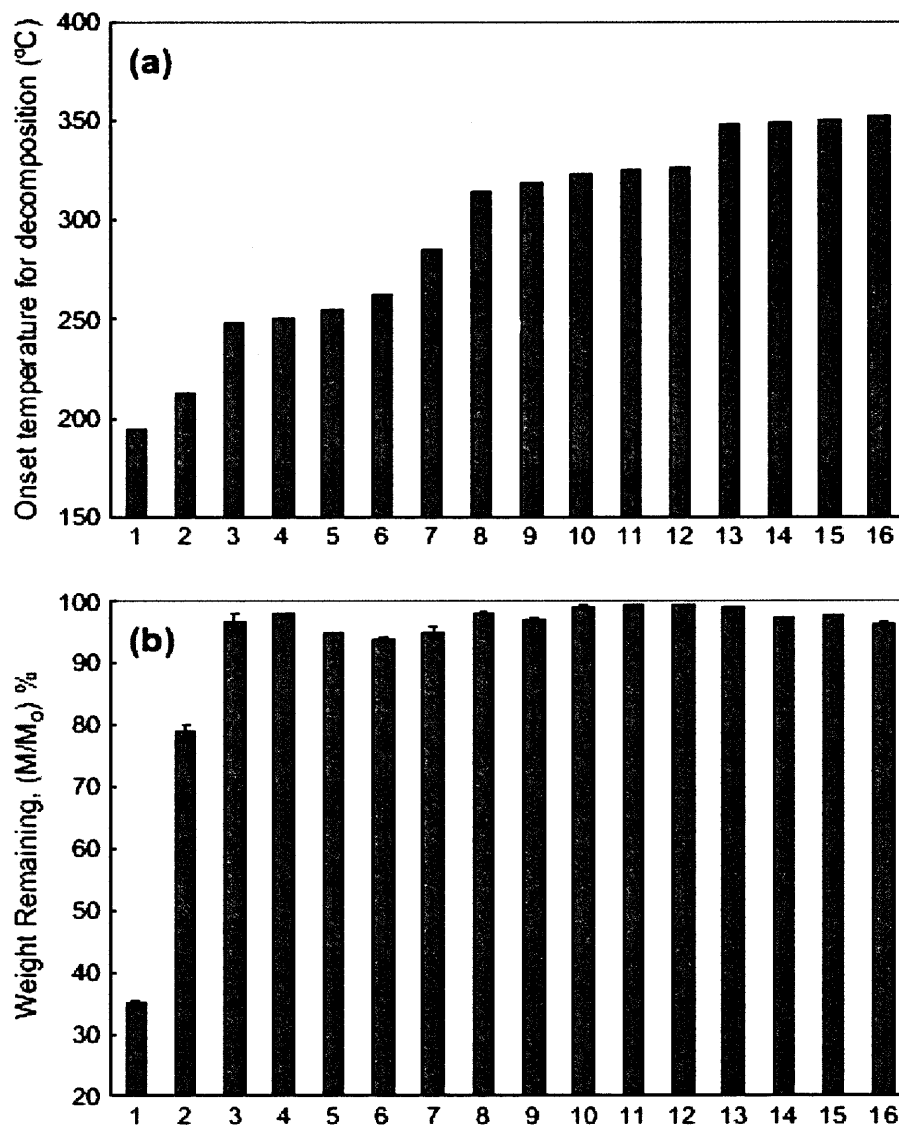


Figure 2.5 (a) Onset temperature for decomposition of different plasticizers when subjected to a temperature ramp of 10 °C/min, (b) percentage of weight remaining for different plasticizers when subjected to an isothermal condition at 200 °C for 30 min. Plasticizers, as denoted by different numbers, are as follows: 1. DEHP, 2. DIDP, 3. TOTM, 4. [tbPh⁺][doss⁻], 5. [hmim⁺][doss⁻], 6. [tbam⁺][doss⁻], 7. [thtdPh⁺][deca⁻], 8. [hmim⁺][BF₄⁻], 9. [thtdPh⁺][Cl⁻], 10. [bmim⁺][PF₆⁻], 11. [thtdPh⁺][Tf₂N⁻], 12. [hmim⁺][PF₆⁻], 13. [tbtdPh⁺][mes⁻], 14. [tbtdPh⁺][dbs⁻], 15. [thtdPh⁺][mes⁻], and 16. [thtdPh⁺][dbs⁻] [29]. For abbreviations see Table 2.1.

Table 2.1 Abbreviations and Chemical Names of Plasticizers and ILs.

Abbreviation	Chemical name
DEHP	Di(2-ethylhexyl) phthalate
DIDP	Diisodecyl phthalate
TOTM	Trioctyl trimellitate
[bmim+][PF6-]	1-Butyl-3-methylimidazolium hexafluorophosphate
[hmim+][doss-]	1-Hexyl-3-methylimidazolium dioctylsulfosuccinate
[hmim+][BF4-]	1-Hexyl-3-methylimidazolium tetrafluoroborate
[hmim+][PF6-]	1-Hexyl-3-methylimidazolium hexafluorophosphate
[tbam+][doss-]	Tetrabutyl ammonium dioctylsulfosuccinate
[tbPh+][doss-]	Tetrabutyl phosphonium dioctylsulfosuccinate
[tbtdPh+][dbs-]	Tributyl (tetradecyl) phosphonium dodecylbenzenesulfonate
[tbtdPh+][mes-]	Tributyl (tetradecyl) phosphonium methanesulfonate
[thtdPh+][Tf2N-]	Trihexyl (tetradecyl) phosphonium bis(trifluoromethane) sulfonylimide
[thtdPh+][Cl-]	Trihexyl (tetradecyl) phosphonium chloride
[thtdPh+][deca-]	Trihexyl (tetradecyl) phosphonium decanoate
[thtdPh+][dbs-]	Trihexyl (tetradecyl) phosphonium dodecylbenzenesulfonate
[thtdPh+][mes-]	Trihexyl (tetradecyl) phosphonium methanesulfonate

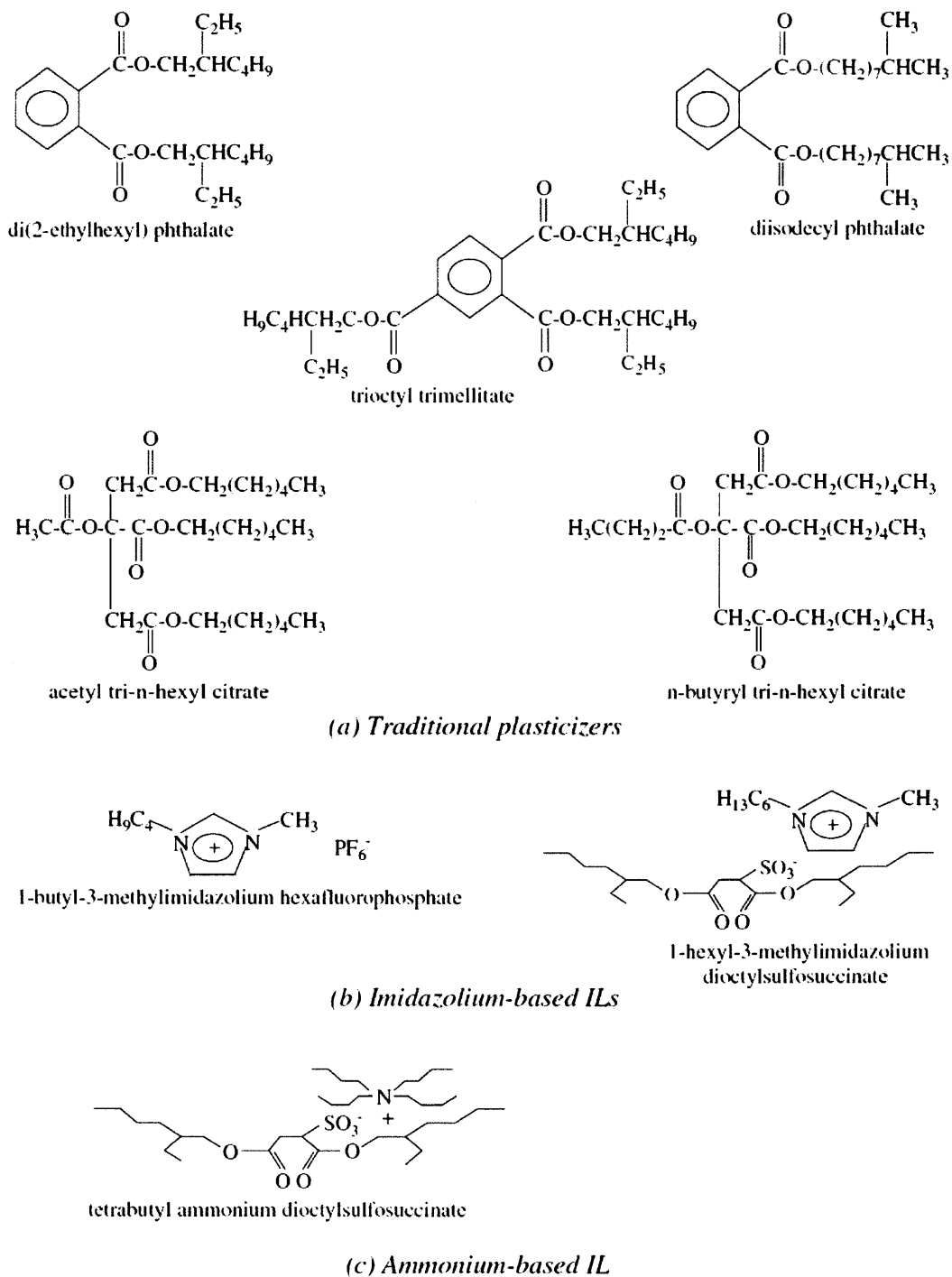


Figure 2.6 Structures of conventional plasticizers and selected ILs [29].

2.2 Ionic Liquids in Polymer Systems

2.2.1 Use of Ionic Liquids as Lubricants

ILs have been recently evaluated as promising versatile external or internal lubricants in several polymers including external or internal lubricants in PVC, polymethyl methacrylate, (PMMA), and polyamides [29].

In order to be used as a lubricant in a polymer, miscibility of the additive with the polymer is a significant factor. From the recent study by Liu et al.[31], certain ILs including the quaternary ammonium based IL, $[\text{Me}_3\text{NC}_2\text{H}_4\text{OH}]^+ [\text{ZnCl}_3]^-$ are miscible with some polymers such as PMMA, PS and PBMA (poly n-butyl methacrylate). For PS and PBMA, the miscibilities of the IL were up to 40 v%. The miscibility of these polymers with the room temperature ILs estimated by storage stability is in the order: PMMA > PBMA > PS.

Sanes et al. [32] reported on the tribological properties of thermoplastics-steel pairs using ILs, both as neat external lubricants and as polymer dispersed internal lubricants. The main objective was to establish the polymer lubricating ability of ILs by determining friction and wear values as a function of IL content, and relating them to real-time observation of the sliding contact and to the possible material degradation effects. They used several kinds of ionic liquids as internal lubricants of polystyrene (PS) and polyamide (PA6). Table 2.2 shows that the coefficient of friction of PS was reduced by adding up to 10% 1-butyl-3-methyl-imidazolium tetrafluoroborate, IL1. However, further friction and wear reduction were not necessarily obtained by increasing the concentration of IL [32].

Table 2.2 T_g Values and Dry Friction and Wear Coefficients for PS Against AISI 52100 Steel as a Function of IL1 Content [32]

Material	T _g (°C)	Friction coefficient	Wear coefficient (mm ³ N ⁻¹ m ⁻¹)
PS	101.54	0.784	1.3 × 10 ⁻²
PS+ 1.35 wt% IL1	105.29	0.258	5.0 × 10 ⁻³
PS+ 3 wt% IL1	105.74	0.232	1.7 × 10 ⁻⁴
PS+ 10 wt% IL1	103.34	0.163	3.3 × 10 ⁻⁵
PS after 100h. immersion in IL1	104.70	NA	NA

These results confirm a strong interaction between AISI 52100 steel and the IL lubricant, which contains a reactive (BF₄) anion and are in accordance with the tribochemistry of ILs at metal–metal interphases described previously [33].

Ye et al. [34] also reported that alkyimidazolium tetrafluoroborates are versatile lubricants which show excellent friction reduction for the contact of steel/steel, steel/aluminum, steel/copper, etc. Chemical structures of these lubricants are shown in Figure 2.7. Ionic liquid L106 showed the lowest friction coefficient as compared to two fluorine-containing lubricants, phosphazene (X-1P) and perfluoropolyether (PFPE) which are widely used as lubricants for head/disk interface or space applications (Table 2.3) [35].

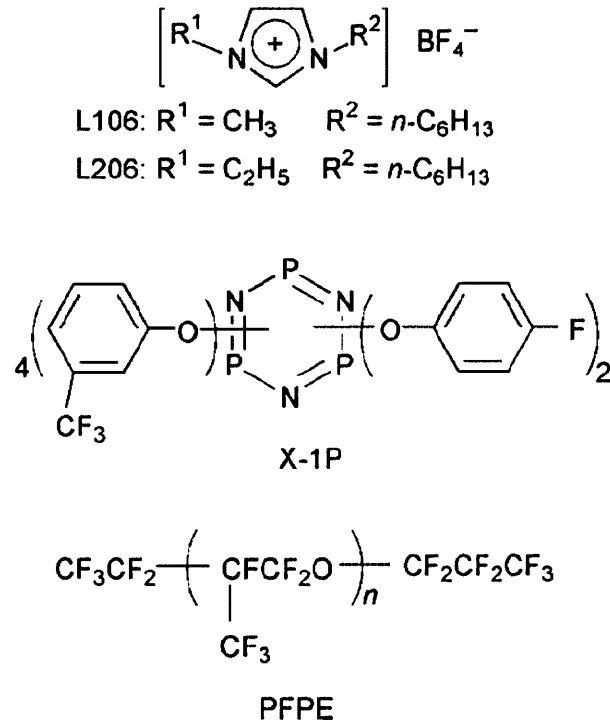


Figure 2.7 Molecular structures of the ionic liquids L106 and L206 and traditional lubricants X-1P and PFPE [34].

Table 2.3 Friction Coefficients for Several Frictional Pairs Lubricated with Various Lubricants [34]

Friction pair (ball/disk)	Friction Coefficient		
	L106	X-1P	PFPE
Steel/Steel	0.065	0.098	0.145
Steel/Al	0.040	0.128	NA
Steel/Cu	0.025	0.117	0.145
Steel/SiO ₂	0.060	0.110	0.132
Si ₃ N ₄ /SiO ₂	0.083	0.125	0.132
Steel/Si(100)	0.050	0.102	0.145
Steel/sialon	0.065	0.100	0.120
Si ₃ N ₄ /sialon	0.065	0.102	0.130

2.2.2 Plasticization of Polymers with Ionic Liquids

Plasticizers have been widely used with polymers for producing flexible plastics to be used in engineering and medical applications. In the polymer matrix, plasticizers act as high temperature solvents by breaking up the primary bonds holding the polymer chains together and forming secondary polymer-plasticizer bonds, and thus rendering mobility to polymer chains or chain segments [29]. Since polymer-plasticizer interactions are weak, there exists a dynamic process where a plasticizer molecule attached to one site in the polymer network may be dislodged and be readily replaced by another [36]. Different plasticizers give different plasticization effects because of differences in strength in plasticizer-polymer and plasticizer-plasticizer interactions as a result of functional groups present in the plasticizer molecule, its structure, chain length, molecular weight (MW), etc. [30, 29]. Traditional plasticizers offer a wide range of end-use properties to various polymers. However, uses of many of these plasticizers are frequently faced with potential problems. Limited compatibility, poor stability at high temperatures or when exposed to ultra violet (UV) rays, diminished lubricity at low temperatures, and flammability are some of the common technical challenges in the plasticizer industry [37]. The most debated issue concerning plasticizers, especially of the commonly used phthalates, is their leaching and migration. One of the unique applications of ILs is as novel plasticizers, as shown above and as reported in several publications [38, 39, 40, 41].

ILs were also found to increase the thermal stability of many polymers. Imidazolium-based hydrophobic ILs were found to be compatible with PMMA up to 50 vol% as plasticizers. In addition to lowering the T_g of PMMA from 120 °C to 20 °C, and producing polymer samples with mechanical properties similar to those produced by

traditional plasticizers, imidazolium based PF_6^- ILs offered better high temperature stability when compared to di-(2-ethylhexyl) phthalate, DEHP or DOP, in both short-term (Figure 2.8) and long-term (Table 2.4) experiments. As a plasticizer for PVC, a phosphonium-based IL, trihexyl(tetradecyl) phosphonium bis(trifluoromethane) sulfonylimide, showed superior short-term high temperature stability compared to DEHP [42].

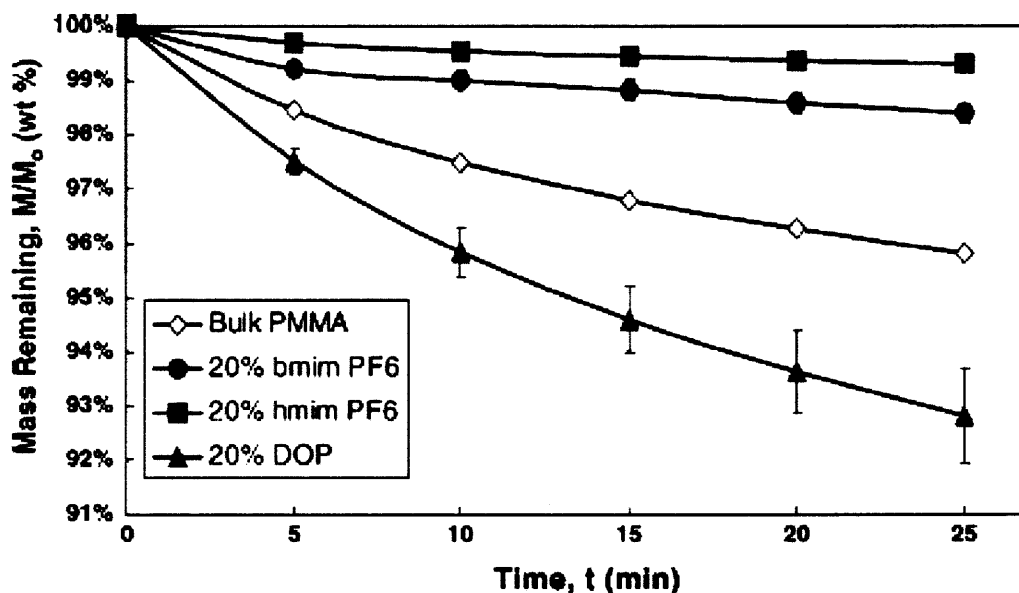


Figure 2.8 Short-term thermal stability of bulk PMMA and samples containing 20 wt% 1-butyl-3-methylimidazolium hexafluorophosphate [$\text{bmim}^+[\text{PF}_6^-]$], 20 wt% 1-hexyl-3-methylimidazolium hexafluorophosphate [$\text{hmim}^+[\text{PF}_6^-]$], and 20 wt% di(2-ethylhexyl) phthalate (DOP) at 250 °C [38].

Table 2.4 Long-term Thermal Stability of Bulk PMMA and Samples Plasticized with 1-butyl-3-methylimidazolium Hexafluorophosphate [bmim⁺][PF₆⁻] and Di(2-ethylhexyl) phthalate (DOP) at 170 °C for 21 Days [43]

Plasticizer and content	Sample mass loss (wt% of initial plasticized polymer) (%)	Plasticizer mass loss (wt% of initial plasticizer) (%)
None (bulk PMMA)	2.3	0
10% [bmim ⁺][PF ₆ ⁻]	2.9	8.3
15% [bmim ⁺][PF ₆ ⁻]	3.4	9.6
20% [bmim ⁺][PF ₆ ⁻]	4.6	13.8
30% [bmim ⁺][PF ₆ ⁻]	5.7	13.6
35% [bmim ⁺][PF ₆ ⁻]	6.7	14.9
40% [bmim ⁺][PF ₆ ⁻]	6.9	13.8
20% DOP	15.2	66.8
30% DOP	24.2	75.3

Research interest in the plasticizer industry has recently focused on biodegradable plasticizers as an alternative to the conventional non-degradable ones. This is related to the growth of the biodegradable plastics industry, as a result of growing concerns about the environmental impact of persistent plastics and their recycling. It is understood, however, that the lack of biodegradability and possible toxicity would restrict the use of many commonly used ILs as plasticizers in biodegradable polymers; however, understanding of the effects of adding ILs having different chemical structure on the properties and degradation characteristics of degradable polymers would encourage further research efforts to design benign, degradable and bio-renewable ILs [44].

2.2.3 Ionic Liquids and Nanoclays

2.2.3.1 Nanoclays

Clays are versatile materials that are used in many different areas such as building materials, ceramics, paper coatings, pharmaceuticals, adsorbents, ion exchangers, etc. [45]. Clay minerals such as phyllosilicates with a sheet structure having individual layers with thickness in the order of 1 nm and surfaces of around 50 – 150 nm in one dimension, are generally referred to as nanoclays [46].

The mineral base of clays is hydrophilic and it can be natural or synthetic. Cationic clays (e.g., montmorillonite, MMT) are widespread in nature, whereas anionic clays (e.g., hydrotalcite) are rarer in nature but relatively simple and inexpensive to synthesize. The clay surface can be changed into organophilic by chemical modification. Therefore, it can be compatible with organic polymers. Nanocomposite is the term generally applied when large surface area nanoclays ($750\text{m}^2/\text{g}$) are added to a host polymer [46].

Generally, the clays used in nanocomposites are normally 2:1 phyllosilicates as shown in Figure 2.9 where the octahedral structure is surrounded by two tetrahedral structures. The cationic clays have negatively charged aluminosilicate layers, which have cations (Na, Li, etc) in the interlayer space to balance the charge. Clay minerals have a cation exchange capacity which results from broken bonds around their edges. This capacity increases as the particle size decreases. Cationic clays, with a cation exchange capacity, include many aluminum silicates such as montmorillonite, vermiculite, smectite, and swelling mica.

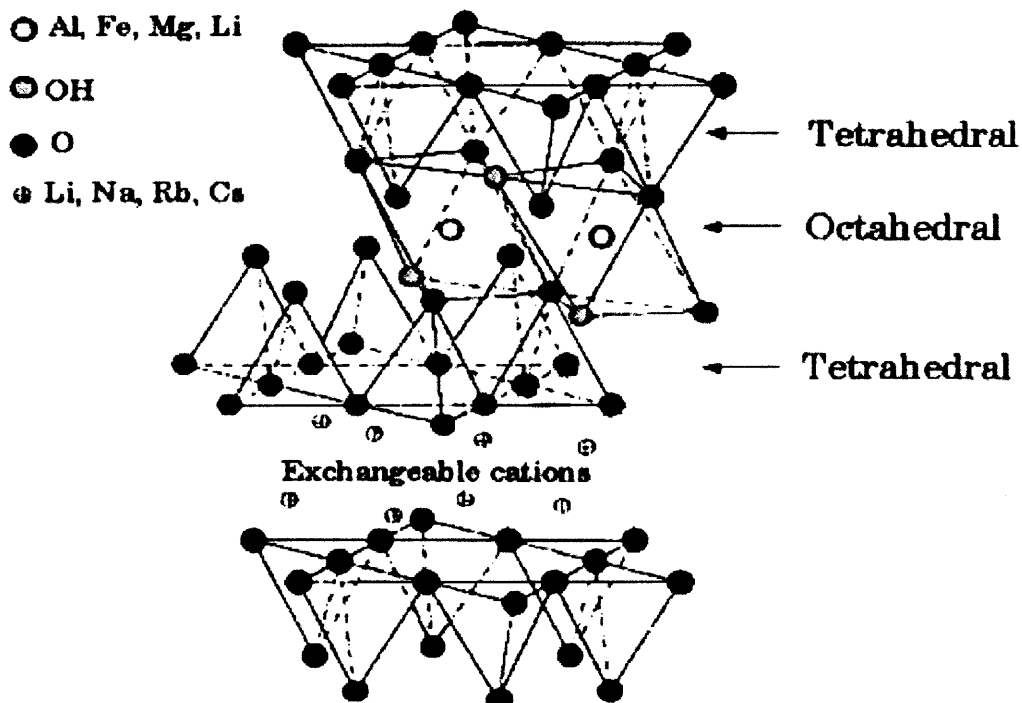


Figure 2.9 Structure of 2:1 phyllosilicate clay [47].

2.2.3.2 IL Modified Nanoclays

In addition to conventional quaternary ammonium organomodifiers a variety of ILs have been used as montmorillonite modifiers to improve dispersion, thermal stability and properties of many thermoplastics [48, 49, 50]. While a great attention has been given to quaternary nitrogen-based ILs (e.g., ammonium, imidazolium, pyridinium, etc.), specific accounts of ILs containing quaternary phosphorus cations have been less common. It has been shown that certain phosphonium-based ILs have better properties than nitrogen-based ILs, particularly thermal stability. For example, thermal stability of phosphonium-based ILs is over 300 °C for many species, even though their decomposition point upon heating varies depending on the anion. Hence, research on nanoclay composites

containing clays modified with phosphonium-based ILs has recently increased as a result of the projected higher thermal stability of the modified clays [51, 52]. For example, Byrne et al. [52] produced MMTs modified with a trihexyltetradecyl phosphonium tetrafluoroborate and showed an expansion of the basal spacing (1.8 nm compared to 1.1 nm in pristine MMT) and improved thermal stability up to 330 °C. Tributylhexadecyl phosphonium bromide was also used with MMT to produce organoclays with expanded d-spacing, high thermal stability, and partially exfoliated structures in linear low density polyethylene, LLDPE, nanocomposites [51, 49]. Similarly, phosphonium based cations present in the ionic liquid IL-4 used in the present work were successfully intercalated into MMT by increasing the basal spacing to 1.5 nm and used in PP nanocomposites [27]. Such phosphonium modified MMTs were also used with PLA in the present work to study possible catalytic degradative effects.

2.3 Degradation Mechanisms of Polylactic Acid

2.3.1 Mechanisms of Thermal Degradation

Thermal degradation of PLA is a complex reaction and various mechanisms have been postulated. As reported by Wachsen et al. [53], the degradation of PLLA during thermal processing is mainly caused by intramolecular transesterification reactions leading to cyclic oligomers of lactic acid and lactide. Doi et al. [54] claimed that thermal degradation of microbial aliphatic polyesters occurred via random chain scission regardless of the type and the chemical composition, by showing that there was a linear relationship between the inverse of the number average degree of polymerization and time.

Kopinke et al. [54] suggested five possible reaction pathways from their experimental data: intra- and intermolecular ester exchange (lactide and cyclic oligomers), cis-elimination, radical and concerted nonradical reactions, radical reactions, and selective, Sn-catalyzed depolymerization. Their thermo-analytical techniques concluded that the dominant reaction pathway is an intramolecular transesterification for pure polylactic acid which gives rise to the formation of cyclic oligomers.

Arraiza et al. [55] proposed a thermal degradation mechanism for PLLA in which a carbon-oxygen bond is broken forming an acid and an unsaturated ester as shown in Figure 2.10.

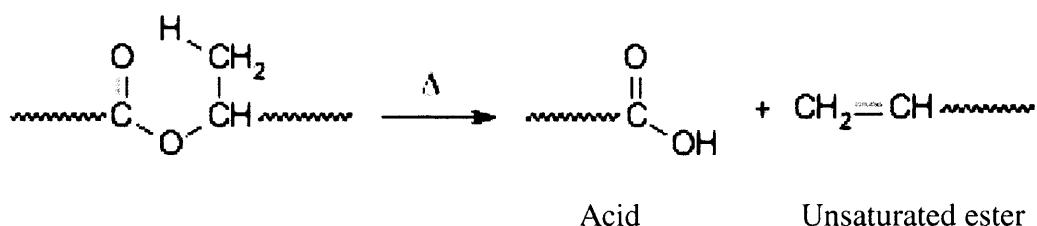


Figure 2.10 Mechanism of thermal degradation of PLLA [55].

The activation energy for the decomposition of the PLA is important in assessing the reaction mechanisms. The rate equation that was used by Friedman (Equation 2.3) is related to temperature by an Arrhenius relationship as shown in equation 2.1.

$$\ln k = \ln Z - \frac{E_a}{RT} \quad (2.1)$$

where k is the rate constant, Z is a frequency factor, E_a is the activation energy, R is the gas constant, and T is temperature in Kelvin.

The Friedman and Chang techniques are among the common techniques used to

study the pyrolytic behavior of polymers [56]. The thermal decomposition kinetics related to thermogravimetric weight loss data (TGA) may be calculated by the Friedman technique from the kinetic equation:

$$d\alpha/dt = Z(1-\alpha)^n e^{-E_a/RT} \quad (2.2)$$

where α is the weight loss of the polymer undergoing degradation at time t , $d\alpha/dt$ denotes the decomposition rate or weight-loss rate, n represents the decomposition reaction order, [56].

The Friedman technique suggests that a plot of $\ln(d\alpha/dt)$ versus $1/T$ is linear with the slope corresponding to the overall activation energy. The order of decomposition can be obtained from the plot $\ln(1-\alpha)$ versus $1/T$.

The relation is given by

$$\ln\left(\frac{d\alpha}{dt}\right) = \ln(Z) + n \ln(1-\alpha) - \frac{E_a}{RT} \quad (2.3)$$

Chang's method uses a rewritten form of the Friedman equation as:

$$\ln\left(\frac{1}{(1-\alpha)^n} \frac{d\alpha}{dt}\right) = \ln(Z) - \frac{E_a}{RT} \quad (2.4)$$

In this study, the activation energy for the thermal decomposition of PLA and PLA/IL blends was determined through the Friedman technique (2.3) from TGA measurements at a single heating rate of 20 °C/min.

2.3.1.1 Effect of Fillers/Additives on the Thermal Degradation of PLA.

Although PLA has an excellent balance of physical and rheological properties, many additives have been combined with it to further extend the range of properties achievable and, thus, optimize the material for specific end use applications. Fillers that have

valuable properties with blended with PLA are talc, mica, kaolin, glass, a variety of inorganic carbonates and sulfates, as well as starch [57].

Usually a large amount of fillers can significantly increase viscosity, cause shear heating and degradation. Appearance may also be a potential problem with flow lines, poor colorability, and opacity being among the main issues [57].

Lee et al. [58] studied the thermal stability of PLA/wood flour blended materials by thermogravimetric analysis. As the wood flour content increased, the decomposition temperature of the composites decreased slightly which may be due to the decomposition of wood components. The lower decomposition temperatures of the PLA/wood flour composites indicated that the composites were less thermally stable than the neat PLA matrix.

Chang et al. [59] compared the organo-montmorillonite (C16-MMT) to dodecyltrimethyl ammonium bromide-montmorillonite (DTA-MMT) and the commercially available Cloisite 25A in the preparation of PLA nanocomposites. From morphological studies using transmission electron microscope (TEM), most clay layers were found to be dispersed homogeneously in the matrix polymer, although some clusters or agglomerated particles were also detected. The authors found the degradation temperature (at a 2% weight loss) of the PLA nanocomposite films with C16-MMT and Cloisite 25A decreased linearly with an increasing amount of organoclay.

On the contrary, Pluta et al. [60] investigated PLA/MMT nanocomposites by studying dispersions of MMT modified with dimethyl 2-ethylhexyl ammonium cation and unmodified MMT prepared by melt blending. X-ray diffraction, XRD, showed that the good affinity between the organo-modified clay and the PLA was sufficient to form

an intercalated structure in the nanocomposite. Thermogravimetric analysis, TGA, showed that the PLA-based nanocomposites exhibited improvement in their thermal stability under oxidative conditions and both types of clays showed a tendency to limit PLA degradation.

Paul et al. found that MMT organo-modified by bis-(2-hydroxyethyl)-methyl (hydrogenated tallow alkyl) ammonium cations produced the greatest increase in thermal stability. Increasing the amount of clay was shown to delay the onset of thermal degradation of the poly(ethylene glycol) (PEG) plasticized PLA matrix. Finally, Zhou [61] showed that thermomechanical degradation of semicrystalline and amorphous PLA polymers was affected by the presence of different MMT and hydrotalcite (HT) fillers, which apparently acted catalytically to different degrees.

2.3.2 Mechanisms of Hydrolytic Degradation

Generally the hydrolytic degradation of aliphatic polyesters in aqueous media proceeds through random ester bond cleavage in the bulk of the sample or a device [62, 63, 64].

It has been shown that thick samples of PLA lead to a heterogeneous degradation with faster degradation inside than at the surface [65, 66, 67, 68]. This heterogeneous degradation was assigned to the contribution of two phenomena: (1) easier diffusion of soluble oligomers from the surface into the external medium than from inside, and (2) neutralization of carboxylic endgroups located at the surface by the external buffer solution [69]. Both phenomena contribute to the reduction of the acidity of the surface layer, whereas in the internal part the degradation rate is enhanced by autocatalysis due to carboxylic end groups. A parameter that indicates which way a degradable polymer will

erode is the ratio of the rate of bulk to surface erosions. Applying penetration theory, it can be shown that the thickness (w) associated with each mechanism is related to a characteristic time, by the following equations:

$$w = \sqrt{\frac{4Dt_{diff}}{\pi}} \quad \text{in the case of bulk erosion} \quad (2.5)$$

and

$$w = \sqrt{Dt_{reaction}} \quad \text{in the case of surface erosion} \quad (2.6)$$

where $t_{diffusion}$ and $t_{reaction}$ are characteristic times of the two processes and D is the diffusion coefficient.

In order to identify parameters that determine surface or bulk erosion pathways, Burkersroda et al. [70] proposed a model in which the two characteristic times of Equations 2.5 and 2.6 are expressed in terms of a dimensionless number (can be considered as a Deborah number) named “erosion number”

In the case of amorphous PLA, material degradation proceeds through surface erosion and is faster in the inner part than at the surface due to the autocatalysis phenomena while degradation of semi-crystalline PLA proceeds through the amorphous regions since these have higher water uptake ability than crystalline parts. The degraded fragments from semi-crystalline PLA diffuse and recrystallize and this results in increasing the degree of crystallinity [71].

Several relationships have been derived relating the changes in number average molecular weight, M_n , with time and hydrolysis rate of ester linkages since M_n is directly related to the scission of polymer chains and is considered to be the most sensitive parameter for modeling polymer degradation.

Anderson [72] proposed a statistical method for relating M_n and hydrolysis rate. They suggested the following relationship assuming that the extent of degradation was not large:

$$1/\overline{M}_n = 1/\overline{M}_{no} + kt \quad (2.7)$$

where \overline{M}_{no} is \overline{M}_n at time $t=0$ and k is the rate constant. Under this assumption, a linear relationship should exist between $1/\overline{M}_n$ versus time. The weak point of this mechanism is that it does not take into account the possibility of acid autocatalysis that would significantly influence the degradation rate.

Pitt and Gu [73] derived an equation based on the kinetics of the ester-hydrolysis reaction and taking into account the autocatalytic effect.

$$d[E]/dt = -d[\text{COOH}]/dt = -k[\text{COOH}][\text{H}_2\text{O}][E] \quad (2.8)$$

where $[\text{COOH}]$, $[\text{H}_2\text{O}]$ and $[E]$ represent the concentration of the carboxyl end groups, water and ester groups, respectively.

By assuming that the ester and water concentrations remain constant and the concentration of acid groups is equal to $1/M_n$ it can be shown that

$$\overline{M}_n = \overline{M}_{no} e^{-kt} \quad (2.9)$$

If this relationship holds true, a linear relationship should exist between $\ln \overline{M}_n$ versus time up until mass loss occurs:

$$\ln \overline{M}_n = -kt + \ln \overline{M}_{no} \quad (2.10)$$

2.3.2.1 Parameters Influencing the Hydrolytic Degradation of PLA. According to Scliccker et al. [22], the hydrolytic degradation process of polyesters is affected by four parameters, specifically: the degradation rate constant, the amount of water that has been

absorbed, the diffusion coefficient of the chain fragments, and the solubility of degradation byproducts in the aqueous media. Several more factors that influence the rate of the hydrolysis reaction are known from many studies: the type of chemical bond, pH, and temperature are the most important [74]. Chemical and physical changes accompany the degradation of biodegradable polymers, such as crystallization of oligomers [56] and monomers [75] or pH changes [71]. Some of these factors can have a considerable feedback effect on the degradation rate.

pH affects reaction rates through catalysis. After shifts in pH, reaction rates of esters may change by some orders of magnitude due to catalysis [76]. The effect of pH on degradation has been investigated carefully for most biodegradable polymers. For poly(glycolic acid) and poly(lactic-co-glycolic acid) sutures, the breaking strength was found to depend markedly on the pH of the degradation medium and was found to be highest at neutral pH [77] reflecting the fastest degradation at low and high pH. This faster chain scission at low pH explains the heterogeneous erosion of PLA due to autocatalysis. The generated monomers, which are carboxylic acids, accelerate polymer degradation by lowering pH [68]. For poly(bis-(p-carboxyphenoxy)propane anhydride) cylinders, for example, the degradation rate increases by a factor of 10 when increasing the pH of the degradation medium from 7.4 to 10 [78]. Poly(ortho esters), in contrast, are resistant against basic pH and degrade substantially faster at acidic compared to neutral pH [79]. By using acidic or basic excipients, the degradation rate of polymer hydrolysis can be varied in a controlled way. The internal pH can, thus, effectively be used to influence the degradation rate of polymers [80]. From a recent study, it is known that the erosion kinetics of PLA and PLGA change tremendously under base catalysis [70]. While

polymers eroded at pH 2 and 7.4 changed their original shape within a few days to an irregular form, matrices eroded at pH>13 maintained their shape up to 6 days. In the case of alkaline medium, one can conclude that the mechanism of erosion has changed from bulk to surface erosion which was confirmed by GPC and SEM [70].

The type of bond within the polymer backbone determines the rate of hydrolysis [81]. Several classifications for ranking the reactivity exist which are either based on hydrolysis kinetics data for polymers [82, 83] or are extrapolated from low-molecular weight compounds containing the same functional group [84]. Reactivities can change tremendously upon catalysis [85, 86] or by altering the chemical environment of the functional groups [76] through steric and electronic effects. The influence of steric effects on degradation can be seen with poly(α -hydroxy esters). In the case of PLA, hydrolysis is relatively slow due to steric effects [87], because the methyl group hinders the attack of water.

In general, hydrolysis is a bimolecular reaction in which water and the functional group possessing the labile bond are involved. The reaction rate is determined by the concentration of both reaction partners [74]. Lipophilic polymers cannot take up large quantities of water and decrease, thereby, their degradation velocity [78, 88]. Hydrophilic polymers, in contrast, take up large quantities of water and increase, thereby, degradation rates.

As shown by Zhou and Xanthos (2008) [61] degradation rate constants were higher for amorphous PLA and its composites than semicrystalline PLA and its MMT composites as a result of increased permeation through the amorphous domains. Since the MMT- Na^+ lost its neutralization ability after treatment with the organic modifiers the

degradation rate constants of the nanocomposites were significantly higher than those of the unfilled polymers with certain differences observed depending on the type of modifier; by contrast, those of the MMT- Na^+ microcomposites were lower or slightly lower than those of the unfilled polymers possibly due to the reduction of the carboxyl group catalytic effect through neutralization with the hydrophilic alkaline filler.

2.4 Objectives

Little or no work has been reported in the polymer modification field using ionic liquids as additives for polylactic acid. Although several plasticizers and lubricants have been used for polylactic acid modification, little attention has been given to the combined effects of ILs on physical, rheological and mechanical properties, thermal stability and thermal/hydrolytic degradation rates.

The aim of this work is to investigate the role of ILs with long chain hydrophobic cations and different anions as process and property modifiers of PLA including plasticization, lubrication, and thermal/hydrolytic degradation. In addition to processability, this research addresses the effects of the selected ILs on the rates of hydrolytic and thermal degradation of PLA, compares with existing models and also attempts to separate the corresponding effects of cations and anions by using model compounds including cation exchanged montmorillonite, MMTs. Thus, an amorphous PLA polymer is mixed with two phosphonium- based ILs which have different anions, at various ratios by melt-blending and solvent casting. The choice of the particular IL structures was based on literature evidence that alkylphosphonium surfactant cations exchanged in the structure of saponite clay tend to accelerate the soil degradation of

aliphatic polyesters including PLA [89]. The efficiency of plasticization and lubrication is measured from changes in thermal, rheological and frictional properties. Changes in polymer molecular weight, changes in pH and acid number of the hydrolytic degradation medium and weight losses are followed during thermal/hydrolytic degradation and are related to morphology by scanning electron microscopy and visual observation, and ultimately to the structure of the ionic liquids.

CHAPTER 3

EXPERIMENTAL

3.1 Materials

3.1.1 Polylactic Acid

Poly lactide polymer pellets PLA 4060D purchased from Natureworks® had a reported glass transition temperature of 58°C and density of 1.25g/cc. This grade was selected because of its amorphous structure that could lead to accelerated degradation. The pellets are transparent and start to become tacky at 45°C as per manufacturer's technical data sheet [90].

3.1.2 Ionic Liquids

The phosphonium based ionic liquids used in this study include the following:

- trihexyltetradecylphosphonium decanoate ([THTDP][DE])
- trihexyltetradecylphosphonium tetrafluoroborate ([THTDP][BF₄])

[THTDP][DE], with MW 655.13 (designated as IL-4) and [THTDP][BF₄], with MW 570.68, (designated as IL-5), were obtained from Sigma-Aldrich and Structures of IL-4 and IL-5 are shown in Figure 3.1.

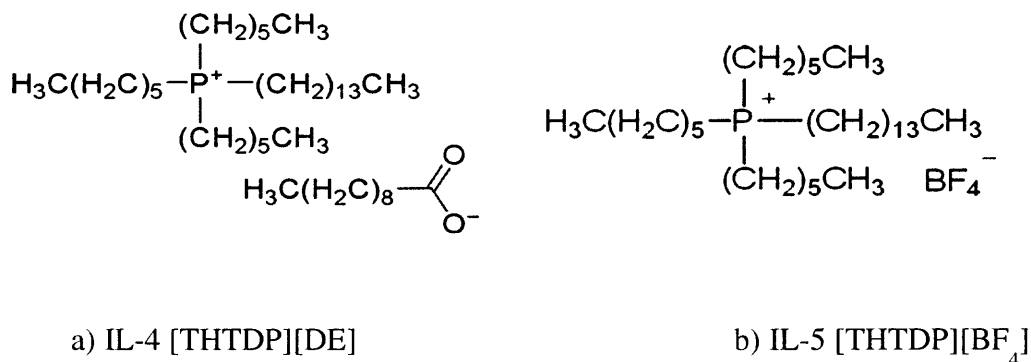


Figure 3.1 Structures of ILs: a) IL-4, b) IL-5 (Source: Sigma Aldrich).

IL-4 with a density less than 1g/cc is sparingly soluble in water and can dissolve up to 21.1% water when fully saturated. When dry, it is totally miscible with a wide range of organic solvents such as toluene, tetrahydrofuran (THF), and dichloromethane. IL-5 has a low melting point of 37 °C and is immiscible with water. When fully saturated, it will contain up to 1.8% water. It is miscible with most common organic solvents such as toluene, THF and dichloromethane [16].

3.1.3 Other Chemicals

Chloroform (CAS No 67-66-3) and the model compound decanoic acid, CH₃ (CH₂)₇CH₂COOH, designated as DECA, (CAS No. 334-48-5) were obtained from Sigma Aldrich.

3.1.4 Nanoclays

Sodium montmorillonite (MMT-Na⁺), used in this study was obtained from Southern Clay Products Inc. (CAS# 1318-93-0, trade name: Cloisite[®]-Na⁺). MMT-Na⁺ contains 4 - 9% moisture and sodium ions in the basal spacing without added organic modifiers. Its

cationic exchange capacity (CEC) has been reported as 92.6 meq /100g clay. Molecular structure and other technical data are shown in Figure 3.2 and Table 3.1.

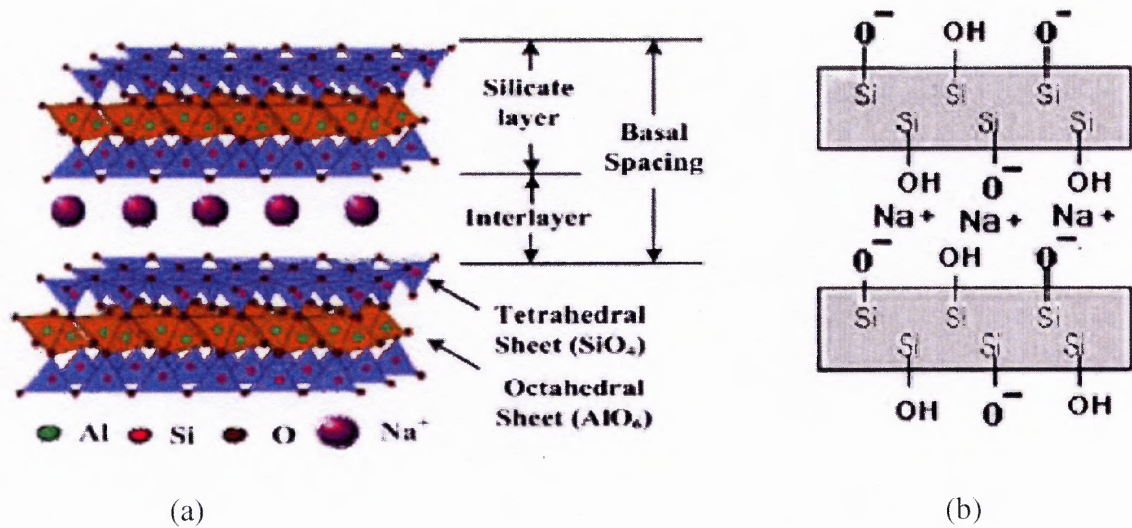


Figure 3.2 (a) Schematic of molecular structure of MMT- Na^+ , (b) Schematic side view of MMT- Na^+ between layers [91].

Table 3.1 Technical Data of Cloisite[®] Na^+ (MMT- Na^+)

X-ray results		
d001 = 11.7 Å		
Density		
Loose bulk (lbs/ft ³): 12.45	Packed bulk (lbs/ft ³): 20.95	Density (g/cc): 2.86
Typical Dry Particle size (Microns, by volume)		
< 10%: 2µm	< 50%: 6µm	< 90%: 13µm
Color		
Off white		

Source: Product Bulletin from Southern Clay Products Inc.

3.1.5 Degradation Media

3.1.5.1 Phosphate Buffer Saline Solution (PBS). In order to follow the hydrolytic degradation behavior of the polylactic acid and its mixtures with ILs, pouches of phosphate buffer saline (PBS) were obtained from Sigma Aldrich. PBS is commonly used for hydrolytic degradation in *in vitro* controlled release experiments. Contents of one pouch, when dissolved in one liter of distilled or ionized water, yielded 0.01 M PBS (NaCl 0.138 M; KCl 0.0027 M) with a pH of 7.4 at 25 °C. The composition of the PBS aqueous solution is 1.38 mM NaCl, 1.15 mM Na₂HPO₄, 1.2 mM KH₂PO₄ and 2.7 mM KCl.

3.1.5.2 Soil. For the soil degradation of polylactic acid and its mixtures with ILs, Miracle-Gro[®] soil (The Scotts Company, Maryville, OH) was used. The compost contains 0.21% nitrogen (0.12% ammonia-nitrogen, 0.09% nitrate nitrogen), 0.07% of P₂O₅, and 0.14% of K₂O. Measured pH of the soil was 8.1 at 25 °C. Sterilized soil (pH 6.8) was prepared by heating up the above soil at 200 °C for 24 hours in the oven followed by storing in a vacuum desiccator.

3.2 Sample Preparation

3.2.1 Melt Compounding

Direct addition of IL-4, and IL-5 at concentrations up to 10 wt% into the molten PLA in the counter rotating Brabender batch mixer (PL2000, C.W. Brabender) created segregated samples since the ILs tended to concentrate on the surface of the mixer bowl.

IL-4 or IL-5 were then dissolved in EtOH/H₂O (4:1) and PLA pellets were added in this solution until thoroughly immersed for 24hrs. The solvent was removed by heating at 70°C for 24hrs in a ventilated oven. The concentrations of IL-4 and IL-5 in the solution

were selected so that the dried pre-mix contained 10 wt% IL. Different weight percentages of ILs in PLA were used. To produce 1 wt% and 5 wt% of IL-4 or IL-5 in PLA, proper amounts of PLA pellets were added along with the pre-coated pellets in the mixer bowl and melt blended at 50 rpm and 160°C for 10 minutes under nitrogen until the torque stabilized. After melt processing, PLA and PLA/ 5wt% IL-5 samples were transparent and had brown color; PLA/ 5wt% IL-4 was dark brown probably the result of excessive degradation. The mixtures produced were then compression molded in a hydraulic compression press for 2 minutes at 180 °C into 10mm thick films.

3.2.2 Solvent Casting

5 wt% (based on PLA) of IL-4 or IL-5 was dissolved in chloroform and PLA pellets were added in each solution. Model compounds containing only decanoic acid and MMT/phosphonium cation (MMT-4) were also prepared in order to separate the effect of the anion from that of the cation in IL-4. To keep the same concentration of decanoate anions and phosphonium cations as in IL-4, 1.6 wt% of DECA and 50 wt% of MMT-4 were dissolved/dispersed, respectively in the PLA solution. As a control, a MMT-Na⁺ slurry containing 50wt% clay based on PLA was also produced. After homogenization, the polymer/additive solution was poured into glass petri dishes and kept for 48 hrs under the hood. After most of the chloroform had evaporated, the remaining solids were dried under vacuum. The thicknesses of the dried films were 1mm with a diameter of 7.5 cm.

3.2.3 Preparation of Nanoclay Modified with IL-4

The cationic exchange reaction was carried out according to [27]. IL-4 was added at 2X the stoichiometric amount of the cationic exchange capacity (CEC) (3.65 g respectively

in 250 ml solution) of MMT-Na⁺. IL-4 was dissolved in ethanol (200 ml) and deionized water (50 ml) solution by vigorous stirring for 10 minutes at room temperature. MMT-Na⁺ (3 g) was then added to the solution. The cationic exchange reaction was performed at 60 °C under reflux. The modified MMT was collected by vacuum filtration (Genuine Whatman filter paper, 7cm diameter, 1.6µm pore size). The modified MMT was washed many times in the funnel with EtOH / H₂O solution and then three more times with vigorous stirring in a 500ml (EtOH 80 %, H₂O 20 %) beaker in order to remove residual anions. The finally filtered MMT (designated as MMT-4) was dried at room temperature for 24 hours and then at 90 °C for 24 hours under vacuum. The final products were ground with a mortar and pestle and dried at 90 °C for 24 hours under vacuum once again.

3.3 Testing and Characterization

3.3.1 Thermal Properties

PLA, ILs, and their compounds were characterized by thermogravimetric analysis, TGA, (TA Instruments, QA 50 analyzer) from room temperature to 500°C, at a heating rate of 20°C/min in a nitrogen atmosphere to determine thermal stability.

PLA, ILs, and their compounds were characterized by differential scanning calorimetry, DSC, (TA Instruments, QA 100 analyzer) from 0°C to 150°C at a heating rate of 10°C/min to determine glass transition temperatures.

3.3.2 Rheological Characterization

3.3.2.1 Helical Barrel Rheometer. The HBRTM is a portable on-line viscosity measuring instrument with a single screw that measures pressure drop across a flight at a

given shaft speed. The data set can be converted to determine viscosity as a function of shear rate. Viscometric behavior of PLA, PLA/ 5wt% IL-4, and PLA/ 5wt% IL-5 was determined by the HBR™ (Figure 3.3) over a period of 70 minutes at constant shaft speed. To eliminate air in the feed compound and stabilize it before measuring viscosity, 20g of PLA and pre-coated PLA pellets with 5 wt% IL-4 and 5 wt% IL-5 were fed and compressed for a period of 1 minute. Measurements were taken at 160°C and 5 RPM in order to minimize excessive thermomechanical degradation.

With the geometry as noted in Figure 3.3 b, the viscosity, η , changes as function of time can be calculated from equation 3.2 using the rotor speed and pressure drop at closed discharge.

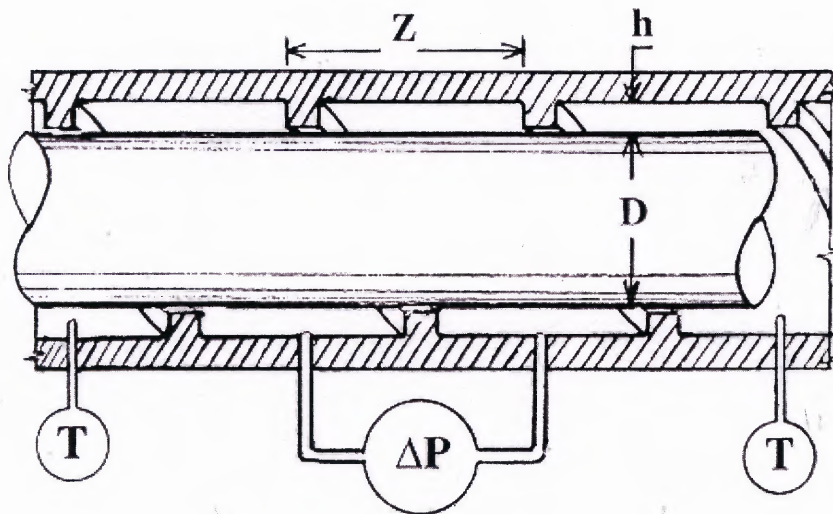
$$\Delta P = 6 \left(\frac{\pi D_r}{h} \right)^2 \eta N \quad (3.1)$$

$$\eta = \frac{1}{6} \left(\frac{h}{\pi D_r} \right)^2 \frac{\Delta P}{N} \quad (3.2)$$

h = Channel depth (1mm), D_r = Diameter of rotor (23 mm), ΔP = pressure difference over one flight, and N = rotor speed



(a)



(b)

Figure 3.3 Helical Barrel Rheometer. (a) Outside view, (b) Cross section.

3.3.2.2 Capillary Rheometer. Information on apparent viscosities of PLA/IL-4, PLA/IL-5 melt mixed compounds were determined using a capillary rheometer (Instron, Model 4204) in the shear rate range of 15 s^{-1} to 38 s^{-1} at $190 \text{ }^\circ\text{C}$. A series of capillary dies of length/diameter (l/d) ratio of 38.3 and diameter of 1.59 mm was used to obtain the die wall shear stress, shear rate, and apparent viscosity. Viscosity was obtained from Equation 3.5 by using values of the shear stress (τ_{wall}) and the shear rate ($\dot{\gamma}_{\text{wall}}$) at the capillary wall derived from equations 3.3 and 3.4. No Bagley or Rabinowitsch corrections were applied in this study.

$$\tau_{\text{wall}} = (\Delta P R_c) / 2L = (\Delta P H) / 4L \quad (3.3)$$

ΔP = pressure drop across the capillary tube

H = inside capillary tube diameter

R_c = inside capillary tube radius

L = capillary tube length.

$$\dot{\gamma}_{\text{wall}} = (4Q) / (\pi R_c^3) \quad (3.4)$$

Q = volumetric flow rate, cm^3/sec

v = average fluid velocity, cm/s .

$$\tau_{\text{wall}} = \eta \dot{\gamma}_{\text{wall}} \quad (3.5)$$

η = viscosity of fluid.

3.3.3 Isothermal Degradation

Isothermal degradation experiments were carried out at 160 °C for 7 days in a ventilated oven in air. An initial amount of 2 grams of each sample (PLA, PLA/5 wt% IL-4, PLA/5 wt% IL-5,) from the melt mixing process was ground to a powder and placed in uncovered glass jars. IL-4 and IL-5 were also used as controls. All samples were weighed every two hours for the first day and then weighed at intervals of 24 hours for seven days. Another set of five samples was placed in the uncovered glass jars at 160 °C in the same oven. Samples collected at pre-determined time intervals were analyzed by GPC.

3.3.4 Hydrolytic Degradation

PLA, PLA/ 5wt% IL-4, and PLA/ 5wt% IL-5 processed by melt mixing were compression molded using a circular plate at 160 °C. Specimens with diameter of 30 mm and thickness of 1.5 mm were then cut into four equal pieces. Specimens were placed into small flasks filled with 60 ml of 1M (phosphate buffer solution, PBS) at pH 7.4. The flasks were allowed to stand in a thermostatted oven at 60 °C for predetermined periods of time. Samples were withdrawn from the PBS after 1 day, 4 days, 6 days and 11 days and washed with distilled water followed by drying in the vacuum oven for a week at room temperature. Samples taken on the 6th day were used for MW analysis by gel permeation chromatography (GPC). The pH change of the degradation medium was frequently measured up to 30 days.

3.3.5 Soil Degradation

Biodegradability was determined by measuring weight loss of the pre-cut 1cm × 1cm specimens with 1mm thickness buried in the soil. The buried specimens were incubated at 60 °C. Relative humidity was kept constant at 30-35 % and measured by a moisture meter (HH2, Delta T, Cambridge, England). Each specimen was removed from the soil after burial for 1, 2, 3, 4 weeks, respectively. The specimens were swiped to remove soil on the surface and dried at 40 °C in a vacuum oven overnight. Plans were to calculate weight changes at each time period using the following equation:

$$\% \text{ Weight Change} = 100 \times (W_i - W_t) / W_i$$

Where W_i and W_t respectively are weights of the initial sample and that at time t .

Another set of samples were placed in the sterilized soil in the same manner to compare the % weight changes and visual appearances with those degraded in the unsterilized soil.

3.3.6 Gel Permeation Chromatography

Molecular weights of the samples before and after thermal and hydrolytic degradations were determined by GPC [Waters Co., RI detector, PLgel 5 μm MIXED-C, 300×7.5 mm (PL1110-6500) column] with THF as eluent at 1.0 ml/min at 35 °C. Columns were previously calibrated using poly(methylmethacrylate) standards. Samples were dissolved in THF (concentration up to 5 wt%).

3.3.7 pH and Acid Number

The pH of the buffer solution at different hydrolytic degradation periods, after sample removal, was measured to monitor changes that could be a combination of acidic degradation byproducts resulting from the polymer and the ILs. When the tests were completed, the samples were washed with distilled water and dried under vacuum at room temperature for further characterization.

Acid numbers (mg of KOH/ g of sample) of PLA, PLA/ 5wt% IL-4, PLA/ 5wt% IL-5 (prepared by solvent casting) before and after six days of hydrolytic degradation were determined by titration using 0.05 N KOH solution with phenolphthalein as an indicator in chloroform as a solvent. Acid numbers of IL-4, and IL-5 in chloroform at a concentration of 0.016 wt% (same concentration of ILs as in PLA/ILs) were also measured.

3.3.8 Physical and Mechanical Properties

3.3.8.1 Flexural Properties. Test specimens (100mm length, 13mm width, and 1mm thickness) were prepared by pressing melt mixed samples for 2 min at 160 °C. The flexural strength and flexural modulus by 3-point bending were measured by a Tinius-Olsen (Lo Cap Universal) testing machine using a span to depth ratio of 16:1, up to 5% deformation/strain (ASTM 790) at a crosshead speed of 0.5 cm/min. Flexural strength and modulus were calculated using the following equations 3.6 and 3.7.

$$S = \frac{3fl}{2ba^2} \quad (3.6)$$

$$E = \frac{ml^3}{4bd^3} \quad (3.7)$$

Where:

S = stress in the outer surface at mid-span (Pa)

f = load at a given point on the curve (N)

E = Flexural modulus (Pa)

m = initial slope of the load vs. deflection curve (N/m)

a = thickness of beam (m)

b = width of beam (m)

d = depth of test beam (m)

l = span length between two support points (m)

In the case of PLA/IL-4, the samples broke at about $f= 7.5\text{N}$ load and the calculated strength is indeed the maximum stress at break. PLA and /PLA/IL-5 samples did not break but rather bent excessively and the reported strength refers to the maximum recorded force.

3.3.8.2 Coefficient of Friction. A dynamic friction coefficient was measured using a mobility/lubricity tester (9505A, Altek Co., Torrington, CT) composed of 1kg sled (9793A, Altek, Co.) as shown in Figure 3.4. A steel sled with 1 kg weight contacts three steel balls on the surface of the sample and measures the friction force resisting the movement of the load cell. Three 1 mm thick films (PLA, PLA/ 5wt% IL-4 and PLA/ 5wt% IL-5) were prepared by the melt mixing method followed by pressing for 2 minutes at 160 °C. The string connected to the load cell and sled was pulled by a motor at the selected speed and the measured force converted to coefficient of friction (COF) was recorded by a gauge. COF was the average of three measurements. All friction tests were

conducted at room temperature at a pulling speed of 20.0 mm/s.

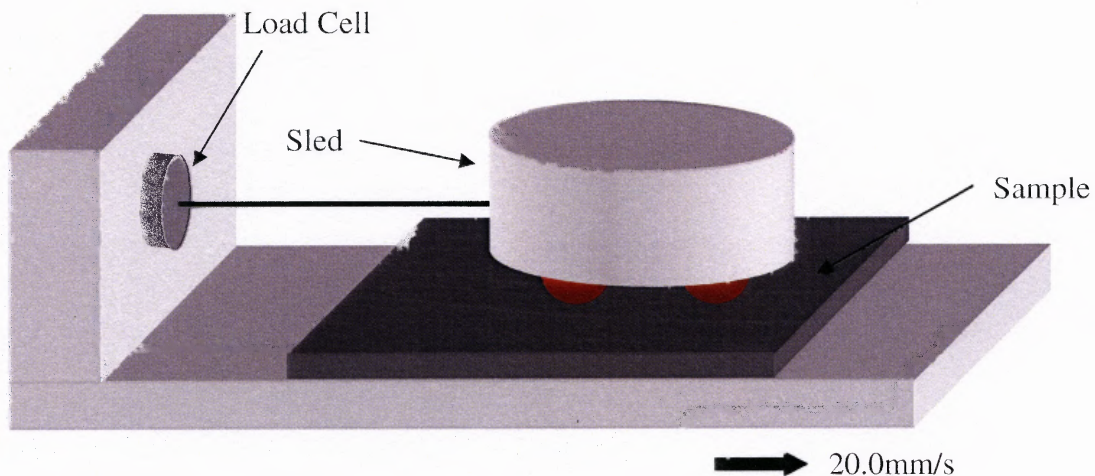


Figure 3.4 Configuration of friction tester.

3.3.8.3 Contact Angle Measurement. One droplet of distilled water was placed on the surface of PLA, PLA/IL-4, and PLA/IL-5 films with thickness of 1mm using a drop shape analysis system (DSA 10MK2, KRUSS, Germany). Contact angle was determined by measuring the angle between the tangent of the drop surface at the contact line and the surface.

3.3.9 Surface Structure, Morphology and Crystallinity

3.3.9.1 Scanning Electron Microscopy (SEM). The surface and cross-section morphologies of PLA, PLA/IL-4, and PLA/IL-5 samples before and after exposure to the PBS solution were examined by SEM (LEO Field Emission Gun 1530-VP Digital SEM).

The samples were carbon coated using a Bal-Tee Med 020 Sputter Coater and then viewed by varying the working voltage (from 1 to 10 kV).

3.3.9.2 Energy Dispersive X-Ray Analysis (EDX). Elemental analysis was performed by EDX on the surfaces and cross-sections of samples examined by SEM. The distribution of IL-4 and IL-5 in the PLA matrix was investigated by analyzing for elements such as *P* and *F* present in the cations of IL-4 and IL-5 and in the anion of IL-5, respectively. The *P/F* ratio was calculated and compared with the theoretical ratio of *P/F* in the case of IL-5.

3.3.9.3 X-Ray Diffraction (XRD). Philips PW3040 diffractometer (Cu $K\alpha$ radiation $\lambda=1.5406 \text{ \AA}$, generator voltage = 45 kV, current = 40 μA) was used to evaluate the crystallinity of the PLA before and after soil degradation. The scanned 2θ range was from 5° - 45° for every sample.

CHAPTER 4

RESULTS AND DISCUSSION

4.1 Miscibility of ILs and PLA

There are numerous demands put on plasticizers, but an especially important factor is that plasticizers should be miscible with PLA, thus creating a homogeneous blend. Solubility parameter, δ (Equation 4.1) [92] is the most effective indicator to predict the miscibility and solubility of ILs with various polymers and in the present case PLA.

$$\delta = \sqrt{\frac{E_{coh}}{V}} \quad (4.1)$$

Where E_{coh} is cohesive energy and V is molar volume for plasticizer or polymer.

Plasticizers are usually miscible with polymers when their solubility parameters are matched or show small differences.

In this study, the solubility parameters of PLA, IL-4 and IL-5 were estimated from group contributions as per procedures summarized by Van Krevelen [92]. For PLA, the methods of Small, Van Krevelen and Hoy, based on group contributions to the molar attraction constant, and by taking PLA density, ρ , as 1.25 g/cm^3 and MW of the repeat unit as 72 gave reasonably close values of 19.6, 18.6 and 19.9 $\text{MPa}^{1/2}$, respectively (Table 4.1).

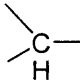
All calculations were based on Equations 4.1 and 4.2 but with different values for E_{coh} and V .

$$E_{coh} = \frac{F^2}{V} \quad (4.2)$$

where F is the group molar attraction constant.

From the a structural point of view [93], IL-4 and IL-5 both have long alkyl chains in the cation which can improve the miscibility with PLA by secondary bonding or interaction with the hydrocarbon backbone in PLA.

Table 4.1 Group Contributions to F [92]

Values	Small	Van Krevelen	Hoy
—CH ₃	438	420	303.4
—COO—	634	512	668
	57	140	176

4.1.1 Predicted Miscibility of IL-4 and PLA

The group contributions to cohesive energy and molar volume method by the Fedors method [94], although apparently less accurate than Small, Van Krevelen and Hoy's methods, contained a larger number of structural groups and could as a result be used for IL-4 that contain elements such as phosphorus. The molar volume of IL-4 is calculated from a density of 0.88 g/cm³ provided from the MSDS (Materials Safety Data Sheet) from Merck & Co., Inc. Fedor's method using equation 4.1, gave a solubility parameter value for PLA of 17.9 MPa^{1/2} (lower than those of the other methods) and a very similar

value for IL-4 (approximately $17.5 \text{ MPa}^{1/2}$). The cohesive energy of groups in IL-4 provided by Fedor and used for the calculation are $-\text{CH}_2$ (4940 J/mol), $-\text{CH}_3$ (4710 J/mol), $-\text{P}$ (9420 J/mol), and $-\text{COO}$ (18000 J/mol) (See Appendix A). Molar volumes of groups used for these calculations were obtained from Table 7.4 of [92] and were very similar to values provided from Cytec [16].

The similarity in the solubility parameters suggests that the IL-4 should be miscible with PLA, as also shown in the literature for other potential PLA plasticizers such as triacetin [95] and citrate oligomers having δ values approaching that of PLA.

It is recognized that the use of the Hansen solubility parameters based on partial parameters corresponding to dispersion forces, dipole-dipole forces and H-bonding would have been more appropriate considering the polar nature of the PLA and the ILs. However, Hansen's data on the phosphorous group necessary for these calculations are not available.

4.1.2 Predicted Miscibility of IL-5 and PLA

The solubility parameter of IL-5 was calculated using a molar volume of $651 \text{ cm}^3/\text{mol}$ [92, 16] by the same group contribution technique described in Section 4.1.1. The cohesive energy of groups provided by Fedors for IL-5 and used for the calculation are $-\text{CH}_2$ (4940 J/mol), $-\text{CH}_3$ (4710 J/mol), P (9420 J/mol), B (13810 J/mol), and F (4190 J/mol) (See also Appendix A). The calculated solubility parameter was $17.4 \text{ MPa}^{1/2}$ which suggests that IL-5 should also be miscible with PLA. It is understood that predictions of miscibility based on solubility parameter are independent of the IL concentration.

4.1.3 Visual Observation

As shown in Figure 4.1, the clarity of PLA/ 5wt% IL-4, and PLA/ 5wt% IL-5 films prepared by melt processing was unchanged, with only a slight yellowish tint vs. the processed neat PLA, indicating either thermodynamic miscibility of PLA with the ILs or an extremely fine dispersion at this particular IL concentration. Incompatibility of the ILs with the amorphous transparent PLA would be expected to result in opacity due to phase separation.

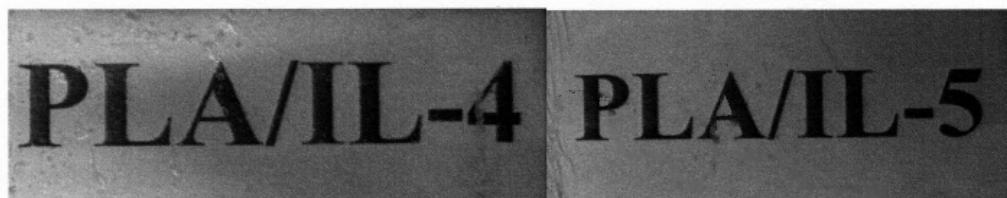


Figure 4.1 Photographs of PLA film samples containing 5 wt% of IL-4 and IL-5.

4.1.4 SEM/EDX

The extent of miscibility or dispersion of the ILs in the cross-sections of PLA/IL-4 and PLA/IL-5 film samples (thickness of 0.1 mm) prepared by melt processing was examined by SEM (Figure 4.2). Some white aggregates of IL-4 particles are observed in Figure 4.2 (b) and fewer aggregates of IL-5 are shown in Figure 4.2 (c). This suggests incomplete dispersion/mixing of the additives in the bulk of the samples.

SEM micrographs and corresponding EDX mapping analysis (Figure 4.3) for PLA/ 5wt% IL-4 film surfaces showed no agglomerates and uniform distribution of the phosphorus element present in the IL cations (Table 4.2). More accurate uniformity in the distribution of the IL-4 anion could not be ascertained by EDX due to the absence of a

characteristic element other than C, H, O. However, from calculations for both cations and anions based on the wt% concentration of the P element, the total amount of IL-4 in PLA was approximately 4.36 wt% which is close to the initial concentration of IL-4 (5 wt%) in the PLA. Considering that EDX results were obtained in various regions of the sample and then averaged, IL-4 appears to be well dispersed and also partly dissolved in the PLA matrix. The presence of the chlorine element in Table 4.2 is attributed to the residual reactants from the IL-4 synthesis [16].

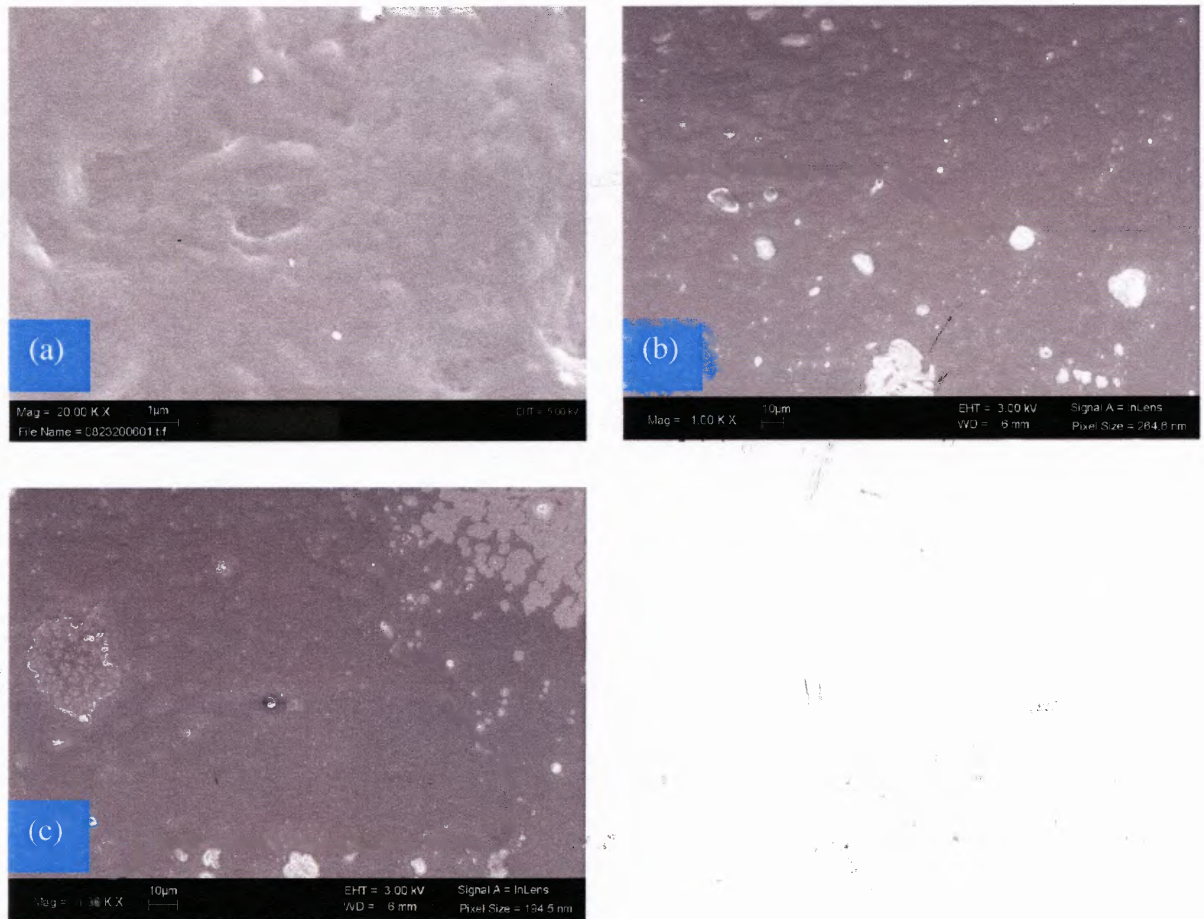


Figure 4.2 SEM micrographs of cross-sections of (a) PLA, (b) PLA/ 5wt% IL-4, and (c) PLA/ 5wt% IL-5 produced by melt processing.

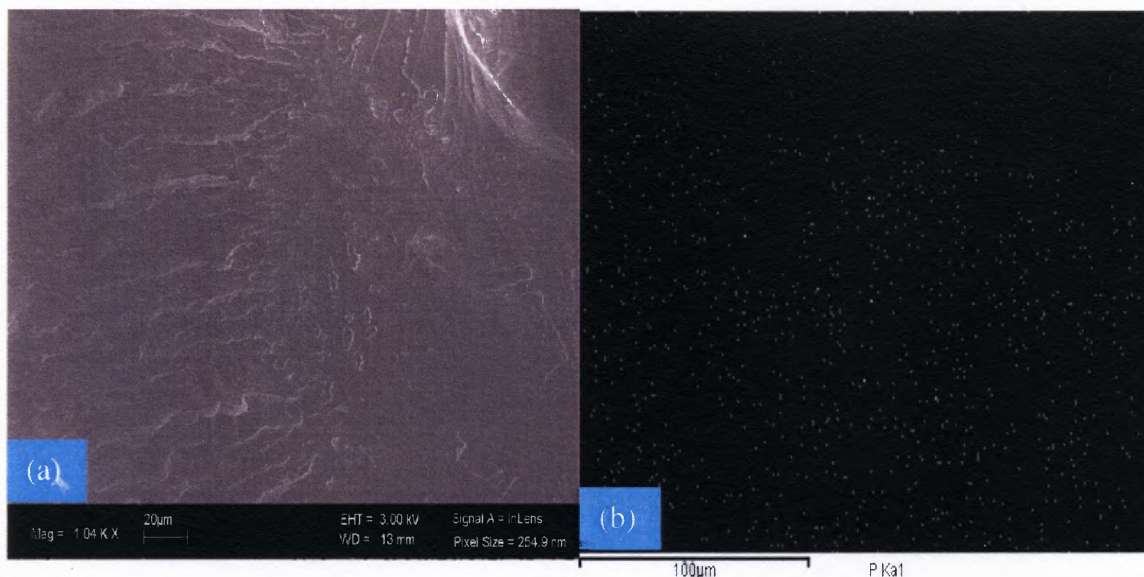


Figure 4.3 (a) SEM micrograph of the surface of PLA/ 5wt% IL-4 and (b) EDX elemental mapping of phosphorous.

Table 4.2 EDX Elemental Analysis of PLA/ 5wt% IL-4 Surface

Element	Weight%	Atomic%
C	56.66	63.91
O	41.59	35.22
P	0.20	0.10
Cl	0.32	0.12
Totals	100.00	

SEM micrograph of a PLA/IL-5 surface and a corresponding mapping for phosphorous (cation) and fluorine (anion) elements are shown in Figure 4.4. Note that the light boron element cannot be detected by EDX. The results suggest uniform distribution of IL-5 on a small scale (and partial dissolution) although the presence of coarser agglomerates is still a possibility.

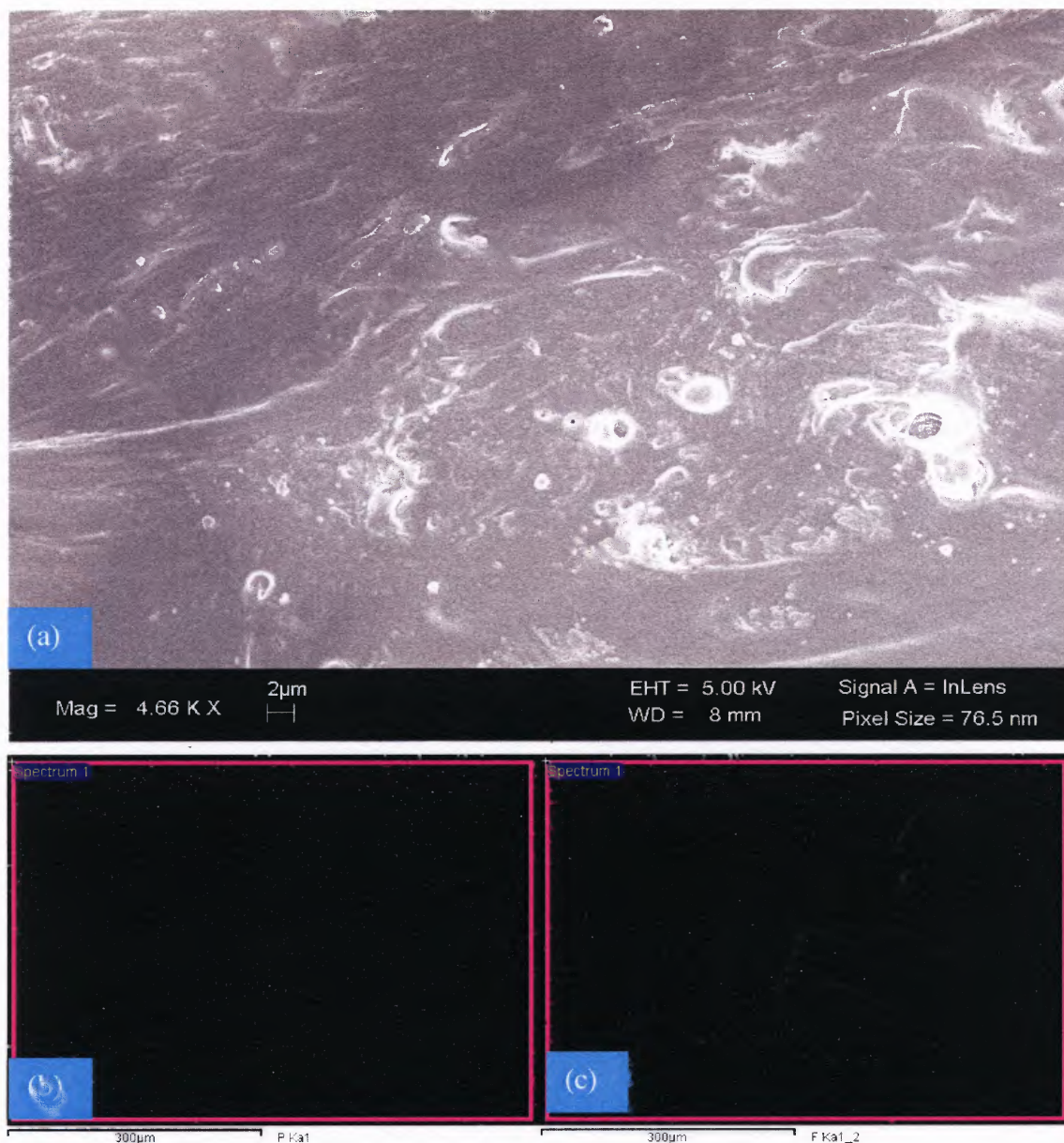


Figure 4.4 (a) SEM micrograph of the surface of PLA/ 5wt% IL-5, (b) EDX elemental mapping of phosphorous, and (c) EDX elemental mapping of fluorine.

As shown in Table 4.3 the P: F ratio 0.29 which is close to the theoretical value of 0.36 calculated from the structural formula of IL-5. This suggests that there is no segregation of cations or anions on the surface of PLA/ 5wt% IL-5.

Table 4.3 EDX Elemental Analysis of PLA/ 5wt% IL-5 Surface

Element	Weight%	Atomic%
C	55.29	62.31
O	43.74	37.01
F	0.96	0.69
P	0.28	0.12
Totals	100.00	

Elemental EDX mapping of ILs has been used by other authors to determine uniformity of their distribution in a polymer matrix. Sanes et al. [32] prepared polymer/ 10wt% IL blends using polystyrene, PS, and 1-ethyl-3-methyl imidazolium tetrafluoroborate, $[EMIM]^+[BF_4]^-$. EDX results of the mixture on fractured surfaces showed a heterogeneous phase distribution where in dark grey regions attributed to the IL elements such as fluorine, nitrogen, etc were detected. This non-uniform IL distribution may due to either the high concentration of IL in PS or the poor miscibility of PS and $[EMIM]^+[BF_4]^-$.

4.1.5 Phase Separation of ILs in PLA

The cross-section of PLA/ 5wt% IL-4 after one year showed uniformly dispersed phases of PLA and IL-4 (Figure 4.5). By contrast, a distinct sign of phase separation (Figure 4.6) of PLA/ 5wt% IL-5 after a long time period of one year was detected by SEM resulting from agglomerated white phases on the cross-section of the fractured sample. This phenomenon suggests that PLA/ 5wt% IL-5 tends to have relatively poor long-term miscibility and compatibility of the IL-5 and PLA.

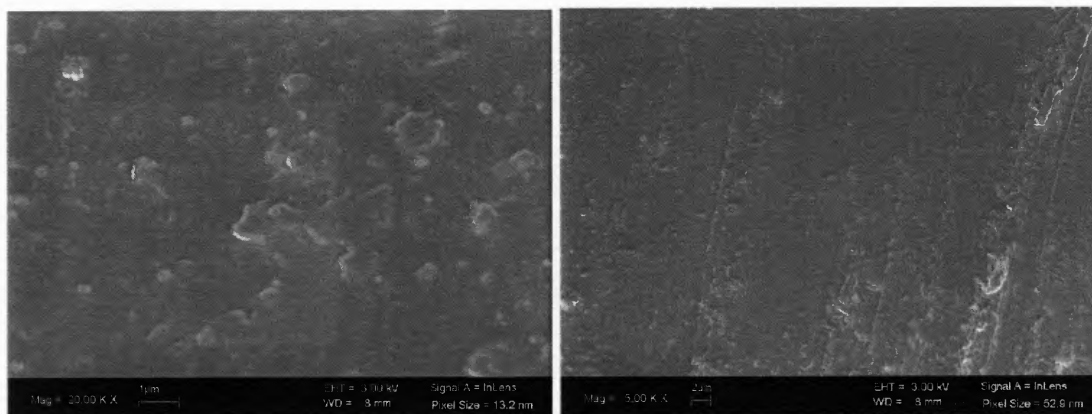


Figure 4.5 SEM micrograph on fractured surface of PLA/ 5wt% IL-4 after one year from melt processing.

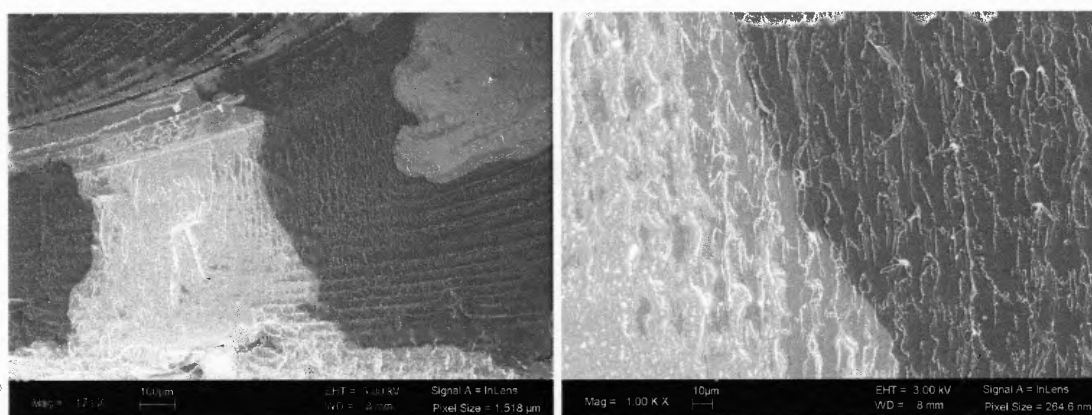


Figure 4.6 SEM micrograph on fractured surface of PLA/ 5wt% IL-5 one year after melt processing.

Compared to PLA/ 5wt% IL-5, PLA/ 5wt% IL-4 contains bulky organic hydrophobic anions with several carbon, oxygen, and hydrogen, atoms, which may possibly form secondary bonding or otherwise interact with PLA, thus restraining their movement and diffusion along the polymer network.

Rahman et al. [29] observed a similar case of phase separation as the one observed in this study. After UV exposure, PVC with 20 wt% [thtdPh⁺][Tf2N⁻] exhibited phase separation that was visually observable. SEM images of cross-sections of the UV exposed sample showed distinct phase separation and layering of the [thtdPh⁺][Tf2N⁻]

molecules along the sides of the sample.

4.1.6 Glass Transition Temperature

DSC scans of melt processed samples were carried out in order to confirm the miscibility of ILs with PLA by determining the T_g of the blends. Figure 4.7 shows DSC scans of the PLA/ILs blends. The T_g was taken as the midpoint of the inflection. For pure PLA, the T_g was observed at approximately 60 °C and decreased with increasing concentration of IL. At 10 wt% IL-4 (the more effective additive), the T_g decreased to approximately 45 °C, which is at the same level as that attained with polyethylene glycol, PEG, conventional plasticizers . No glass transition temperature was detectable for either IL-4 or IL-5 at temperatures as low as -30 °C. Thus, both ILs can be considered as plasticizers with efficiency depending on their type and concentration. (Table 4.4)

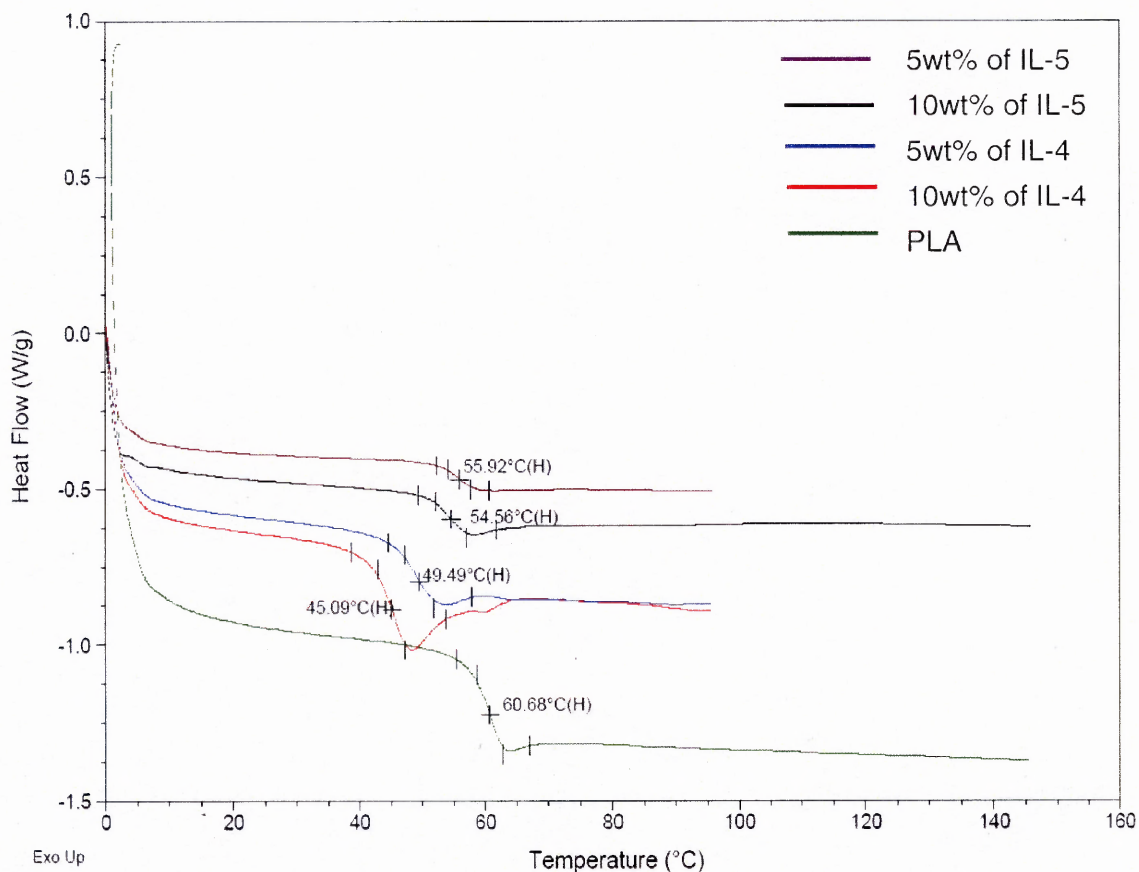


Figure 4.7 DSC comparison of PLA vs. PLA containing different wt% of IL-4 and IL-5.

Table 4.4 T_g Comparison of PLA vs. PLA Containing Different wt% of IL-4 and IL-5

Sample	T_g (°C)
PLA	60.7
PLA/ 5wt% IL-4	49.5
PLA/ 10wt% IL-4	45.1
PLA/ 5wt% IL-5	55.9
PLA/ 10wt% IL-5	54.5

Polymer plasticization involves the entrance of smaller plasticizer molecules into the matrix allowing more slipping and flexibility of the polymer molecules. Thus, the smaller plasticizer molecules increase the interchain distance between the large polymer molecules reducing their entanglements and, thus, lowering the glass transition temperature. ILs used as plasticizers can also change T_g by increasing free space and volume of polymer and allowing polymer segment mobility even at lower temperatures. ILs used in this study have anions with different values of molar volume as calculated from density and MW: IL-4 has a higher molar volume of $744.5\text{cm}^3/\text{mol}$ while the molar volume of IL-5 is $651\text{cm}^3/\text{mol}$. The higher molar volume of the anions in IL-4 and their enhanced organophilic interactions with the PLA hydrocarbon backbone should more effectively lower T_g than IL-5.

It should be noted that T_g decreases with decreasing M_n , according to the Equation 4.7 [96].

$$T_g = T_g^\infty - C/M_n \quad (4.7)$$

T_g^∞ is the glass transition temperature at infinite polymer molecular weight and C is a constant whose units are $^\circ\text{K mol g}^{-1}$.

Thus, direct comparison of the effects of the ILs on T_g would only be possible if no MW changes took place during blending. As will be shown in later chapters, both ILs reduced the MW of PLA to different degrees, acting catalytically. Therefore the reduction of the T_g of PLA could be the result of a combined plasticization/degradation effect.

4.2 Thermal Stability of ILs/PLA by TGA

Figures 4.8 and 4.9 compare the thermal stabilities under nitrogen of single components and blends produced by melt mixing. In terms of increasing thermal stability the blend components are classified as IL-5>PLA pellets>IL-4 (Fig.4.8). IL-5 lost about 50 wt% of its initial weight at approximately 485 °C whereas IL-4 lost half of its initial weight at approximately 360 °C. PLA/IL-4 blends have lower thermal stability than PLA/IL-5 blends (Figure 4.9) (due to the inherent lower thermal stability of IL-4) and both blends have lower thermal stability than the non-processed PLA pellets. Although both ILs have the same phosphonium based cation, IL-4 caused the most rapid weight loss of PLA while PLA/IL-5 was relatively stable. This leads to the conclusion that IL-4 displays a more intensive catalytic degradative effect compared to IL-5.

PLA/ 5wt% IL-5 lost 10 wt% of its initial weight at approximately 360 °C. The temperature at which PLA/PEG (conventional plasticizer for PLA) loses 10wt% of its initial weight is about 300 °C [97] under at similar TGA operating conditions. This may be due to the presence of the phosphonium based cations which are known as thermally stable [98] resulting, thus, in a plasticized compound with higher stability than PLA/PEG.

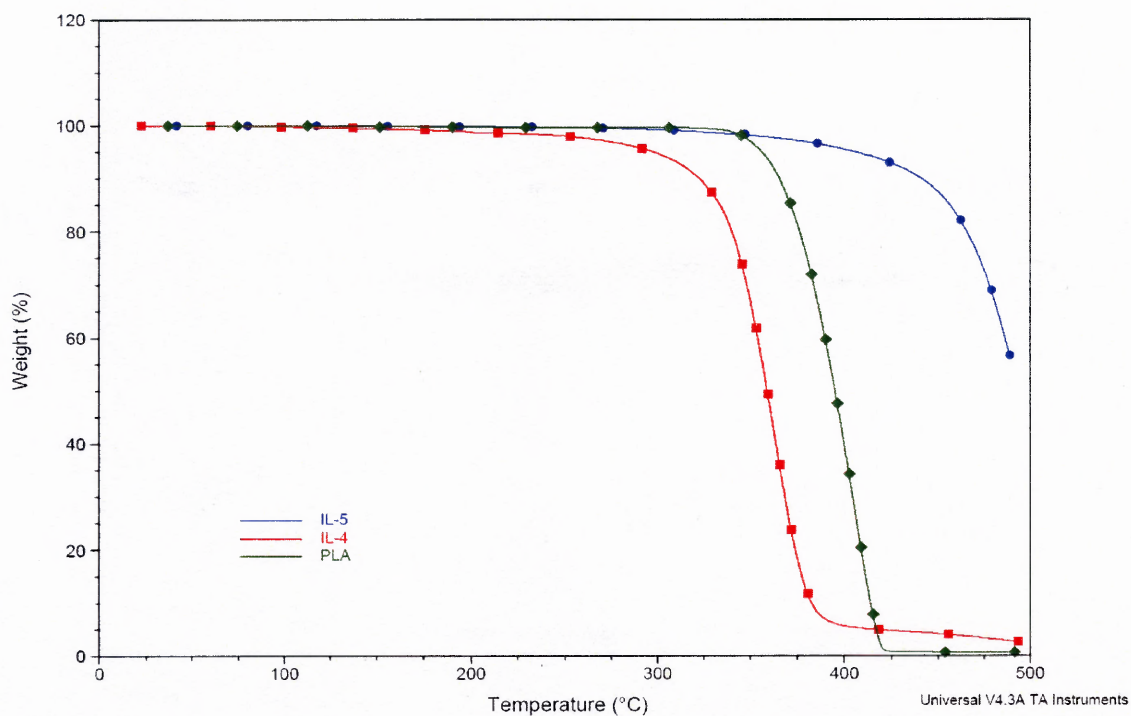


Figure 4.8 TGA comparison of IL-4, IL-5 and processed PLA.

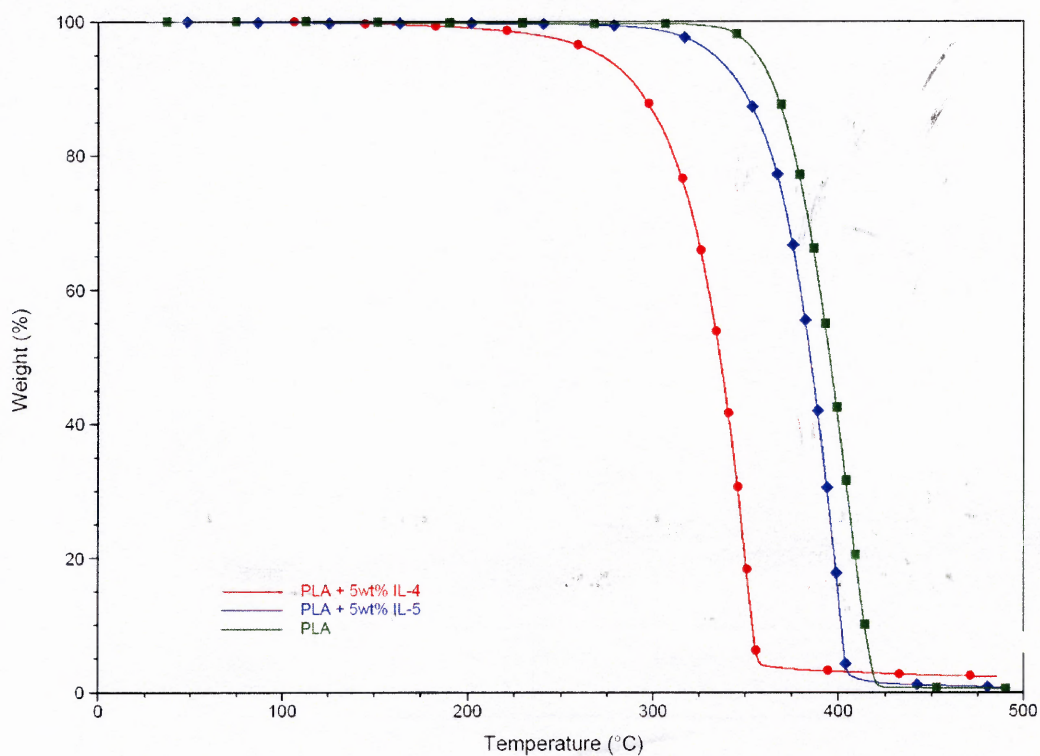


Figure 4.9 TGA comparison of processed PLA with PLA containing 5wt% of IL-4 and IL-5.

4.2.1 Activation Energy by TGA

The thermal decomposition activation energy, E_a , of PLA, PLA/IL-4, and PLA/IL-5 was calculated based on the TGA results in Section 4.2. In general, E_a is associated with the lowest energy needed for degradation and, thus, high E_a indicates high thermal stability. The kinetic parameters given by the Friedman technique (Section 2.3.1) are somewhat lower than those derived from the Freeman-Carroll and Chang methods [99]. The reason that the Friedman technique was used in this study is that the E_a values represent the thermal decomposition behavior in the temperature range from (onset degradation temp. – [20 ~ 40] K) to the onset degradation temp., in which the linear relation between $\ln(d\alpha/dt)$ and $1/T$ (Eq. 2.3) is available [100].

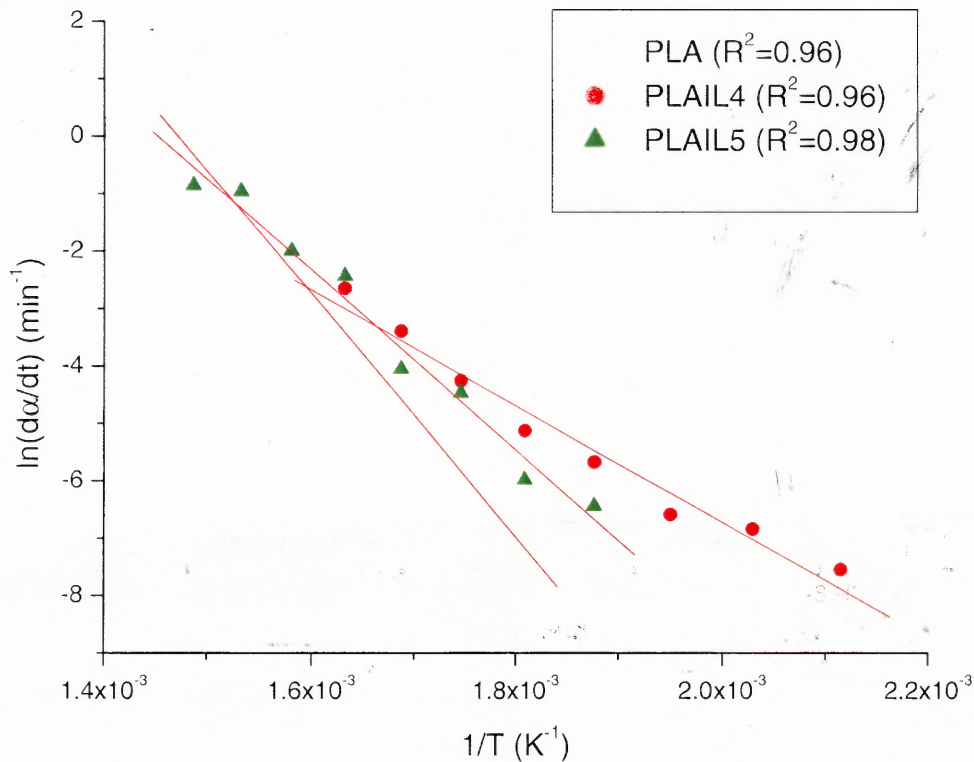


Figure 4.10 Friedman plots of $\ln(d\alpha/dt)$ or $\ln(1-\alpha)$ vs. $1/T$ for the direct calculation of E_a of thermal degradation at a heating rate of $20 \text{ }^\circ\text{C}/\text{min}$ under nitrogen.

In plotting TGA data, the temperature range was from about 200 °C to a temperature corresponding to 10% weight remaining for each sample.

The calculated E_a values from Figure 4.10 are 176.3 kJ/mol, 84.8 kJ/mol, and 130.3 kJ/mol for PLA, PLA/IL-4, and PLA/IL-5 respectively. High R^2 are calculated for each case. This suggests that PLA and PLA/IL-5 have higher thermal stability than PLA/IL-4 in agreement with Section 4.4.1.

4.3 Flow Characteristics of ILs/PLA

4.3.1 Capillary Rheometer

Figure 4.11 contains viscosity /shear rate curves for PLA and PLA/IL-5 samples prepared by melt mixing. It is evident that IL-5 produces significant reductions in the PLA apparent viscosity, proportional to its increasing concentration. The apparent viscosity of PLA/IL-5 (10 wt%) is 57.3 Pa·s while that of PLA is 531.6 Pa·s at 384 s^{-1} and 190 °C. In addition, while PLA/IL-5 (10 wt%) exhibits a marked negative dependence of apparent viscosity vs. apparent shear rate in the range relevant for processing, the viscosity of PLA decreases only slightly when the shear rate increases.

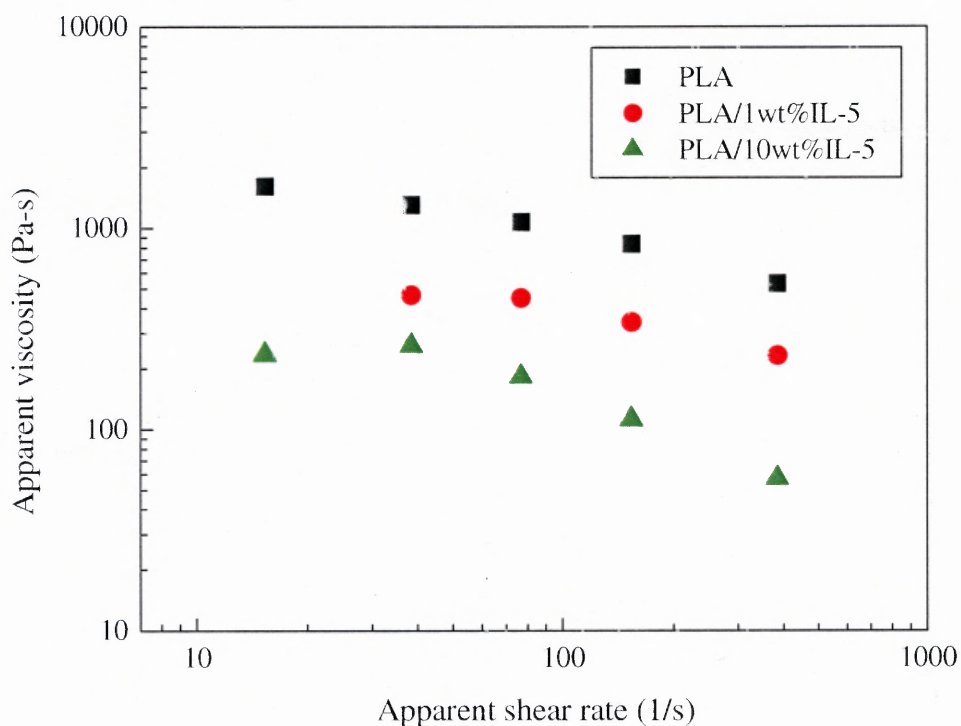


Figure 4.11 Apparent viscosity vs. apparent shear rate curves of PLA and PLA/IL-5 blends.

Viscosity reduction was observed for PLA/IL-4 (1wt% IL-4). However, viscosity measurements at any of the other IL-4 concentrations used (5 % and 10 %) were not possible, even with a smaller diameter die due to very low values as a result of degradation and lubrication effects. This is consistent with reports that carboxylic acids (including decanoic acid) additives in thermoplastics migrate to the steel walls of the capillary instrument and induce slippage by the formation of a lubricating layer; also, with our batch mixing results where torque could not be measured when ILs were added directly in the molten PLA (See also Section 4.3.3).

4.3.2 Helical Barrel Rheometer (HBR)

Figure 4.12 shows the shear viscosity obtained with HBR of PLA, PLA/ 5wt% IL-4, and PLA/ 5wt% IL-5 versus time at 160 °C. The results show that PLA/ 5wt% IL-4 has the lowest viscosity decreasing continuously during the entire experimental period. After 20 minutes, no shear viscosity data could be collected similarly to the absence of data in the batch mixer at higher than 1wt% IL-4 concentration.

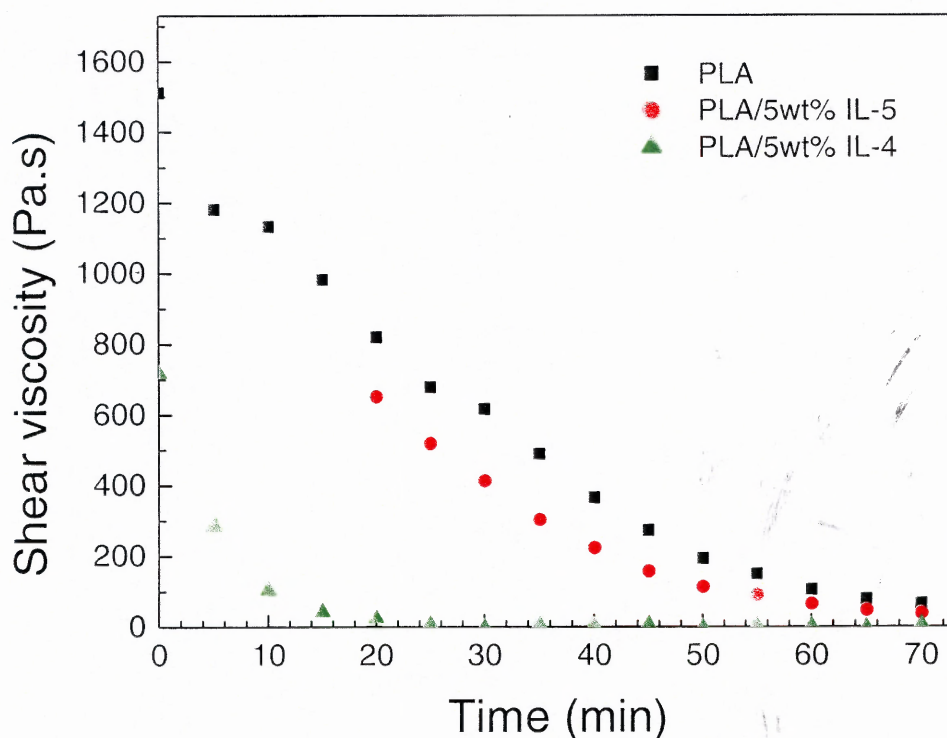


Figure 4.12 Shear viscosity comparison of PLA, PLA/ 5wt% IL-4 and PLA/ 5 wt% IL-5.

This may be due to lubrication and also excessive thermal degradation within the first 20 minutes catalyzed by the decanoate anions and the lubricating effect of carboxylic

groups of IL-4 as mentioned also in Section 4.3.1. In the case of PLA and PLA/ 5wt% IL-5, in agreement with the results of the capillary viscometry, PLA/IL-5 showed a lower viscosity and less tendency to degradation. As shown in Sections 4.3.1 and 4.3.2, both IL-4 and IL-5 reduced viscosities of PLA/ILs, to different degrees, and could be potentially used as internal lubricants to improve flow characteristics.

4.3.3 Torque Curves during Melt Mixing

As shown in Figure 4.13, at a concentration of 5 wt% IL-4 in PLA, torque dropped to zero, two minutes after addition of the neat PLA pellets to 10 wt% PLA/IL-4 pre-coated pellets. Again, this may be due to migration of the carboxylated additive in PLA to the steel rotors of the batch mixer to induce slippage by the formation of a lubricating layer [101].

At 5 wt% IL-5 the torque increased somewhat at approximately 1 minute after the addition of the PLA pellets and remained more or less steady throughout the mixing period. At all times, torque values of PLA/ILs were lower than the torque levels attained by the PLA alone. At 10 wt% IL-4 concentrations (data not shown), torque was practically zero at the time of addition and remained zero until the end of the mixing period. At 10 wt% of IL-5 (data not shown), torque decreased gradually from the time of addition but was still measurable. At 1 wt% of ILs, (data not shown) torque values were measurable for both ILs, however, torque decreased much more rapidly in the case of PLA/IL-4.

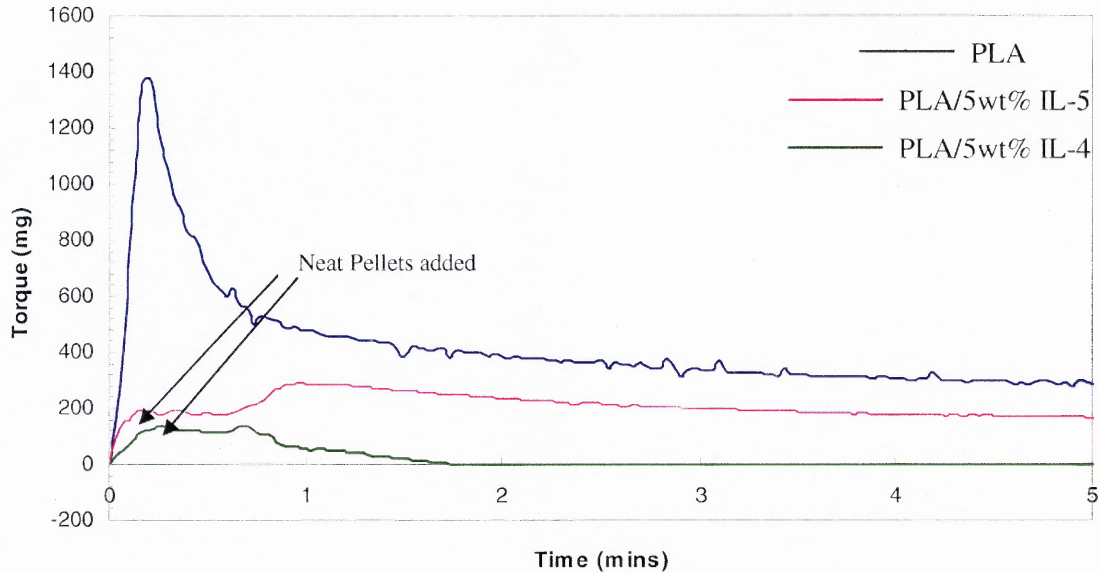


Figure 4.13 Torque curves of PLA and PLA/IL blends during batch mixing.

These experiments confirm the significant differences of the effects of the two ILs on the flow characteristics of PLA in terms of lubrication, plasticization and degradation, all at much more pronounced levels in the case of IL-4.

4.4 Isothermal Degradation of PLA and PLA/ILs

4.4.1 Weight Changes as a Function of Time

As shown in Figure. 4.14, unmodified PLA was relatively stable up to 140 hours, whereas the addition of both ILs deteriorated its thermal stability to different extents. The times at which samples lost 10 wt% of their initial weights are 120 hours (PLA), 55 hours (PLA/IL-5), and 12 hours (PLA/IL-4). IL-5 produced a more thermally stable plasticized PLA sample than IL-4. PLA/IL-4 lost weight rapidly after few hours and ended up losing 60 wt% of its initial weight at around 140 hours. A significant observation was that, up to

45 hours, PLA/IL-5 was the most stable sample while PLA and PLA/IL-4 had lost up to 10 wt% and 38 wt% of their weights, respectively. (Figure 4.14)

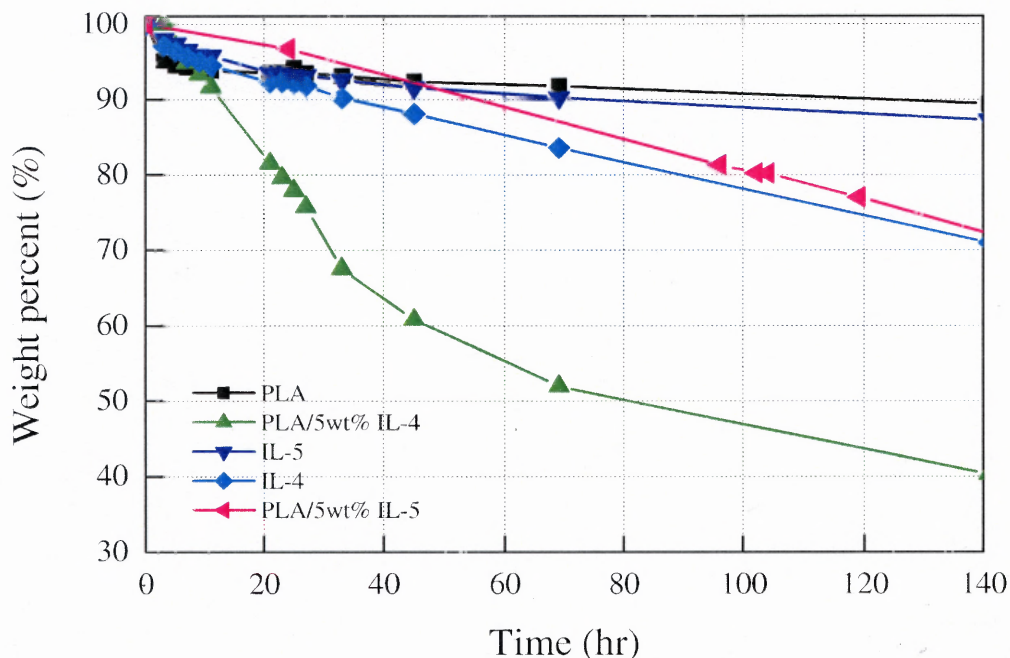


Figure 4.14 Weight loss of PLA, IL-4, IL-5, PLA/ 5wt% IL-4, and PLA/ 5wt% IL-5 as a function of thermal degradation time at 160 °C in air.

With respect to the ILs, IL-5 displayed better thermal stability compared with IL-4, losing ~12 wt% or less of its initial weight up to 140 hours, whereas IL-4 lost ~30 wt% weight of its initial weight. Same stability trends were observed earlier by TGA (Figure 4.9) although in the latter case the experiments were conducted under nitrogen. The significantly higher weight loss for the PLA/IL-4 cannot only be explained by the inherent lower thermal stability of IL-4; a catalytic degradative effect due the presence of the decanoate anion may play a major role as also shown by [29] for PVC/[thtdPh⁺][deca⁻] (Table 2.1).

4.4.2 Molecular Weight Changes as a Function of Time

Table 4.5 contains molecular weight data, obtained by GPC, for PLA and its blends with IL-4 and IL-5, before and after isothermal degradation.

Table 4.5 MW Changes of Melt Processed PLA, PLA/ 5wt% IL-4 and PLA/ 5wt% IL-5 before and after Isothermal Heating at 160°C; M_p , M_n , and M_w are Peak MW, Number Average MW, and Weight Average MW, Respectively

Samples Thermal treatment	PLA $M_p (M_n, M_w)$	PLA/IL-4 $M_p (M_n, M_w)$	PLA/IL-5 $M_p (M_n, M_w)$
None	168880 (113200, 172260)	N/A	N/A
After melt processing	154950 (113200, 161090)	62930 (39327, 62520)	185900 (126740, 196920)
4 hours heating	143030 (103620, 145040)	-	139640 (97080, 142900)
6 hours heating	145470 (96350, 141360)	22620 (20930, 25380)	128310 (78260, 129630)
8 hours heating	129230 (91900, 131270)	17550 (16500, 18560)	140630 (89890, 137470)
19 hours heating	138280 (88640, 146450)	24060 (19020, 27170)	95330 (57300, 99350)
50 hours heating	109110 (85790, 117460)	-	79120 (52030, 86240)

Molecular weights in the Table are expressed as M_p (Peak MW), M_n (number average MW) and M_w (weight average MW). The data were most often based on single point measurements on degraded, small samples, having complex and possibly non-uniform composition; as a result some observed discrepancies are as expected. Overall, however, some reasonable trends can be observed.

As expected the MW of PLA decreases somewhat after melt processing and by about 27% after 50 hours isothermal heating at 160 °C. The PLA/ 5wt% IL-4 underwent the most rapid degradation after melt processing and the polymer MW decreased further to very low values after 19 hours isothermal heating. Although the PLA/ 5wt% IL-5 had an abnormally high MW value after melt processing, the polymer MW began decreasing upon isothermal heating, however, more rapidly than that of the unmodified PLA. The data are in agreement with the previously obtained differences in thermal stability of the three materials.

4.4.3 Thermal Degradation and Modeling

4.4.3.1 Degradation Rate Constant. Many researchers have studied degradation mechanisms of aliphatic polyesters and derived mathematical models to fit experimental data [102, 103]. Emsley and Heywood [104] used the following equation that accounts for the relationship between degree of polymerization and time based on random chain scission model.

$$1/DP_t - 1/DP_0 = kt \quad (4.8)$$

where DP_t is degree of polymerization at time t , DP_0 is initial degree of polymerization, and k is degradation rate constant.

Calculated DP values in this work were based on number average molecular weight. $1/DP$ of was plotted vs. time according to Equation 4.8. As shown in Figure 4.15, all systems obeyed a reasonable linearity up to 19 hours which allowed the calculation and comparison of the initial rate constants. The derived k values were $8.5 \times 10^{-6} \text{ s}^{-1}$, $3.05 \times 10^{-4} \text{ s}^{-1}$, and $3.42 \times 10^{-5} \text{ s}^{-1}$, for PLA, PLA/IL-4, and PLA/IL-5, respectively. The corresponding R^2 values were 0.88, 0.99, and 0.96. The calculated rate constant values by equation 4.81 were higher for both ILs modified PLA than the unmodified polymer. The high R^2 values also confirm that the thermal degradation of PLA in the presence of the ILs occurs by the same chain scission mechanism that is assumed in the derivation of Equation 4.8.

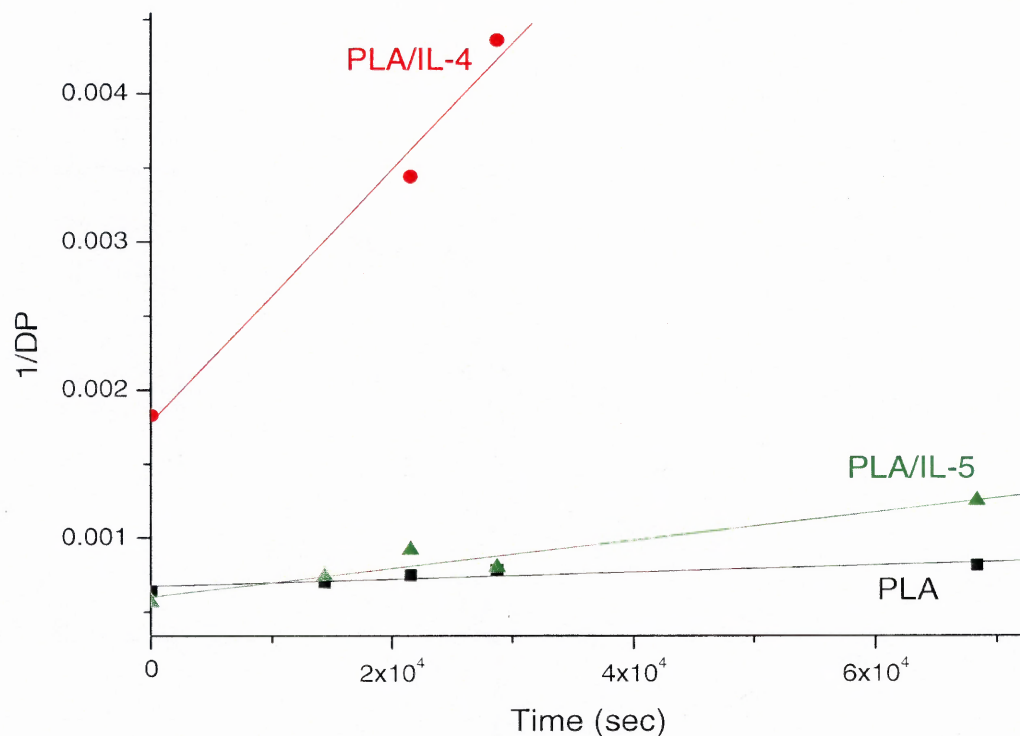


Figure 4.15 Thermal degradation data up to 19 hours for PLA, PLA/IL-4, and PLA/IL-5 based on $1/DP$ and Equation 4.8.

4.5 Hydrolytic Degradation of PLA and PLA/ILs

4.5.1 Visual Observation

PLA, PLA/ 5wt% IL-4 and PLA/ 5wt% IL-5 plates used for hydrolytic degradation were initially transparent in agreement with the amorphous structure of the PLA and the assumed PLA/IL miscibility as suggested by our T_g data (Figure 4.7) and the calculated solubility parameters. In the degradation medium, PBS, at 60 °C, the surface of all samples became rapidly white in the order : PLA/ 5wt% IL-4,>PLA/ 5wt% IL-5,> PLA which is presumably due to the crystallization of the amorphous PLA as its MW decreases (see also Section 4.6.3). For all samples, differentiation between surface and interior was clearly detectable, surface being white while interior being transparent. This

may due to the the neutralization of carboxylic end groups located at the surface by the external buffer solution and the diffusion of the soluble oligomers from the surface [105].

In the case of PLA/ 5wt% IL-4, after 144 hours, full breakdown took place and residues remained in the form of a white powder. Both PLA and PLA/ 5wt% IL-5 samples after 144 hours, as shown in Figure 4.16, became rough on their surface and very fragile when bent.

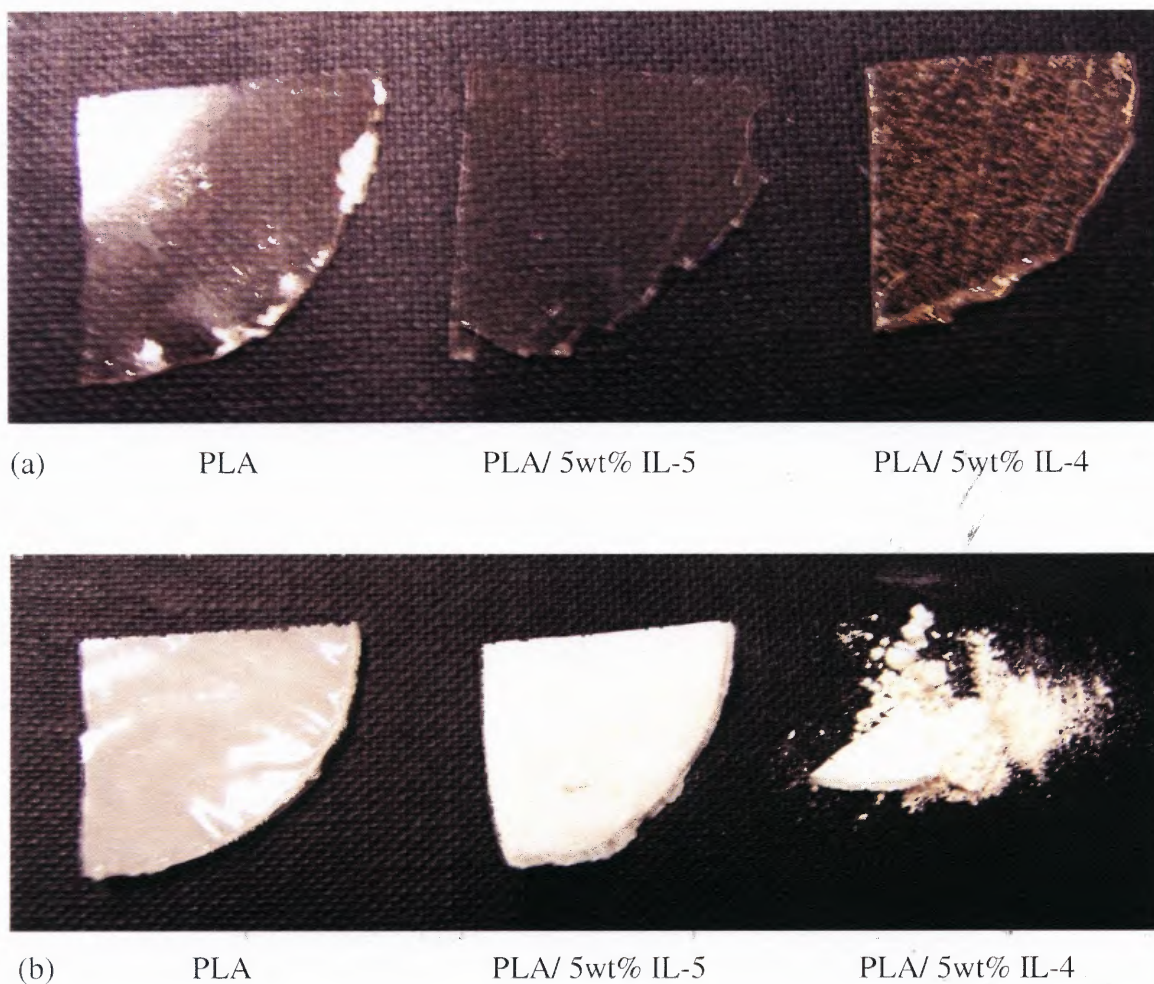


Figure 4.16 (a) PLA, PLA/ 5wt% IL-5 and PLA/ 5wt% IL-4 before hydrolytic degradation. (b) PLA, PLA/ 5wt% IL-5 and PLA/ 5wt% IL-4 after 144 hours of hydrolytic degradation.

4.5.2 Molecular Weight Changes as a Function of Time

MW changes of melt mixed samples after 6 days of hydrolytic degradation indicate that both IL-4 and IL-5 accelerate the degradation of PLA (Table 4.6); however, as in the case of thermal degradation, the effects of IL-4 are much more pronounced. Peak molecular weight, M_p , values by GPC after 144 hours were 65,353 (PLA) vs. 3,543 (PLA/IL-4) and 37,053 (PLA/IL-5).

Table 4.6 Peak MW, M_p , Changes of PLA, PLA/ 5wt% IL-4 and PLA/ 5wt% IL-5 before and after Hydrolytic Degradation (144 hrs)

Treatment \ Samples	M_p PLA	M_p PLA/IL-4	M_p PLA/IL-5
None	168880	N/A	N/A
After melt processing	154950	62970	185900
After melt processing followed by 144 hrs hydrolytic degradation	65350	3540	37050

It is known that PLA degradation is acid catalyzed, particularly in the presence of carboxylic groups [106]; this could explain the significant effect of the decanoate anion. On the other hand, the BF_4^- anion of IL-5 could also accelerate the degradation by forming HF in water [16]. To investigate the relative contributions of the cation and the anion to the degradation of PLA, model compounds (PLA/DECA, PLA/MMT-0, and PLA/MMT-4) were prepared. The effects of the cations and anions on the polymer peak

MW after 144 hrs hydrolytic degradation are shown in Table 4.7

Table 4.7 Peak MW, M_p , Changes of PLA, PLA/MMT-0, PLA/MMT-4, PLA/IL-4, and PLA/decanoic Acid Prepared by the Solvent Casting Method after 144 hrs Hydrolytic Degradation

	As prepared	After 144 hrs hydrolytic degradation
PLA	162280	89100
PLA/MMT-0 (untreated MMT control)	167950	80310
PLA/MMT-4 (phosphonium cation modified MMT)	156810	34650
PLA/IL-4(phosphonium cation/decanoate anion)	29000	750
PLA/DECA	111260	20010

Unmodified MMT-0 appears to have little, if any, catalytic effect on the polymer degradation. The presence, however, of the phosphonium cation on the MMT (MMT-4) although having little effect on the polymer MW of the “as prepared” samples does have a significant effect on the samples subjected to hydrolytic degradation. Decanoic acid and its anion contribute somewhat to degradation of both the “as prepared” samples and

much more to the ones subjected to hydrolytic degradation. IL-4 containing a combination of phosphonium and decanoate ions appears to catalyze degradation of both the “as prepared” samples and also those subjected to hydrolytic degradation. In summary, both phosphonium cations and decanoate anions play a significant role in the PLA degradation with the catalytic effect more pronounced for the decanoate anion. It should be noted that IL tributylhexacecyl phosphonium bromide containing the same phosphonium cation has been reported to be an effective catalyst in the alkaline hydrolysis of polyethylene terephthalate (PET) [107].

4.5.3 Scanning Electron Microscopy

The morphological changes due to the incubation in PBS were visualized by SEM micrographs of specimens collected at certain time periods of time. Figure 4.17 shows SEM micrographs of PLA, PLA/IL-4 and PLA/IL-5 before and after 144 hours of hydrolytic degradation. Both PLA/IL-4 and PLA/IL-5 samples display rough surfaces and porosity compared to PLA. The pictures, clearly, revealed that all the surfaces of PLA/IL blends were degraded. The effects are much more pronounced for the PLA/IL-4 sample that is characterized by accelerated degradation.

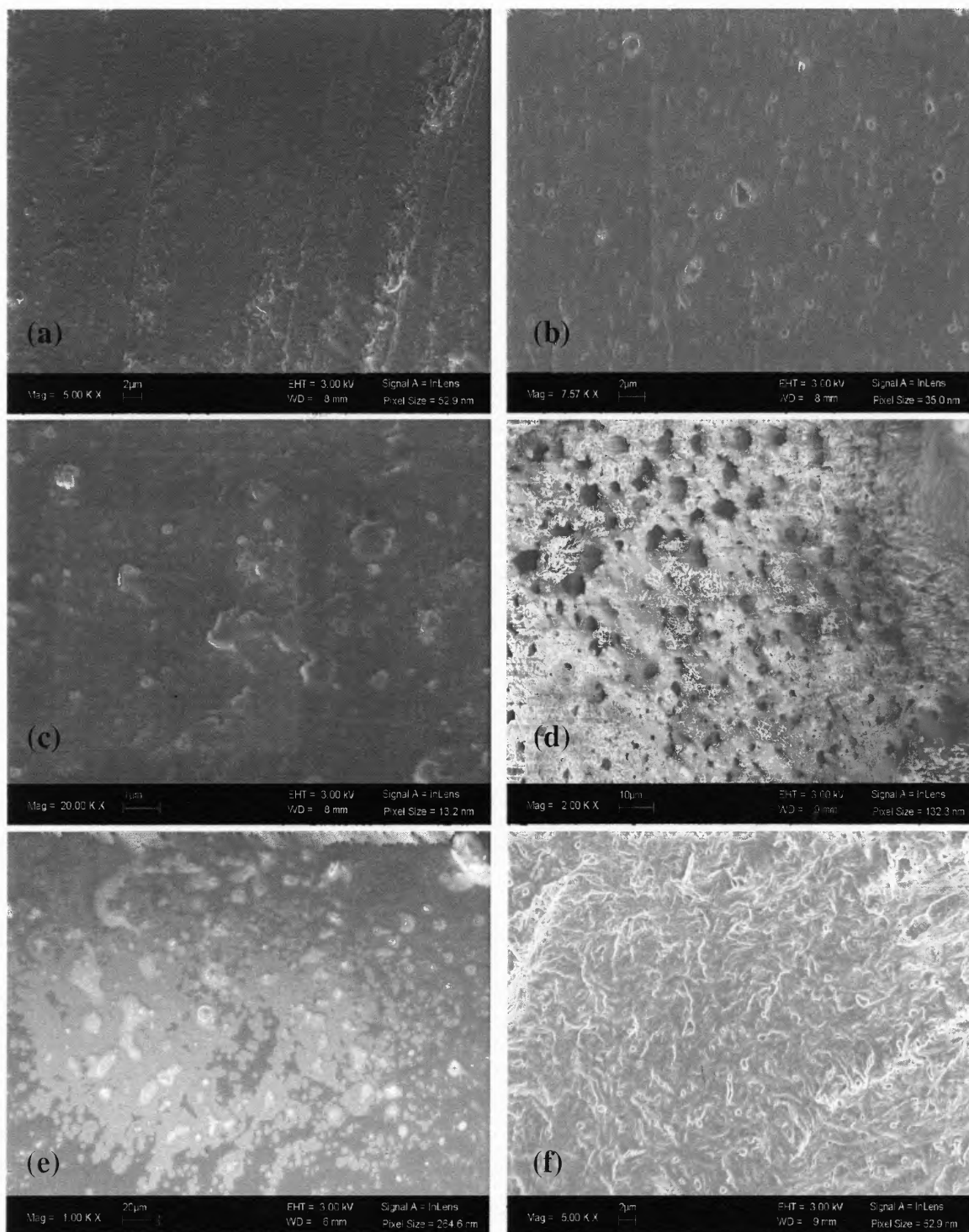


Figure 4.17 (a) SEM micrograph of PLA before immersion in PBS. (b) SEM micrograph of PLA after 144 hours of immersion in PBS. (c) SEM micrograph of PLA/ IL-4 before immersion in PBS. (d) SEM micrograph of PLA/IL-4 after 144 hours of immersion in PBS. (e) SEM micrograph of PLA/ IL-5 before immersion in PBS. (f) SEM micrograph of PLA/IL-5 after 144 hours of immersion in PBS.

Average pore sizes increased in the order of PLA, PLA/IL-5, and PLA/IL-4 (0.3 μm , 1 μm , 5 μm) (see Appendix B), confirming the rapid acceleration of degradation by both IL-4 and IL-5, but in particular IL-4. It is known that degradation causes an increase in the number of carboxylic acid chain ends which are known to autocatalyze ester hydrolysis. In the case of IL-4, additional degradation appears to be due to the presence of decanoate anions/decanoic acid in the hydrolysis medium.

4.5.4 Acid Number and pH Changes as a Function of Time

Figure 4.18 shows the pH of the degradation medium at different incubation times. In the case of PLA/ 5wt% IL-4, as mentioned before, the presence of decanoic acid in the degradation medium could catalyze and accelerate the hydrolysis of other ester bonds. The pH decreases due to polymer degradation involving autocatalysis, resulting in increase of $-\text{COOH}$ concentration. PLA/ 5wt% IL-5 is forming a byproduct (HF) which could also decrease the pH value of the degradation medium [16]. However, it is understood that HF could react with the silicate glass of the container thus affecting the pH reading. The pH of the PBS containing immersed PLA and PLA/ 5wt% IL-5 remained stable for the first 3 days whereas for the PLA/ 5wt% IL-4 system it dropped down to 3.5 in 5 days. In the case of PLA, pH decreased slightly between 10 and 12 days followed by rapid decrease to 4 between 13 and 16 days, due to formation of acidic oligomers/monomer. The pH change of PLA/ 5wt% IL-4 was the most rapid among the samples, in agreement with the MW changes of PLA/ 5wt% IL-4 after 6 days of hydrolytic degradation.

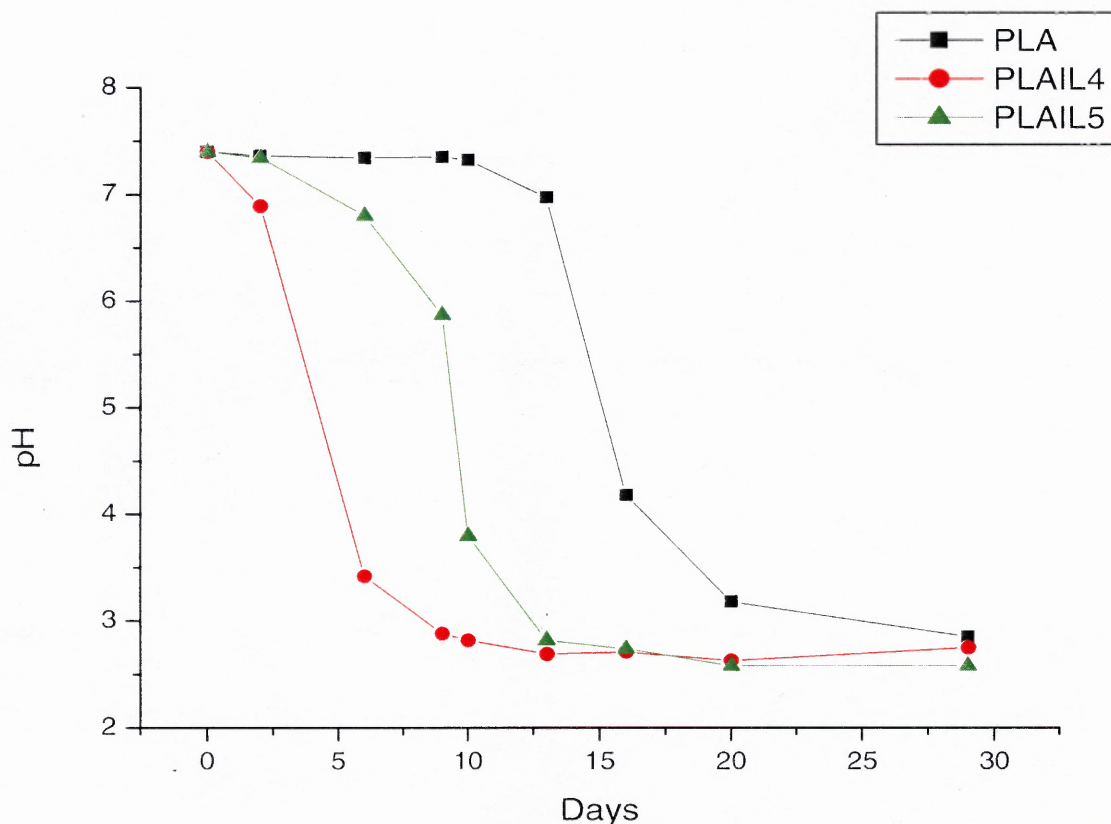


Figure 4.18 pH changes of PBS during hydrolytic degradation.

During hydrolytic degradation, as shown in Table 4.8, acid numbers of PLA, PLA/ 5wt% IL-4, and PLA/ 5wt% IL-5 increased as a result of the formation of acidic oligomers, lactic acid monomer as well as the contributions of the individual ILs. The initial value of PLA/ 5wt% IL-4 is relatively higher than that of other samples due to the contribution of the more acidic IL-4. The system PLA/ 5wt% IL-4, contributing to the most rapid degradation showed again the largest increase of acid number after immersion.

Table 4.8 Acid Numbers before and after Hydrolytic Degradation

Sample	Acid number (control)	Acid number (after 6 days of hydrolytic degradation)
PLA	2.21	9.2
PLA/ 5wt% IL-4	7.57	35.6
PLA/ 5wt% IL-5	5.02	8.4
IL-4	7.15	N/A
IL-5	2.52	N/A

4.6 Soil Degradation Characteristics of PLA and PLA/ILs

4.6.1 Visual Observation

There was no significant visual difference between PLA and PLA/ILs blends until 7 days. The apparent decay after 7 days of the neat PLA is slower than that of PLA/ 5wt% IL-5 and PLA/ 5wt% IL-4, indicating that PLA/ILs blends have higher biodegradability than PLA. After 21 days, samples could not be fully recovered due to a considerable fragmentation, as shown in Figure 4.19. PLA/ILs blends were already cracked and crumbled after 14 days, and recovery of the degraded fragments was difficult after that time period. For all samples, color change to opaque white started on the 7th day as in the case of hydrolytic degradation. This is due to crystallization promoted by the formation of low MW polymer during degradation (See Section 4.6.3). It should be mentioned that weight losses could not easily be measured due to excessive fragmentation of the samples

after removal and during washing. Thus, only visual examination was possible.

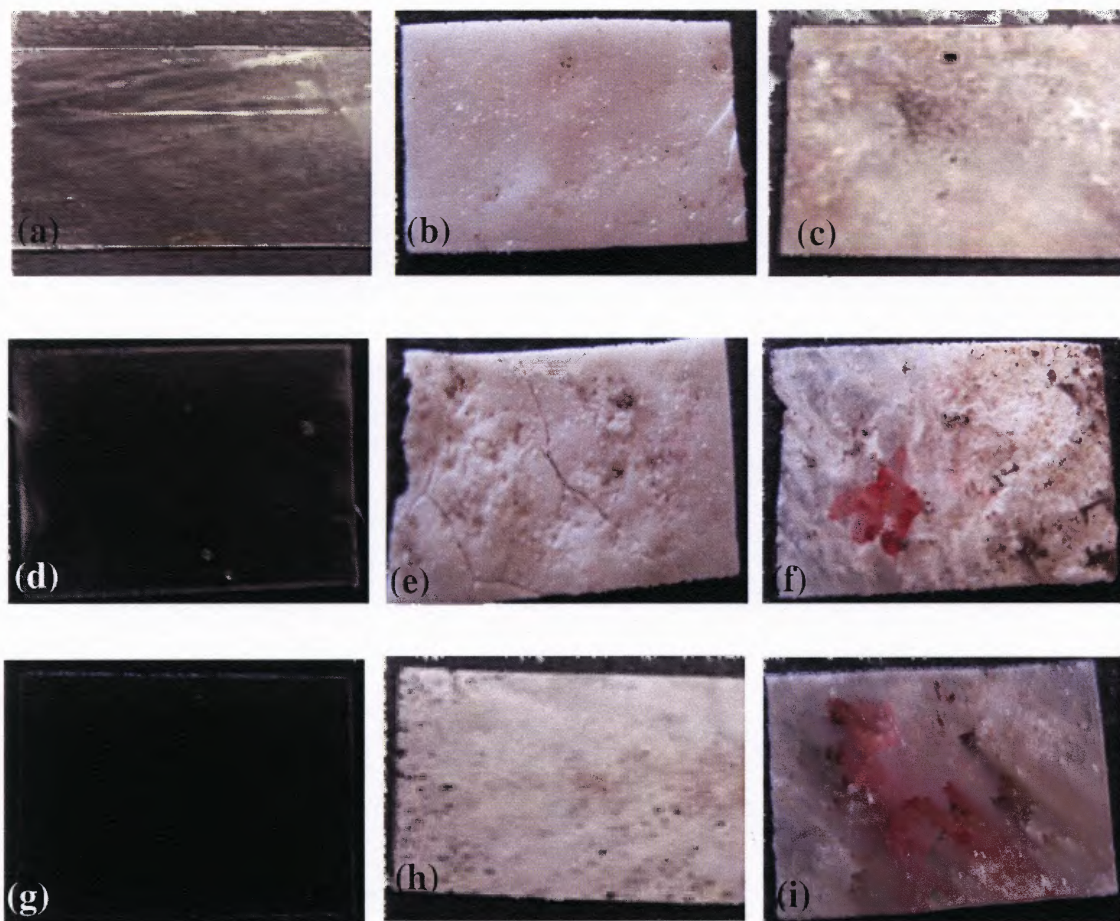


Figure 4.19 Photographs of neat PLA and PLA/ILs blends before and after burial in soil/sterilized (s.) soil for 28 days: (a) PLA before burial (b) PLA after burial in soil (c) PLA after burial in s.soil (d) PLA/IL-4 before burial, (e) PLA/IL-4 after burial in soil ,(f) PLA/IL-4 after burial in s.soil (g) PLA/IL-5 before burial (h) PLA/IL-5 after burial in soil (i) PLA/IL-5 after burial in s.soil

*s.soil: sterilized soil

Figure 4.19 shows pictures of PLA and PLA/ILs blends degraded in soil and sterilized soil. The buried specimens of PLA/ILs blends were very fragile and some parts were broken in the washing process that prevented the measurement of weight loss. In the case of specimens in soil, the PLA /ILs blends were expected to be degraded by both the action of water and enzymatic interactions while the degradation process in the sterilized

soil system was expected to be controlled by moisture only. The surface of the matrix PLA appears unchanged except for the color change and shrinkage after the burial-test (Figs 4.19 b, c). In the case of PLA/ILs blends, many cracks were observed especially for the PLA IL-4 in soil. The cracks were thought to be formed by the excessive degradation of the polymer and shrinkage of the sample due to PLA crystallization as a result of its MW reduction. Such cracks were not observed in the case of PLA and PLA/IL-5 blend in both soil and sterilized soil. In general, samples degraded in sterilized soil were less opaque than samples degraded in the “as received” soil.

4.6.2 Change of Crystallinity after Soil Degradation

Figure 4.20 shows the X-ray spectrum of PLA before and after 4 weeks of soil degradation. The spectrum of the initial polymer was typical of an amorphous polymeric material. After 4 weeks of degradation a peak (17°) clearly appeared, indicating morphological changes. A second narrow peak (18.5°) appeared at the expense of the scattered energy due to the amorphous domains as also shown by Miyajima et al. [108]. The peaks indicate that amorphous PLA crystallized during/after soil degradation due to its lower molecular weight. This is supported by the results of Miyajima et al. [108] who studied the hydrolytic degradation of amorphous PLA prepared by quenching. They obtained similar peaks after 16 hours immersion in pH 7.4 PBS at 37°C . Degradation gives shorter chains that are more mobile than longer ones, and more susceptible to crystallize. Since PLA/IL-4 and PLA/IL-5 also became whitish after 4 weeks, it is assumed that crystallization of the amorphous polymer also took place. As a result, XRD experiments were not carried out with the exposed blends. The results of this Section

could be directly applicable to the case of hydrolytic degradation (Section 4.5) where initially transparent samples became opaque after immersion.

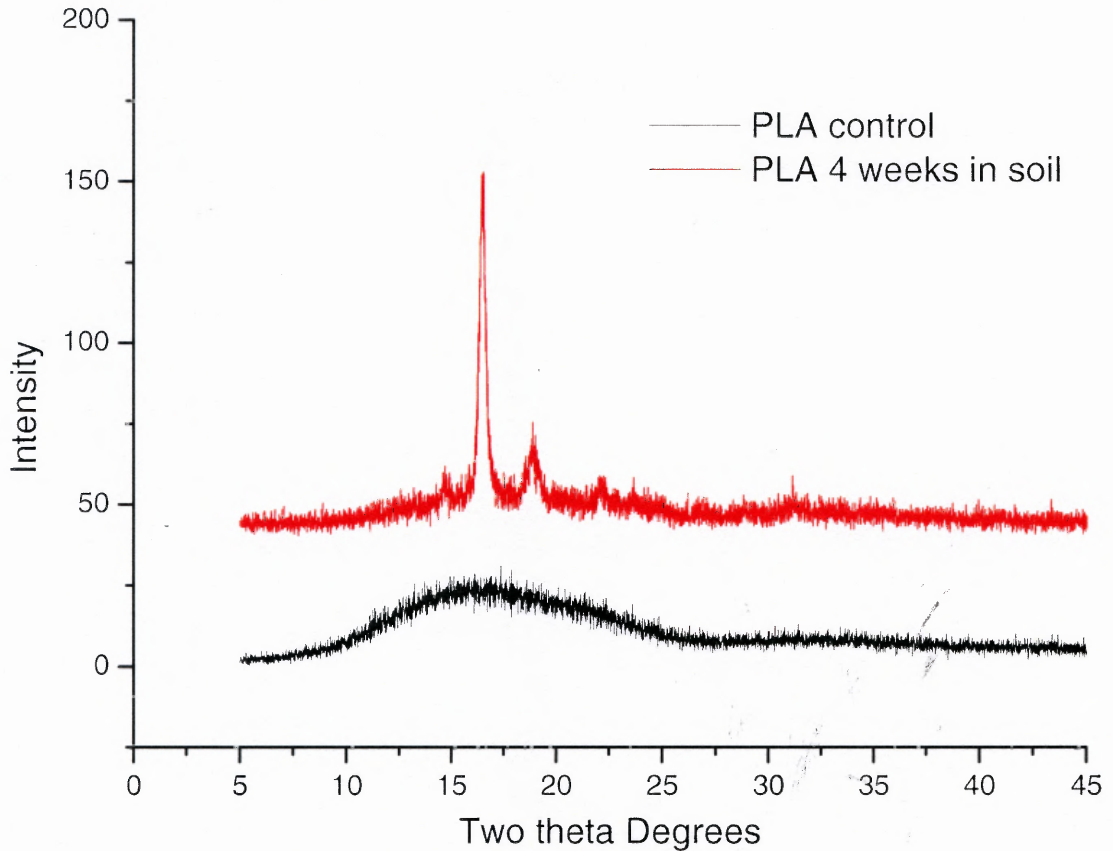


Figure 4.20 XRD spectra of PLA before and after 4 weeks of soil degradation.

4.7 Physical / Mechanical Properties

4.7.1 Coefficient of Friction of PLA and PLA/ILs

For all samples, the friction force showed a sudden increase to a maximal value (static friction) and then decreased to a steady state value indicating the kinetic friction force.

After each measurement, values were averaged to calculate the average kinetic friction

force for the run. The resulting COF values of ILs in PLA are compared with PLA in Table 4.9. Two important observations are made: (i) for both PLA/IL-4 and PLA/IL-5 compositions, COF values were significantly lower than that of PLA. (ii) PLA/IL-5 showed a lower COF than PLA-IL-4. Both IL-4 and IL-5 appear to be good internal lubricants which would tend to migrate to the surface of the PLA matrix.

Table 4.9 Contact Angle and Coefficient of Friction Results.

Sample	Coefficient of friction (ALTEK)	Contact angle (deg)
PLA	0.45±0.07	71.10
PLA/ 5wt% IL-4	0.17±0.05	66
PLA/ 5wt% IL-5	0.08±0.02	58.9

In the absence of ILs, friction is between the PLA surface and the steel balls and, as a result, the COF is very high (~0.45). Incorporation of ILs into the composite results in ILs covering some fraction of the PLA matrix surface and causing a reduction in the measured COF. ILs may be uniformly distributed in the PLA matrix including its surface resulting in a reduction of COF. A possible explanation on the structure of PLA/ILs blends is that the anion part of the ionic liquid can interact with positively charged sites such as carbonyl group due to the delta (-) charge of oxygen atoms in the PLA chain.

4.7.2 Contact Angle Measurements of PLA and PLA/ILs

According to the results shown in Table 4.8, the presence of IL-4 and IL-5 decrease the contact angle of water on PLA resulting in increasing hydrophilicity that depends on the type of the anion. The more hydrophilic tetrafluoroborate anions [109] appear to be present on the surface of the PLA film reducing, thus, the contact angle to about 59°. In this experiment, it is found that there is a relationship between contact angle and coefficient of friction; lower coefficient of friction corresponds to lower contact angle in agreement with the results of Hiratsuka et al. [110].

4.7.3 Flexural Properties of PLA and PLA/ILs Blends

The effects of ILs on the mechanical properties of PLA can be derived from the summarized data in Figure 4.21. Please note that in the case of PLA/IL-4, the samples broke at about 7.5N load and the calculated strength is indeed the maximum stress at break that caused brittle fracture. PLA and /PLA/IL-5 samples were more ductile and did not break but rather bent excessively; the reported strength refers to the maximum recorded force.

As discussed in Section 4.1.6, the low T_g of PLA/ILs samples could not only be due to plasticization but also thermo-mechanical degradation. PLA/IL-4 was the most highly degraded sample with the lowest T_g and exhibited brittle fracture and a high modulus. PLA/IL-5 underwent less thermo-mechanical degradation, had a higher T_g , was more ductile and had also a lower modulus. Therefore, it appears that IL-5 can be considered as a better plasticizer. By contrast, processed PLA underwent relatively little thermo-mechanical degradation and retained its high modulus and ductility.

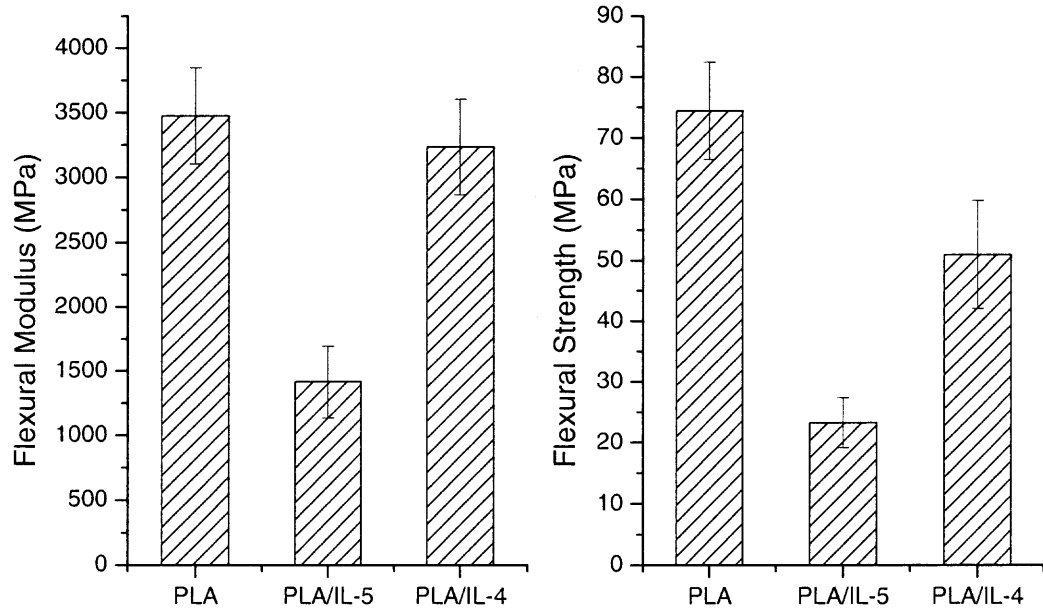


Figure 4.21 Flexural modulus and flexural strength of PLA, PLA/ 5wt% IL-4, and PLA/ 5wt% IL-5 by three point bending test. *Error bars indicate mean values \pm one standard deviation.

CHAPTER 5

CONCLUSIONS AND RECOMMENDATIONS

In this study, two ILs with different anions (decanoate, tetrafluoroborate) but with the same phosphonium based cation were evaluated as potential plasticizers and lubricants for PLA and also for their effects on its hydrolytic and thermal degradation. Both IL-4 and IL-5 were well dispersible and partly miscible with PLA at 5 wt% content as evidenced by SEM and T_g characterization, as well as from solubility parameter calculations. However, in the case of PLA/ 5wt% IL-5, phase separation was observed one year after melt processing.

The effects of the IL containing the decanoate anion (IL-4) were more pronounced on lubrication and degradation as evidenced by reduced melt viscosities and accelerated thermal/hydrolytic degradation; it could also be considered as a more effective plasticizer based on T_g suppression results although degree of plasticization could also be affected by the observed excessive MW degradation during processing. The IL containing the tetrafluoroborate anion increased the thermal stability of PLA, at least up to 40 hours at 160°C in air, and accelerated its hydrolytic degradation, but to a lesser extent than the decanoate based IL. The catalytic role of the decanoate anion in hydrolytic degradation was confirmed through experiments with model compound (PLA/DECA).

Hydrolytic chain scission of ester bonds catalyzed by carboxylic groups of PLA and IL-4 and HF formed from IL-5 are the suggested mechanisms of the hydrolytic degradation from results of pH and acid number changes, although it appears that the presence of the phosphonium cation contributes also to accelerated degradation.

SEM micrographs confirm that both ILs accelerate hydrolytic degradation by increasing pore size. In the “as received” soil, PLA and their IL blends (particularly the PLA/IL-4 blend) appeared to degrade faster than in a sterilized soil, presumably as a result of additional enzymatic degradation. Different surface characteristics of the PLA/ILs were manifested in differences in COF and contact angle measurements; PLA/IL-5 showed lower COF towards steel and more hydrophilic characteristic than PLA and PLA/IL-4. The effects of IL-5 on the mechanical properties of PLA blend demonstrated lowest flexural strength and modulus but still higher ductility than IL-4.

Based on the results of this study, IL-5 could be considered as a more desirable multifunctional additive for PLA offering a better balance of adverse vs. beneficial effects than IL-4.

Further understanding of the biodegradation of PLA/ILs blends remains for future studies. Research in the toxicity of ILs may be helpful to find applications of studied PLA/ILs blends. Given the potential toxicity of ILs towards living organisms, further experiments are recommended in order to separate the biodegradation of PLA from the effects of ILs that could be released from the matrix in a controlled manner. Potential applications for the studied PLA/ILs systems could be as additives in antibacterial coatings or insecticide/pesticide containing devices.

APPENDIX A

CALCULATION OF SOLUBILITY PARAMETERS USING FEDORS METHOD [92]

Solubility parameter of IL-4, IL-4, and PLA were calculate as shown in the follwings;

1. Solubility Parameter of IL-4

CH2: 4940 J/mol (Cohesive energy according to Fedors)

CH3: 4710 J/mol

P: 9420 J/mol

COO: 18000 J/mol

Molar volume: 744.46 cm³/mol

$$\delta = \sqrt{\frac{(4940 \times 36) J / mol + (4710 \times 5) J / mol + 9420 J / mol + 18000 J / mol}{744.46 \text{ cm}^3 / mol}} = 17.53 (J / \text{cm}^3)^{\frac{1}{2}}$$
$$= 17.53 (\text{MPa})^{1/2}$$

2. Solubility parameter of IL-5

CH2: 4940 J/mol

CH3: 4710 J/mol

P: 9420 J/mol

B: 13810 J/mol

F: 4190 J/mol

Molar volume: 651 cm³/mol

$$\delta = \sqrt{\frac{(4940 \times 28) J / mol + (4710 \times 4) J / mol + 9420 J / mol + 13810 J / mol + (4190 \times 4) J / mol}{651 \text{ cm}^3 / mol}}$$
$$= 17.4 (\text{MPa})^{1/2}$$

3. Solubility parameter of PLA

CH: 3430 J/mol

CH₃: 4710 J/mol

COO: 18000 J/mol

Molar volume: 58 cm³/mol

$$\delta = \sqrt{\frac{3430 \text{ J/mol} + 4710 \text{ J/mol} + 1470 \text{ J/mol} + 18000 \text{ J/mol}}{58 \text{ cm}^3/\text{mol}}} = 21.8 \text{ J/cm}^3$$
$$= 21.8 \text{ (MPa)}^{1/2}$$

APPENDIX B

SEM OF PLA AND PLA/ILS BLENDS AFTER HYDROLYTIC DEGRADATION

SEM micrographs show differences in pore size depend on types of PLA/ ILS.

B.1 PLA

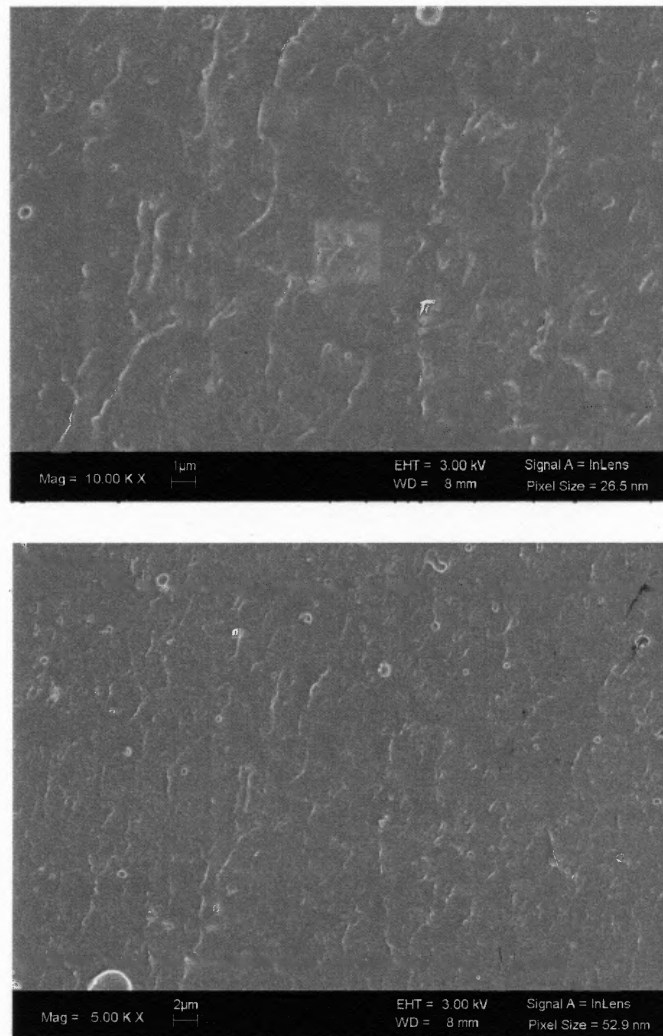


Figure B.1 SEM micrographs of PLA after 144 hours of immersion in PBS.

B.2 PLA/ 5wt% IL-4 blends

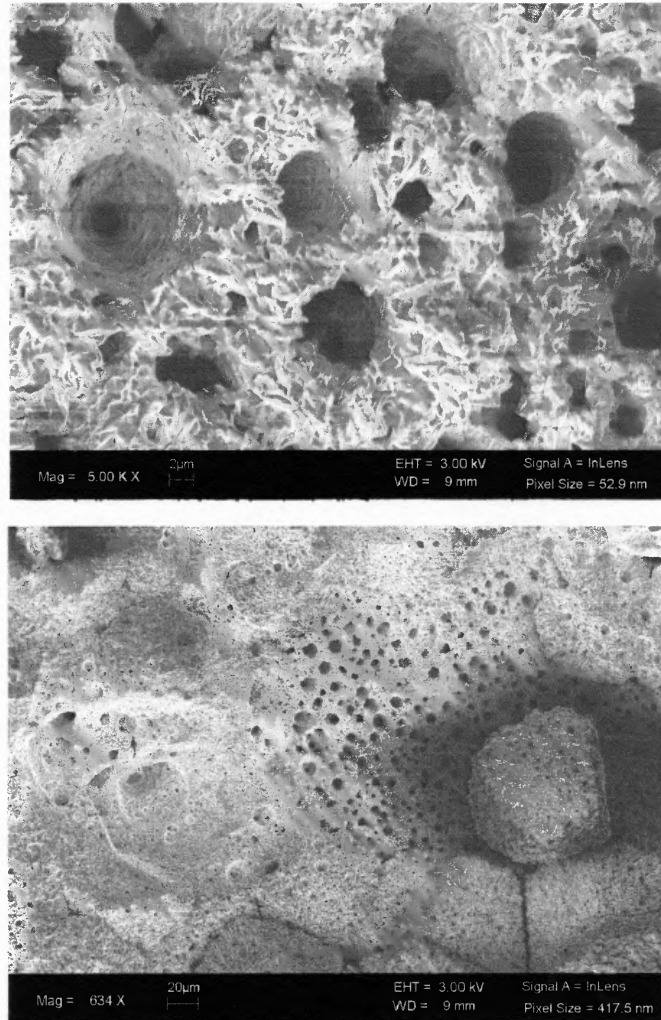


Figure B.2 SEM micrographs of PLA/IL-4 after 144 hours of immersion in PBS.

B.3 PLA/ 5wt% IL-5 blends

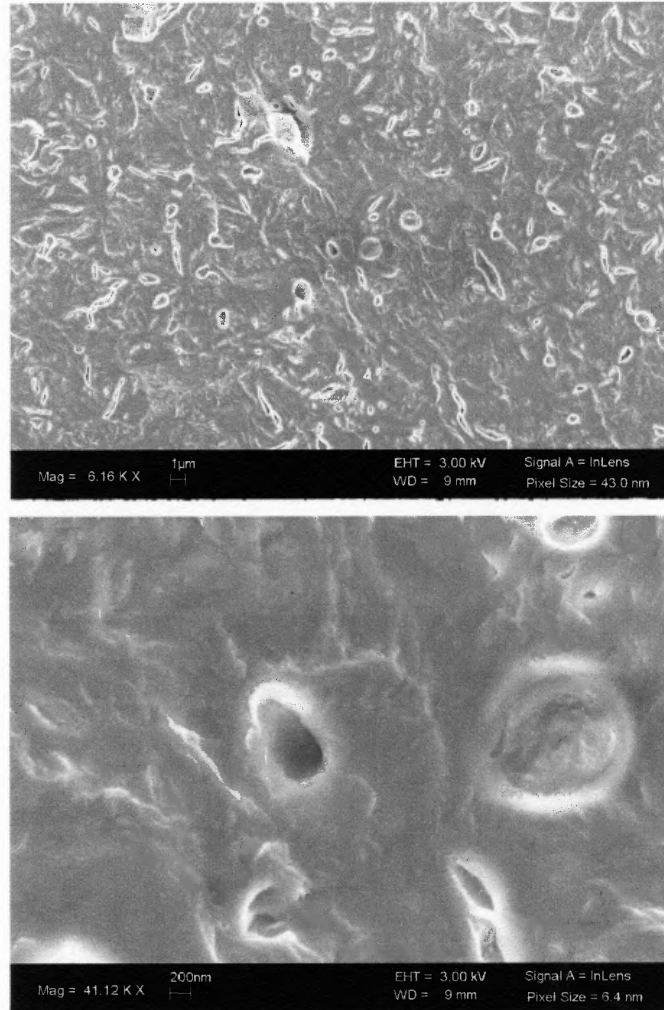


Figure B.3 SEM micrographs of PLA/IL-5 after 144 hours of immersion in PBS.

Missing Page

Missing Page

Missing Page

Missing Page

Missing Page

REFERENCES

1. R. E. Drumright, P. R. Gruber and D. E. Henton, Polylactic acid technology. *Advanced Materials* **2000**, 12, (23), 1841-1846.
2. W. H. Carothers, G. L. Dorrough and F. J. Van Natta, Studies of polymerization and ring formation. X. The reversible polymerization of six-membered cyclic esters. *Journal of the American Chemical Society* **1932**, 54, (2), 761-772.
3. N. Teramoto, K. Urata, K. Ozawa and M. Shibata, Biodegradation of aliphatic polyester composites reinforced by abaca fiber. *Polymer Degradation and Stability* **2004**, 86, (3), 401-409.
4. H. Pistner, R. Gutwald, R. Ordnung, J. Reuther and J. Muhling, Poly(L-lactide): A long term degradation study in vivo I. Biological results. *Biomaterials* **1993**, 14, (9), 671-677.
5. D. P. Mobely, *Plastics from microbes: microbial synthesis of polymers and polymer precursors. Hanser Publishers* **1994**.
6. D. M. Bigg Effect of Copolymer Ratio on the Crystallinity and Properties of Poly(lactic Acid) Copolymers, *Society of Plastics Engineers-Annual Technical Conference*, 1996; pp 2028-2039.
7. J. J. Cooper-White and M. E. Mackay, Rheological properties of poly(lactides). Effect of molecular weight and temperature on the viscoelasticity of poly(l-lactic acid). *Journal of Polymer Science Part B: Polymer Physics* **1999**, 37, (15), 1803-1814.
8. D. Garlotta, A literature review of poly(lactic acid). *Journal of Polymers and the Environment* **2001**, 9, (2), 63-84.
9. T. Welton, Room-temperature ionic liquids. Solvents for synthesis and catalysis. *Chemical Reviews* **1999**, 99, (8), 2071-2083.
10. R. A. Reich, P. A. Stewart, J. Bohaychick and J. A. Urbanski, Base oil properties of ionic liquids. *Lubrication Engineering* **2003**, 59, (7), 16-21.
11. N. H. Kim, S. V. Malhotra and M. Xanthos, Modification of cationic nanoclays with ionic liquids. *Microporous and Mesoporous Materials* **2006**, 96, (1-3), 29-35.
12. H. Zhao and S. V. Malhotra, Applications of ionic liquids in organic synthesis. *Aldrichimica Acta* **2002**, 35, (3), 75-83.

13. K. R. Seddon, Ionic liquids for clean technology. *Journal of Chemical Technology and Biotechnology* **1997**, 68, (4), 351-356.
14. C. Zhong, T. Sasaki, A. Kobayashi, E. Fujiwara, A. Kobayashi, M. Tada and Y. Iwasawa, Syntheses, structures, and properties of a series of metal Ion-containing dialkylimidazolium ionic liquids. *Bulletin of the Chemical Society of Japan* **2007**, 80, (12), 2365-2374.
15. R. G. Reddy, Ionic liquids: How well do we know them? *Journal of Phase Equilibria and Diffusion* **2006**, 27, (3), 210-211.
16. Cytec Phosphonium Salts. <http://www.cytec.com/specialty-chemicals/products/phosphonium-salts.htm> (June 26, 2007).
17. J. H. Davis Jr, K. J. Forrester and T. Merrigan, Novel organic ionic liquids (OILS) incorporating cations derived from the antifungal drug miconazole. *Tetrahedron Letters* **1998**, 39, (49), 8955-8958.
18. P. Bonhôte, A. P. Dias, N. Papageorgiou, K. Kalyanasundaram and M. Grätzel, Hydrophobic, highly conductive ambient-temperature molten salts. *Inorganic Chemistry* **1996**, 35, (5), 1168-1178.
19. S. Aki, J. F. Brennecke and A. Samanta, How polar are room-temperature ionic liquids? *Chemical Communications* **2001**, (5), 413-414.
20. J. N. Canongia Lopes, M. F. Costa Gomes and A. A. H. Pádua, Nonpolar, polar, and associating solutes in ionic liquids. *Journal of Physical Chemistry B* **2006**, 110, (34), 16816-16818.
21. P. Wasserscheid and W. Keim, Ionic liquids - New 'solutions' for transition metal catalysis. *Angewandte Chemie - International Edition* **2000**, 39, (21), 3773-3789.
22. G. Schliecker, S. Fuchs, C. Schmidt and T. Kissel, Characterization of a homologous series of D, L-lactic acid oligomers; a mechanistic study on the degradation kinetics in vitro. *Biomaterials* **2003**, 24, 3835-3844.
23. N. H. Kim, S. V. Malhotra and M. Xanthos, Ionic liquids as modifiers for cationic and anionic nanoclays. In *ACS Symposium Series*, 2007; Vol. 975, pp 234-246.
24. J. F. Brennecke, R. D. Rogers and K. R. Seddon, ACS Symposium Series: Preface. In *American Chemical Society Symposium Series*, 2007; Vol. 975, pp xi-xiii.
25. C. M. Gordon, New developments in catalysis using ionic liquids. *Applied*

26. L. G. Bonnet and B. M. Kariuki, Ionic liquids: Synthesis and characterisation of triphenylphosphonium tosylates. *European Journal of Inorganic Chemistry* **2006**, 2, 437-446.
27. J. U. HA and M. Xanthos, Functionalization of nanoclays with ionic liquids for polypropylene composites. *Polymer Composites*, accepted DOI 10.1002/pc.20583 **2008**.
28. C. J. Bradaric, A. Downard, C. Kennedy, A. J. Robertson and Y. Zhou, Industrial preparation of phosphonium ionic liquids. *Green Chemistry* **2003**, 5, 143-152.
29. M. Rahman and C. S. Brazel, Ionic liquids: New generation stable plasticizers for poly(vinyl chloride). *Polymer Degradation and Stability* **2006**, 91, (12), 3371-3382.
30. L. G. Krauskopf and A. Godwin., Plasticizers: types, properties and performance. *Encyclopedia of PVC*, 2 **1988**.
31. Y. Liu, G. Wu, D. Long and G. Zhang, 60Co [γ]-Initiated polymerization of vinyl monomers in room temperature ionic liquid/THF mixed solutions. *Polymer* **2005**, 46, (19), 8403-8409.
32. J. Sanes, F. J. Carrión, M. D. Bermúdez and G. Martínez-Nicolás, Ionic liquids as lubricants of polystyrene and polyamide 6-steel contacts. Preparation and properties of new polymer-ionic liquid dispersions. *Tribology Letters* **2006**, 21, (2), 121-133.
33. Z. Mu, F. Zhou, S. Zhang, Y. Liang and W. Liu, Effect of the functional groups in ionic liquid molecules on the friction and wear behavior of aluminum alloy in lubricated aluminum-on-steel contact. *Tribology International* **2005**, 38, (8), 725-731.
34. C. Ye, W. Liu, Y. Chen and L. Yu, Room-temperature ionic liquids: A novel versatile lubricant. *Chemical Communications* **2001**, (21), 2244-2245.
35. B. S. Nader, K. K. Kar, T. A. Morgan, C. E. Pawloski and W. L. Dilling, Development and Tribological Properties of New Cyclotriphosphazene High Temperature Lubricants for Aircraft Gas Turbine Engines. *Tribology Transactions* **1992**, 35, (1), 37-44.
36. L. G. Krauskopf and G. A., *PVC handbook*. Carl Hanser Verlag: Munich, 2005.
37. M. Rahman and C. S. Brazel, The plasticizer market: an assessment of traditional

plasticizers and research trends to meet new challenges. *Progress in Polymer Science* **2004**, 29, (12), 1223-1248.

38. M. P. Scott, C. S. Brazel, M. G. Benton, J. W. Mays, J. D. Holbrey and R. D. Rogers, Application of ionic liquids as plasticizers for poly(methyl methacrylate). *Chemical Communications* **2002**, 7, (13), 1370-1371.
39. M. P. Scott, M. G. Benton, M. Rahman and C. S. Brazel, Plasticizing effects of imidazolium salts in PMMA: high temperature stable flexible engineering materials. Ionic liquids as green solvents: progress and prospects. In *American Chemistry Society Symposium*, 2003; Vol. 856 p468.
40. M. Rahman, M. G. Benton, M. P. Scott and C. S. Brazel Room temperature ionic liquids as environmentally benign plasticizers and reaction media for polymerization reactions, *Proceedings of Green Chemical Engineering Conference*, Sandestin, Florida, 2003; pp 180-183.
41. M. Rahman and C. S. Brazel, Effectiveness of Phosphonium, Ammonium, and Imidazolium-Based. Ionic Liquids as Plasticizers for Poly(vinyl chloride): Thermal and Ultraviolet Stability. *Polymer Preprints* **2004**, 45-1, 301-302.
42. M. Rahman and C. S. Brazel, Effectiveness of phosphonium, ammonium and imidazolium based ionic liquids as plasticizers for poly(vinyl chloride): Thermal and ultraviolet stability. *Polymer Preprints* **2004**, 45, (1), 301-302.
43. New plasticizer joins Bayer's range. *Additives for Polymers* **2003**, 2003, (8), 2-2.
44. D. Zhao, Y. Liao and Z. D. Zhang, Toxicity of ionic liquids. *Clean - Soil, Air, Water* **2007**, 35, (1), 42-48.
45. A. Vaccari, Preparation and Catalytic Properties of Cationic and Anionic Clays. *Catalysis Today* **1998**, 41, 53-71.
46. K. Kamena, *Nanoclays and Their Emerging Markets*. Wiley-VCH: Weinheim, Germany, 2005; p 163-171.
47. M. Alexandre and P. Dubois, Polymer-layered silicate nanocomposites: Preparation, properties and uses of a new class of materials. *Materials Science and Engineering R: Reports* **2000**, 28, (1), 1-63.
48. A. B. Morgan and J. D. Harris, Exfoliated polystyrene clay nanocomposites synthesized by solvent blending with sonication. *Polymer* **2004**, 45, (26), 8695-8703.
49. K. Stoeffler, P. G. Lafleur and J. Denault Polyethylene nanocomposites based on high thermal stability organoclay, *Society of Plastics Engineers Annual*

50. E. Kandare, G. Chigwada, D. Wang, C. A. Wilkie and J. M. Hossenlopp, Nanostructured layered copper hydroxy dodecyl sulfate: A potential fire retardant for poly(vinyl ester) (PVE). *Polymer Degradation and Stability* **2006**, 91, (8), 1781-1790.
51. K. Stoeffler, P. G. Lafleur and J. Denault Thermal Properties of Polyethylene Nanocomposites Based on Different Organoclays, *Society of Plastics Engineers Annual Technical Conference*, 2006; p 263.
52. C. Byrne, T. McNally and C. G. Armstrong Thermally stable modified layered silicates for PET nanocomposites, *Polymer Processing Society America's Regional Meeting*, Quebec, Canada, 2005.
53. O. Wachsen, K. Platkowski and K.-H. Reichert, Thermal degradation of poly-L-lactide -studies on kinetics, modelling and melt stabilisation. *Polymer Degradation and Stability* **1997**, 57, (1), 87-94.
54. F. D. Kopinke, M. Remmler, K. Mackenzie, M. Möder and O. Wachsen, Thermal decomposition of biodegradable polyesters - II. Poly(lactic acid). *Polymer Degradation and Stability* **1996**, 53, (3), 329-342.
55. A. L. Arraiza, J. R. Sarasua, J. Verdu and X. Colin, Rheological behavior and modeling of thermal degradation of poly(ϵ -caprolactone) and poly(L-lactide). *International Polymer Processing* **2007**, 22, (5), 389-394.
56. S. Li and M. Vert, Crystalline oligomeric stereocomplex as an intermediate compound in racemic poly(DL-lactic acid) degradation. *Polymer International* **1994**, 33, (1), 37-41.
57. NatureWorks® *Technology Focus Report: Polylactic Acid Containing Fillers and Fibers*; Minnetonka, MN, 2/19, 2007.
58. S. Y. Lee, I. A. Kang, G. H. Doh, H. G. Yoon, B. D. Park and Q. Wu, Thermal and mechanical properties of wood flour/talc-filled polylactic acid composites: Effect of filler content and coupling treatment. *Journal of Thermoplastic Composite Materials* **2008**, 21, (3), 209-223.
59. J. H. Chang, Y. U. An and G. S. Sur, Poly(lactic acid) nanocomposites with various organoclays. I. Thermomechanical properties, morphology, and gas permeability. *Journal of Polymer Science, Part B: Polymer Physics* **2003**, 41, (1), 94-103.
60. M. Pluta, A. Galeski, M. Alexandre, M. A. Paul and P. Dubois, Poly(lactide)/montmorillonite nanocomposites and microcomposites prepared

by melt blending: Structure and some physical properties. *Journal of Applied Polymer Science* **2002**, 86, (6), 1497-1506.

61. Q. Zhou and M. Xanthos, Nanoclay and crystallinity effects on the hydrolytic degradation of polylactides. *Polymer degradation and stability*, accepted DOI 10.1016/j.polymdegradstab.2008.05.014 **2008**.
62. M. Vert, J. Feijen, A. Albertsson, G. Scott and E. Chiellini, Biodegradable polymers and plastics. *Royal Society of Chemistry* **1992**.
63. M. Vert, J. Mauduit and S. Li, Biodegradation of PLA/GA polymers: Increasing complexity. *Biomaterials* **1994**, 15, (15), 1209-1213.
64. M. Vert, G. Schwach, R. Engel and J. Coudane, Something new in the field of PLA/GA bioresorbable polymers? *Journal of Controlled Release* **1998**, 53, (1-3), 85-92.
65. I. Grizzi, H. Garreau, S. Li and M. Vert, Hydrolytic degradation of devices based on poly(DL-lactic acid) size dependence. *Biomaterials* **1995**, 16, (4), 305-311.
66. S. Li, Hydrolytic degradation characteristics of aliphatic polyesters derived from lactic and glycolic acids. *Journal of Biomedical Materials Research* **1999**, 48, (3), 342-353.
67. M. Therin, P. Christel, S. Li, H. Garreau and M. Vert, In vivo degradation of massive poly(α -hydroxy acids): Validation of in vitro findings. *Biomaterials* **1992**, 13, (9), 594-600.
68. M. Vert, S. Li and H. Garreau, More about the degradation of LA/GA-derived matrices in aqueous media. *Journal of Controlled Release* **1991**, 16, (1-2), 15-26.
69. S. Li and S. McCarthy, Further investigations on the hydrolytic degradation of poly (DL-lactide). *Biomaterials* **1999**, 20, (1), 35-44.
70. F. V. Burkersroda, L. Schedl and A. Göpferich, Why degradable polymers undergo surface erosion or bulk erosion. *Biomaterials* **2002**, 23, (21), 4221-4231.
71. A. Göpferich, R. Gref, Y. Minamitake, L. Shieh, M. J. Alonso, Y. Tabata and R. Langer, Drug delivery from bioerodible polymers: Systemic and intravenous administration. *Formulation and Delivery of Proteins and Peptides* **1994**, 242-277.
72. J. M. Anderson, *Perspectives of the in vivo responses of biodegradable polymers*. CRC Press: Boca Raton, 1995.

73. C. G. Pitt and Z. Gu, Modification of the rates of chain cleavage of poly(ϵ -caprolactone) and related polyesters in the solid state. *Journal of Controlled Release* **1987**, 4, (4), 283-292.
74. A. Göpferich, Mechanisms of polymer degradation and erosion. *Biomaterials* **1996**, 17, (2), 103-114.
75. A. Göpferich and R. Langer, Modeling of polymer erosion. *Macromolecules* **1993**, 26, (16), 4105-4112.
76. A. J. Kirby, Hydrolysis and formation of esters of organic acids. *Comprehensive Chemical Kinetics* **1972**, 10, 57-207.
77. C. C. Chu, A comparison of the effect of pH on the biodegradation of two synthetic absorbable sutures. *Annals of Surgery* **1982**, 195, (1), 55-59.
78. K. W. Leong, B. C. Brott and R. Langer, Bioerodible polyanhydrides as drug-carrier matrices. I: Characterization, degradation, and release characteristics. *Journal of Biomedical Materials Research* **1985**, 19, (8), 941-955.
79. J. Heller, Controlled drug release from poly(ortho esters) - A surface eroding polymer. *Journal of Controlled Release* **1985**, 2, 167-177.
80. J. Heller, Poly (ortho esters). *Advances in Polymer Science* **1993**, 107, 41-92.
81. L. T. Fan and S. K. Singh, *Controlled Release: A Quantitative Treatment* **1989**.
82. R. Baker, *Controlled Release of Biologically Active Agents* **1987**.
83. T. St. Pierre and E. Chiellini, Biodegradability of synthetic polymers used for medical and pharmaceutical applications: Part I - Principles of hydrolysis mechanisms. *Journal of Bioactive and Compatible Polymers* **1986**, 1, 467-497.
84. K. Park, W. W. Shalaby and H. Park, Biodegradable hydrogels for drug delivery. *Pennsylvania: Technomic Publishing* **1993**, 237.
85. P. Sykes, *A Guidebook to Mechanism in Organic Chemistry* **1986**.
86. C. Shih, T. Higuchi and K. J. Himmelstein, Drug delivery from catalyzed erodible polymeric matrices of poly(ortho ester)s. *Biomaterials* **1984**, 5, (4), 237-240.
87. C. G. Pitt, Non-microbial degradation of polyesters: Mechanisms and modifications. *Biodegradable Polymers and Plastics* **1992**, 7-17.
88. E. Ron, T. Turek, E. Mathiowitz, M. Chasin, M. Hageman and R. Langer,

Controlled release of polypeptides from polyanhydrides. *Proceedings of the National Academy of Sciences of the United States of America* **1993**, 90, (9), 4176-4180.

89. K. Okamoto, S. Ray and M. Okamoto, New poly(butylene succinate)/layered silicate nanocomposites. II. Effect of organically modified layered silicates on structure, properties, melt rheology, and biodegradability. *Journal of Polymer Science Part B: Polymer Physics* **2003**, 41, (24), 3160-3172.
90. NatureWorks® Technical data sheet. <http://www.natureworkslc.com/product-and-applications> (05/11 2007).
91. M. U. Kato, A.; Okada, A., Synthesis of PP oligomer clay intercalation compounds. *Journal of Applied Polymer Science* **1997**, 66, 1133-1138.
92. D. W. V. Krevelen, *Properties of polymers*. Elsevire scientific publishing company: Amsterdam, 1976.
93. C. Fu and Z. Liu, Syntheses of high molecular weight aliphatic polyesters in 1-alkyl-3-methylimidazolium ionic liquids. *Polymer* **2008**, 49, (2), 461-466.
94. F. F. Robert, A method for estimating both the solubility parameters and molar volumes of liquids. *Polymer Engineering & Science* **1974**, 14, (2), 147-154.
95. Z. Ren, L. Dong and Y. Yang, Dynamic mechanical and thermal properties of plasticized poly(lactic acid). *Journal of Applied Polymer Science* **2006**, 101, (3), 1583-1590.
96. L. H. Tagle, F. R. Díaz and R. J. Vega, Glass transition temperature - molecular weight relation of a poly(amide-imide). *Polymer Bulletin* **1984**, 11, (6), 523-524.
97. S. Yan, J. Yin, J. Yang and X. Chen, Structural characteristics and thermal properties of plasticized poly(l-lactide)-silica nanocomposites synthesized by sol-gel method. *Materials Letters* **2007**, 61, (13), 2683-2686.
98. S. S. R. M. O. Kazuaki Okamoto, New poly(butylene succinate)/layered silicate nanocomposites. II. Effect of organically modified layered silicates on structure, properties, melt rheology, and biodegradability. *Journal of Polymer Science Part B: Polymer Physics* **2003**, 41, (24), 3160-3172.
99. X.-G. Li, Huang, M.-R., Guan, G.-H., Sun, T., Kinetics of thermal degradation of thermotropic poly(p-oxybenzoate-co-ethylene terephthalate) by single heating rate methods. *Polymer International* **1998**, 46, (4), 289-297.
100. X.-S. Wang, X.-G. Li and D. Yan, Thermal decomposition kinetics of

- poly(trimethylene terephthalate). *Polymer Degradation and Stability* **2000**, 69, (3), 361-372.
101. S. Ahn and J. L. White, Influence of carboxylic acid additives on the flow behavior of molten thermoplastics. *Journal of Applied Polymer Science* **2003**, 90, (6), 1555-1564.
 102. X. Liu, Y. Zou, W. Li, G. Cao and W. Chen, Kinetics of thermo-oxidative and thermal degradation of poly(d,l-lactide) (PDLLA) at processing temperature. *Polymer Degradation and Stability* **2006**, 91, (12), 3259-3265.
 103. F. Rodriguez, *Principles of Polymer Systems* Taylor & Francis: Washington, DC, 1996.
 104. A. M. Emsley, M. Ali and R. J. Heywood, A size exclusion chromatography study of cellulose degradation. *Polymer* **2000**, 41, (24), 8513-8521.
 105. S. Li, H. Garreau and M. Vert, Structure-property relationships in the case of the degradation of massive poly(α -hydroxy acids) in aqueous media - Part 2 Degradation of lactide-glycolide copolymers: PLA37.5GA25 and PLA75GA25. *Journal of Materials Science: Materials in Medicine* **1990**, 1, (3), 131-139.
 106. B. Weyershausen and K. Lehmann, Industrial application of ionic liquids as performance additives. *Green Chemistry* **2005**, 7, (1), 15-19.
 107. R. López-Fonseca, M. P. González-Marcos, J. R. González-Velasco and J. I. Gutiérrez-Ortiz, Chemical recycling of PET by alkaline hydrolysis in the presence of quaternary phosphonium and ammonium salts as phase transfer catalysts *Waste Management and the Environment IV DOI 10.2495/WM080521* **2008**.
 108. M. Miyajima, A. Koshika, J. Okada, M. Ikeda and K. Nishimura, Effect of polymer crystallinity on papaverine release from poly (-lactic acid) matrix. *Journal of Controlled Release* **1997**, 49, (2-3), 207-215.
 109. S. Park and R. J. Kazlauskas, Biocatalysis in ionic liquids - Advantages beyond green technology. *Current Opinion in Biotechnology* **2003**, 14, (4), 432-437.
 110. K. Hiratsuka, A. Bohno and H. Endo, Water droplet lubrication between hydrophilic and hydrophobic surfaces. *Journal of Physics: Conference Series* **2007**, 89, (1).